



Title	A Novel Biofilm-Membrane Reactor for Advanced Drinking Water Treatment
Author(s)	Kimura, Katsuki
Citation	北海道大学. 博士(工学) 乙第5696号
Issue Date	2000-09-29
DOI	10.11501/3175420
Doc URL	<a href="http://hdl.handle.net/2115/32690">http://hdl.handle.net/2115/32690</a>
Type	theses (doctoral)
File Information	5696.pdf



[Instructions for use](#)

A Novel Biofilm-Membrane Reactor  
for  
Advanced Drinking Water Treatment

**Katsuki Kimura**

Hokkaido University

2000

## ACKNOWLEDGMENT

I wish to express my deepest gratitude to Prof. Yoshimasa Watanabe for the guidance and encouragement he has given during the investigation. His coming back to Hokkaido Univ. certainly gave an influence on my life. Thanks to him, I could have many precious experiences.

I am also grateful to Prof. Tetsuo Takakuwa and Prof. Yasumoto Magara for their fruitful suggestions on this thesis.

I also wish to express my gratitude to Prof. Hallvard Ødegaard, Norwegian University of Science and Technology, Trondheim. Without his encouragement, I could not finish writing this thesis. I learned a lot through the communication with him.

I was very lucky to meet Prof. Norihito Tambo, who is working as President of Hokkaido Univ. now. I often remembered his lectures while writing this thesis. I am very proud that I am the "omega" student of him.

I deeply appreciate the friendship and helpfulness of Dr. Satoshi Okabe, Dr. Hisashi Sato, Dr. Shinsuke Kasahara and Dr. Rulin Bian. Their attitude and passion to research have been stimulating me. They have also encouraged me with a lot of beer!

I have gotten sincere supports and assistance from the staff of the laboratory, not least Mr. Genzou Ozawa and Miss Tomoko Kikuchi. Thanks are also given to Dr. Naoki Ohkuma, Hitachi Plant and Construction Co. Ltd., for providing me the experimental apparatuses.

Finally, I would like to thank all my family members for their support and tolerance.

---

# CONTENTS

---

<b>CHAPTER ONE – INTRODUCTION</b>	<b>1</b>
1.1. The Present State of Water Use in Japan	1
1.2. The Present and Future Problems of the Japanese Waterworks	7
1.3. Combination of a Biological Process for $\text{NH}_4^+\text{-N}$ Oxidation and Membrane Filtration for Solid-liquid Separation	11
 <b>CHAPTER TWO – AN ANALYSIS OF THE POTENTIAL OF USING THE ROTATING MEMBRANE DISK MODULE AS THE NOVEL BIOFILM-MEMBRANE REACTOR (BMR)</b>	 <b>19</b>
2.1. The Rotating Membrane Disk Module	19
2.2. Experimental Methods	22
2.2.1. Experimental Apparatus	22
2.2.2. Analytical Methods	24
2.3. Results and Discussion from Introductory Experiments	24
2.3.1. Evaluation of System Applicability (Run 2-1)	24
2.3.2. Evaluation of Membrane Flux on Transmembrane Pressure Development (Run 2-2)	27
2.3.3. Evaluation of the Influence of Seeding Sludge	
2.4. Summary	31

## CHAPTER THREE – MEMBRANE FILTRATION RESISTANCE IN THE NOVEL

	<b>BIOFILM-MEMBRANE REACTOR (BMR)</b>	<b>34</b>
3.1.	Experimental Method	35
3.1.1.	Experimental Apparatus	35
3.1.2.	Analytical Methods	35
3.1.3.	Division of the Total Membrane Filtration Resistance	36
3.2.	Results and Discussion from the Six Long Term Experiments	37
3.2.1.	Experiment Using Pure Cultures of the Nitrifiers (Run 3-1)	37
3.2.2.	Experiment Using Bacteria Acclimated to the Inorganic Substrates (Runs 3-2 and 3-3)	39
3.2.3.	Distribution of the Membrane Filtration Resistance and Analysis of the Deposit Cake on the Membrane	43
3.2.4.	Longer Operation with Periodical Cleaning (Run 3-4)	45
3.2.5.	Substances Causing the Irreversible Membrane Fouling in the Operation of the BMR	50
3.2.6.	Estimation of the Magnitude and the type of the Filtration Resistance Induced by Nitrifiers (Run 3-5)	55
3.2.7.	Experiment Using the Feed Water Pre-treated with the Same Membrane	60
3.3.	Summary	65

<b>CHAPTER FOUR – EFFICIENT CLEANING METHOD FOR THE NOVEL</b>		
<b>BIOFILM-MEMBRANE REACTOR (BMR)</b>		<b>69</b>
4.1.	Simultaneous Oxidation of $\text{NH}_4^+\text{-N}$ and Removal of Suspended Solids Employing the Dead-end Filtration Mode (Run 4-1)	69
4.2.	Modification of the Operating Method for Simultaneous Oxidation of $\text{NH}_4^+\text{-N}$ and Removal of Suspended Solids	72
4.3.	Simultaneous Oxidation of $\text{NH}_4^+\text{-N}$ and Removal of Suspended Solids with the Modified Operation	74
4.4.	Summary	81
 <b>CHAPTER FIVE – KINETIC ANALYSIS OF NITRIFYING BIOFILM</b>		
<b>DEVELOPED IN THE NOVEL</b>		
<b>BIOFILM-MEMBRANE REACTOR (BMR)</b>		<b>84</b>
5.1.	The Conventional Biofilm Model	85
5.2.	Verification of the Feasibility of the Conventional Biofilm Model	88
5.2.1.	Limitation with the Conventional Model	88
5.2.2.	Materials and Methods	89
5.2.3.	Comparison between the Model Calculation and the Microelectrode Measurement	91
5.2.4.	Analysis of Data Obtained in the Continuous Filter Run	96
5.3.	Summary	108

<b>CHAPTER SIX – PILOT SCALE STUDY OF THE NOVEL</b>	
<b>BIOFILM-MEMBRANE REACTOR (BMR)</b>	<b>111</b>
6.1. Materials and Methods	111
6.1.1. Characteristics of Raw Water	111
6.1.2. Experimental Apparatus	112
6.1.3. Experimental Conditions	114
6.1.4. Analytical Methods	114
6.2. Results and Discussion	115
6.2.1. Increase of the Transmembrane Pressure Difference	115
6.2.2. $\text{NH}_4^+$ -N Oxidation Efficiency	121
6.2.2.1. Time Course Change of Nitrification	121
6.2.2.2. Application of the Biofilm Model to the Pilot Study	123
6.2.3. Removal of Other substances	124
6.2.3.1. Humic Substances expressed by E260	124
6.2.3.2. AOC	127
6.2.3.3. Metals	128
6.3. Summary	132
<b>CHAPTER SEVEN – SUMMARY AND CONCLUSION</b>	<b>136</b>
7.1. Summary	136
7.2. Considerations for full scale application	139
7.3. Conclusion	140

---

# CHAPTER

## 1

---

### INTRODUCTION

#### 1.1. THE PRESENT STATE OF WATER USE IN JAPAN

In Japan, water works and sewage system have been widespread through the 20th century. The spread of these water systems has contributed significantly to the improvement of epidemic safety. However, we are now faced with severe water shortages and water pollution problems. So far, the increase of the population and the demand for tap water has been satisfied with the expansion of water collective basin by constructing dams and long distance water transport systems. However, the adoption of this kind of strategy for water supply is now becoming considerably more difficult in many regions. As a result, precipitation below normal can easily cause water shortage problems in many areas. Table 1-1 shows the major water shortage incidents that occurred recently in Japan (Ministry of Construction, the government of Japan, 1998). In addition, the excessive expansion of water collective basin has brought about the undesirable situation that water works have to take raw water from water courses that are effected by pollution, for instance wastewater from other cities. The supply of tap water to the population is, consequently, becoming a problem, quantitatively as well as qualitatively.



## 2 Introduction

Table 1-1 Recent incidents of water shortage in Japan.

	regeon		water supply restriction	
	Location	River	period	duration
1994	in and around Tokyo	Tone-gawa	Jul. 22-Sep. 8 (excepting Aug. 16-Aug. 30)	41 days
		Ara-kawa	Aug. 17-Aug. 21	5 days
	in and around Kamagori	Toyo-kawa	Jun. 16-Oct. 24	131 days
	in and around Nagoya	Kiso-gawa	Jun. 9-Nov. 13	158 days
	in and around Tokai cities along Yodo-gawa (Osaka etc.)	Kiso-gawa	Jun. 1-Nov. 13	166 days
		Yodo-gawa	Aug. 22-Oct. 4	44 days
	in and around Takamatsu	Yoshino-gawa	Jun. 29-Aug. 19 Aug. 31-Nov. 14	128 days
Fukuoka	Chikugo-gawa	Aug. 4-May 31(1995)	295 days	
1995	in and around Kamagori	Toyo-kawa	Aug. 11-Apr. 1(1996)	234 days
	in and around Nagoya	Kiso-gawa	Aug. 25-Mar. 18(1996)	207 days
	in and around Tokai	Kiso-gawa	Aug. 22-Mar. 18(1996)	210 days
	in and around Takamatsu	Yoshino-gawa	Mar. 10-Apr. 28	50 days
			Sep. 6-Oct. 23 Dec. 8-May 21(1996) (excepting Jan. 15-Jan. 18, Mar. 1- Mar. 5, Mar. 15-Apr. 10, Apr. 15-Apr. 26, May 1-May 21(1996))	48 days 166 days
1996	in and around Tokyo	Tone-gawa	Jan. 12-Mar. 27 (excepting Mar. 17-Mar. 27)	76 days
			Aug. 16-Sep. 25	41 days
	Kanagawa prefecture	Sagami-gawa	Feb. 26-Apr. 24	59 days
			Jul. 5-Jul. 23	19 days
	in and around Kamagori	Toyo-kawa	May. 8-Jul. 9	63 days
			Aug. 9-Dec. 5	119 days
	in and around Nagoya	Kiso-gawa	May. 31-Jun. 26	27 days
Aug. 14-Aug. 29			16 days	
in and around Tokai	Kiso-gawa	May. 31-Jun. 25	26 days	
		Aug. 14-Aug. 16	3 days	
in and around Takamatsu	Yoshino-gawa	Sep. 30-Dec. 5	67 days	
1997	in and around Tokyo	Tone-gawa	Feb. 1-Mar. 25 (excepting Mar. 23-Mar. 25)	53 days
	in and around Kamagori	Toyo-kawa	Mar. 28-May. 17	61 days

The present Japanese water quality standard that is regulating the effluent from the wastewater treatment plant, is determined based on the assumption that the receiving water body has 10 times more water volume than the effluent volume. Many rivers have, however, poor quantity of water flows in the middle and lower sections. This is due to the exploitation of water resources in the upper stream area, the increase of non-permeable ground area leading to the direct out flow of rainfall, the discharge of municipal wastewater at seaside as well as other factors. Under these circumstances, it is difficult to achieve sufficient water volume for the dilution effect in the receiving water body. For instance, in a small river running through Tokyo (Kanda river), treated municipal wastewater effluents account for 96 % of the water flowing at dry weather flow (Matsuo, 1999).

Table 1-2 shows annual water balance in Japan on the macroscopic level (Secretary to the Minister of State for National Land Agency, the government of Japan, 1998). As seen from the table, about 10 % of the theoretical maximum water quantity to be used (as defined in Table 1-2) is already consumed in the cities and the same quantity of water is discharged as wastewater. In Japan, most of the precipitation is seen in the rainy season and when Typhoons are occurring. This means that most of the precipitation would flow out to the ocean without being utilized. Consequently, from a macroscopic point of view, it is quite understandable that it is quite difficult to reserve sufficient quantity (e.g. 10 fold to the wastewater) of "natural" water for the dilution of the wastewater discharge throughout the year.

In order to solve the problems mentioned above, strict preservation of water collective basin for drinking water

Table 1-2 Macroscopic annual water balance in Japan.

Theoretical water quantity to be used (average of 1966-1995)	approx. $4.2 \times 10^{11}$ m <sup>3</sup> /year
Theoretical water quantity to be used in water shortage year	approx. $2.8 \times 10^{11}$ m <sup>3</sup> /year
Water consumed in the cities (1995)	approx. $3.2 \times 10^{10}$ m <sup>3</sup> /year
Water utilized for agriculture	approx. $5.9 \times 10^{10}$ m <sup>3</sup> /year

Theoretical water quantity to be used is defined as:

$$(\text{precipitation (m}^3/\text{m}^2/\text{year)} - \text{evaporation (m}^3/\text{m}^2/\text{year)}) \times \text{water collective basin (m}^2)$$

production and development of more efficient water treatment technologies, are needed. One has to take into consideration of the established right of farmers to take water. Sometimes there is plenty of water in a river when a near city is suffering from a severe water shortage. The city cannot use the river water in many cases. This is because a certain part of the river water is traditionally protected as the farmer's water. Educational activity aimed at cutting down the water consumption is important, too. These efforts may contribute significantly, however, they cannot resolve the problems completely.

The dual water distribution system has been proposed for the drastic change in the water metabolism in a city (Tambo, 1976, Watanabe, 1999). Fig. 1-1 shows the concept of the new water metabolic system. In addition to the existing water distribution network, a new distribution network has to be constructed for supplying extremely purified water. Nowadays in Japan, one person uses 400 liters of tap water a day on average (Environment Agency, the government of Japan, 1999). Within the

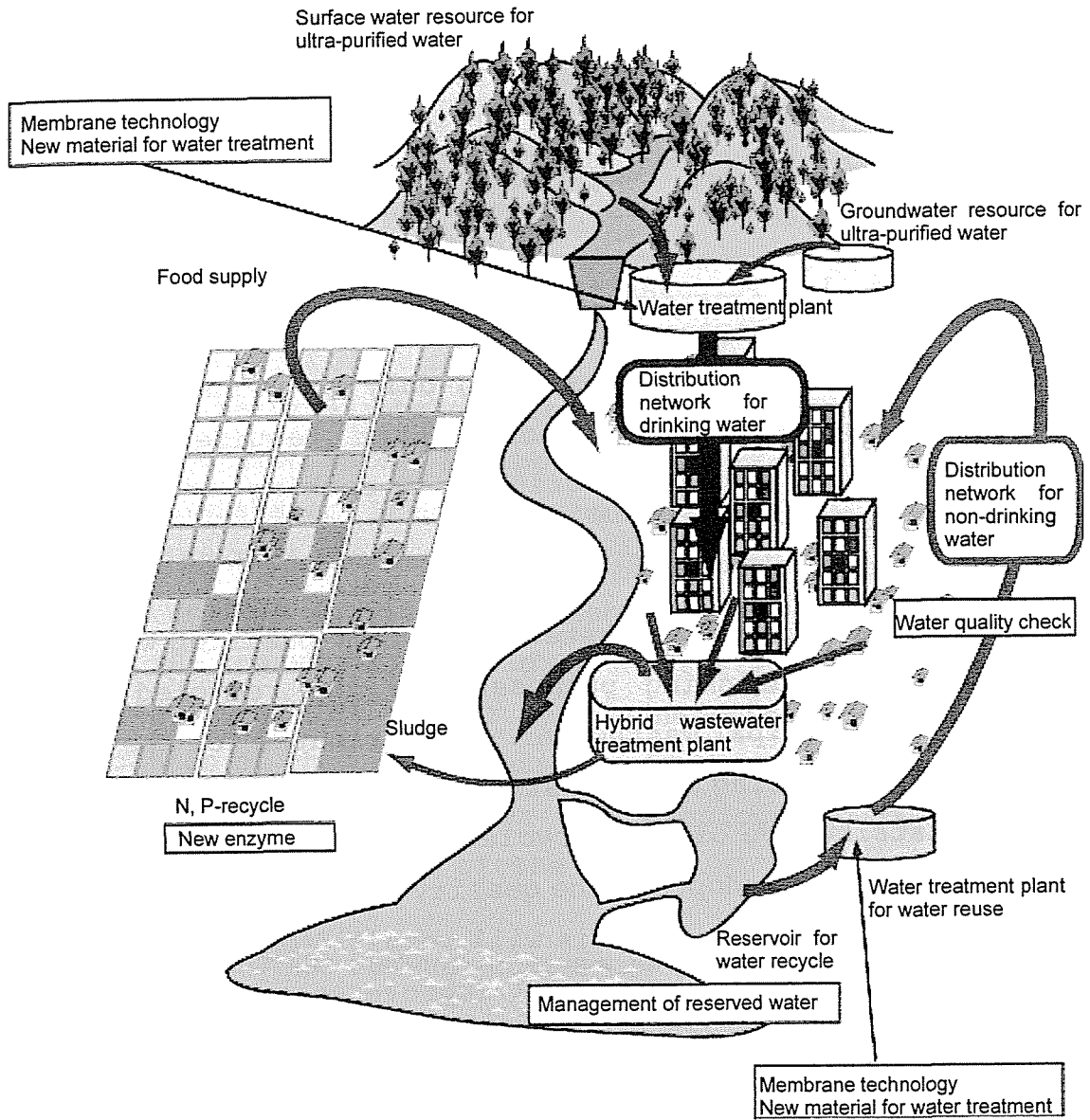


Fig. 1-1 New water metabolic system in a city.

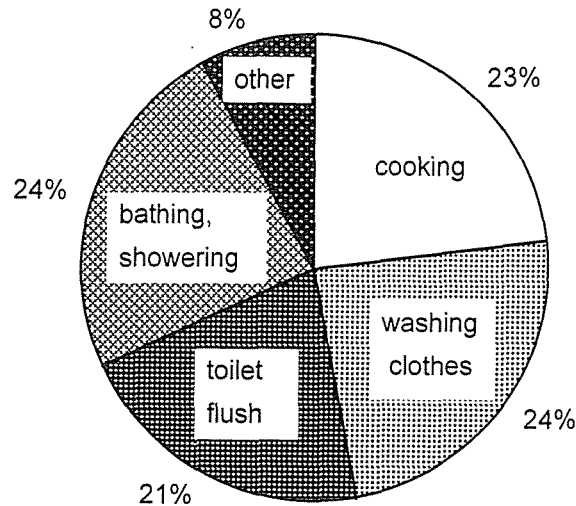


Fig. 1-2 Purposes of water use in a typical Japanese family (Matsuo, 1999).

400 liters of tap water consumption, only about one fourth of the water is used for purposes that require advanced purification such as that for drinking or cooking, see Fig. 1-2 (Matsuo, 1999).

Through the new dual water system, the ultra-purified water is distributed for drinking purposes and the recycled water created from municipal wastewater is distributed for the other purposes. The existing water distribution system is still used for the distribution of the recycled water. If this new water metabolic system is adopted, the quality of drinking water will be significantly improved. This will result from the fact that the quality of the raw water will improve as a result of the decrease of the size of the required water collective basin since consumption of the ultra-purified water would not be large.

Polluted water existing in the middle or lower sections of the water course, would not have to be used for drinking water any more. In addition, an improved dilution effect in the environment as the result of the decrease of the net water

consumption is to be expected.

Finding ample land for new water recourse development including the construction of dams is becoming increasingly difficult. This kind of development is not favored due to its environmental impact. "Expansion" or "consumption" oriented water resource plans can never change the situation and only postpone the problem. In the dual water system described above, the municipal wastewater treatment plant is considered as the new water resource that always has a water quantity approximately equal to the consumed quantity. The dual system would be a reasonable solution of the problems concerned with water.

However, it naturally takes a long time (e.g. 50-100 years) to construct a new water metabolic system such as the dual distribution system. It actually took about a century to prepare the existing Japanese water system. Therefore, the research in water and wastewater engineering should focus on the themes that can fill the gap between the old and new systems or on the topics that can be "seeds" in the next generation. For instance, modification of the conventional rapid sand filtration system is an example of the former and development of membrane technology is an example of the latter.

## **1.2. THE PRESENT AND FUTURE PROBLEMS OF THE JAPANESE WATERWORKS**

As described in the previous section, many of the waterworks in Japan have to use polluted raw water and therefore the importance of the preservation of the water collective basin has been recognized. Thus the rule for the preservation of drinking water sources was formed in February 1994. This rule provides the framework for the activities to improve water quality especially in the upper stream of the water intake point,

including the construction of wastewater treatment facilities, dredging and so on. With this legal support, improvement of the raw water quality was expected. However, this rule has not been utilized to its full potential. Only 11 waterworks had requested the application of the rule until the end of 1998 (Environment Agency, the government of Japan, 1999). Far from the water quality improvement, deterioration of surface water quality is recently reported particularly in mega-cities such as Tokyo or Osaka (Ministry of Construction, the government of Japan, 1998). Nevertheless, rapid improvement of raw water quality is improbable, the demand for the safety and taste of tap water is still growing.

Under these circumstances, ammonia nitrogen ( $\text{NH}_4^+\text{-N}$ ) is one of the problematic substances. Rapid sand filtration system (coagulation, sedimentation, sand filtration and disinfection) is widely used in Japan. They cannot remove  $\text{NH}_4^+\text{-N}$ , however.  $\text{NH}_4^+\text{-N}$  increases the chlorine demand and creates undesirable disinfection by-products (DBPs) such as trihalomethene. In addition, chlorine reacts with  $\text{NH}_4^+\text{-N}$  to produce chloramines which deteriorate the taste of tap water (Nabeta and Nishikawa, 1997). In order to reduce the production of the DBPs, chloramins are employed in USA as the disinfection agent instead of free chlorine. However, this procedure would not be adopted in Japan because of the taste problem associated with it. There are also reports indicating that the chloramines themselves promote cancer (Duddles *et al.*, 1994; Bull *et al.*, 1990).

In the Netherlands, some water suppliers have already abandoned post-chlorination in order to prevent the formation of halogenated organic compounds (van der Kooji *et al.*, 1999). Abandoning chlorine disinfection can diminish the  $\text{NH}_4^+\text{-N}$

problems described above. However, distributed water containing  $\text{NH}_4^+\text{-N}$ , allows the growth of nitrifying bacteria on the surface of the distribution pipe, which allows heterotroph growth that utilizes the organic substances secreted by the nitrifiers (Rittman and Brunner, 1984, Wilzac *et al.*, 1996). Biomass development in the distribution system not only decreases the microbiological safety of tap water, but also adds an unpleasant taste and/or odor to the water (Allen *et al.*, 1980). For the reduction of  $\text{NH}_4^+\text{-N}$  concentration, breakpoint chlorination has so far been the dominating method in Japan. Since the breakpoint chlorination is accompanied by an increase of DBPs or the deterioration of taste, a biological process such as biological activated carbon (BAC) is expected to be preferred in the future. However, the detachment and leakage of bacteria from the activated carbon surface (AWWA Committee Report, 1981; Stringfellow *et al.*, 1993) may cause other problems.

In addition to the  $\text{NH}_4^+\text{-N}$  related problems mentioned above, the pollution of drinking water sources with chlorine resisting pathogenic microorganisms such as *Cryptosporidium* or *Giardia* has become a serious problem in Japan. In a recent survey conducted by Ministry of Health and Welfare, the government of Japan, *Cryptosporidium* and *Giardia* was detected in samples from 6 watersheds (8 sampling points) and 16 watersheds (24 sampling points) out of 94 watersheds (277 sampling points), respectively (Kitazawa *et al.*, 1999). For the control and removal of these pathogenic microorganisms, it is clearly important to regulate the finished water more stringently. However, from a practical point of view, it is impossible to enumerate *Cryptosporidium* or *Giardia* in the finished water frequently, especially in local and small waterworks since the detection of such microorganisms requires well-skilled analysts and a lot of time. Although Ministry of Health and



Welfare, the government of Japan, has instructed the waterworks to maintain the turbidity unit (TU) of the finished water below 0.1, as a measure to prevent the outbreak of *Cryptosporidium*, it is considerably difficult to measure turbidity exactly at such a low concentration range. In a study focused on the direct measurement of the particle numbers in the sand-filtered water (Hayashi, 1999), particles as large as 3-7  $\mu\text{m}$  (representative of *Cryptosporidium*) leaked from the filter at the order of  $10^4$  particles/L even when the TU of the filtered water was maintained less than 0.1. Considering that the concentration of *Cryptosporidium* in the finished water should be less than  $10^0$  oocysts/L, it can be concluded that the conventional sand filter is insufficient to control the *Cryptosporidium* outbreak, as pointed out by Rose (1990).

The membrane process has received a lot of attention recently due to its extremely high solid-liquid separation efficiency. The efficiency is so high that the membrane system can remove *Cryptosporidium* or *Giardia* almost completely (Jacangelo et al., 1995). Several full-scale membrane filtration plants for drinking water treatment have recently been installed in the USA, France, England, the Netherlands, Norway, South Africa, Japan and Australia. Wiesner et al. (1994) estimated costs of ultrafiltration and nanofiltration processes and compared it with the cost of conventional solid-liquid separation for small facilities. They concluded that costs of membrane processes were lower compared with conventional treatment for small facilities (<200,000  $\text{m}^3/\text{d}$ ). Additionally, membrane technology has the potential to reduce concentration of DBPs, both by reduction of natural organic matter (the DBP precursors) and by limiting the amount of chemical reagent needed for disinfection. Thus, the membrane technology is very promising, however, it cannot remove  $\text{NH}_4^+\text{-N}$  efficiently.

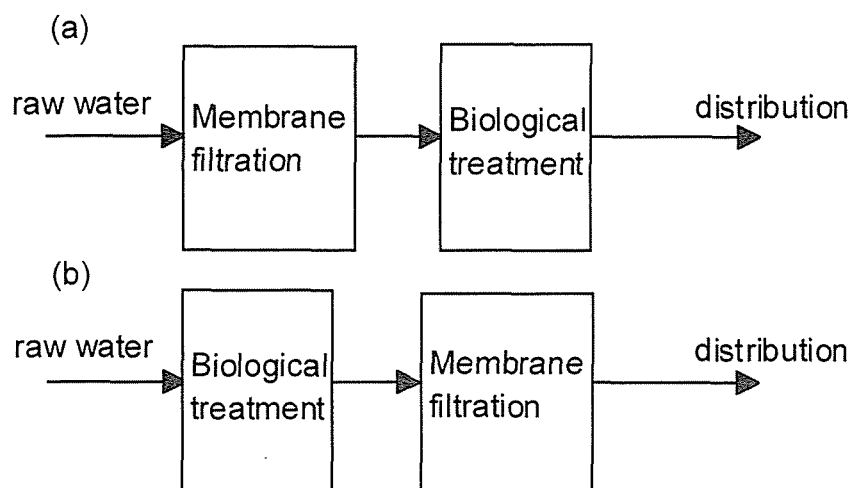


Fig. 1-3 Combination of membrane filtration and biological treatment.

### 1.3. COMBINATION OF A BIOLOGICAL PROCESS FOR $\text{NH}_4^+\text{-N}$ OXIDATION AND MEMBRANE FILTRATION FOR SOLID-LIQUID SEPARATION

As stated in the previous section, both the oxidation of low concentrations of  $\text{NH}_4^+\text{-N}$  and the strict solid-liquid separation are strongly needed in the future drinking water treatment. In order to achieve this goal, the combination of a biological process and membrane filtration seems to be adequate. It is of importance, however, how these two processes are combined. The simplest way is by installing a biological process stage such as a biological activated carbon (BAC) filter, prior or subsequent to a membrane filtration stage (See Fig. 1-3 (a), (b)). This kind of process combination has one distinct advantage in that the operating conditions of the two processes can be controlled individually. It would, however, result in a complicated operating procedure and would require large space. This diminishes the merits that the membrane technology itself has. Additionally, the arrangement of biological process subsequent to membrane shown in Fig. 1-3 (a) will cause bacteria leakage from the biological process. If possible, biological

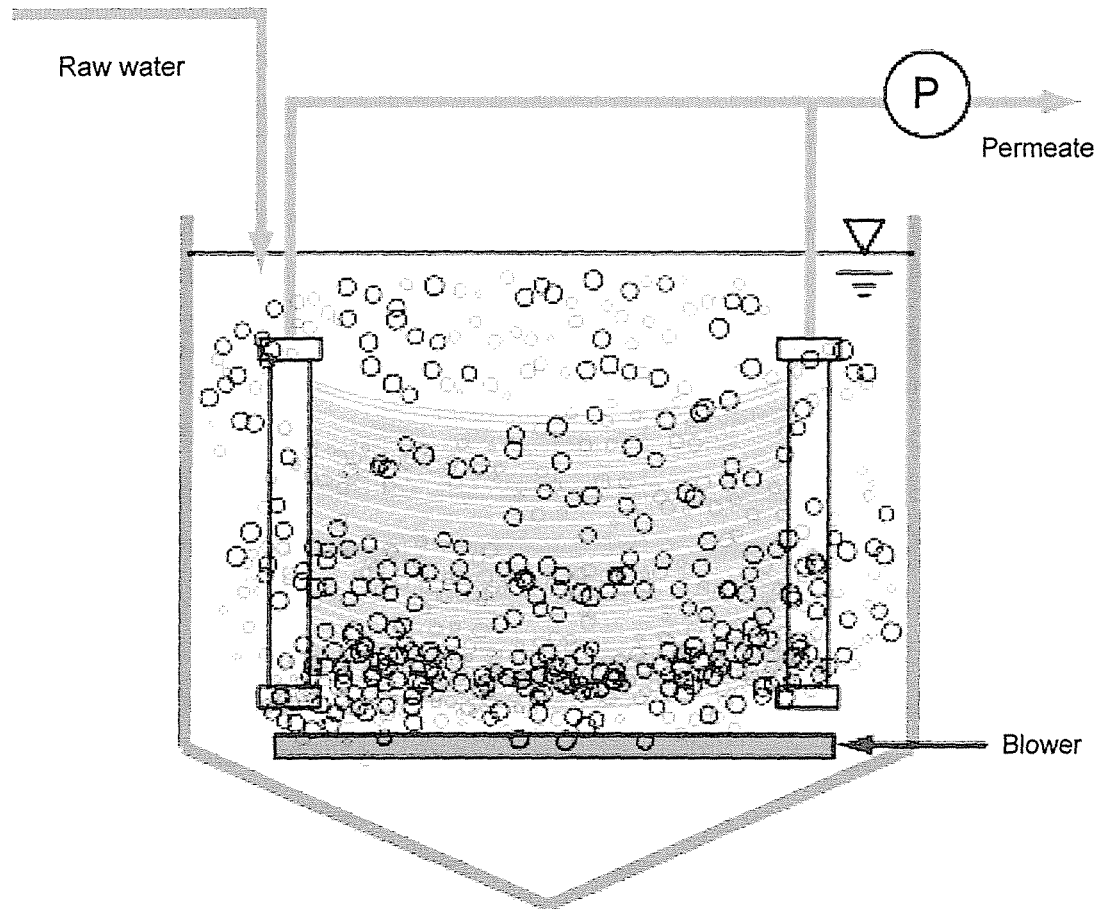


Fig. 1-4 Submerged membrane configuration.

treatment and membrane filtration should be integrated into one reaction tank.

When integrating both biological treatment and membrane filtration into one reactor, the crossflow membrane configuration is not efficient because it requires circulation of raw water. The submerged membrane configuration (shown in Fig. 1-4) may be more adequate for this design. Several studies have been done to examine the use of the submerged membrane for the integration, mostly aimed for industrial and municipal wastewater treatments (Kayawake *et al.*, 1991; Shimizu *et al.*, 1996; Ueda *et al.*, 1997; Bouhablia *et al.*, 1998). This kind of combination of the processes is referred as integrated membrane bioreactor (MBR) (Manem and Sanderson, 1996). In the operation

of integrated MBR, suspended biomass is usually utilized. Aeration is implemented vigorously inside the reactor in order to supply oxygen to the biomass, mix the liquid well and give shear stress on the membrane surface for membrane cleaning and fouling prevention.

It is not feasible, however, to apply the conventional integrated MBR configuration directly to the oxidation of low concentration of  $\text{NH}_4^+\text{-N}$  in drinking water treatment. Although the amount of biomass required for the oxidation of low concentration of  $\text{NH}_4^+\text{-N}$  is supposed to be small, a lot of energy would be consumed through the aeration to disperse that small quantity of biomass uniformly inside the reactor. In order to maintain a sufficient population of the slow-growing  $\text{NH}_4^+\text{-N}$  oxidizers (nitrifiers) in the MBR, the dead-end filtration mode must be employed, resulting in a water recovery rate close to 100%. The raw water usually contains suspended particles, however, that can be retained inside MBR. If the retained particles accumulate on the membrane surface, deterioration of the membrane permeability will occur. Additionally, the particles retained in the reactor (sludge) would have to be discarded at appropriate intervals, and it is quite difficult, therefore, to keep required nitrifiers selectively within MBR.

In order to solve the problems described above, the author proposes a novel bio-membrane process for the integration of biological oxidation of low concentrations of  $\text{NH}_4^+\text{-N}$  and membrane filtration. The principle of the process is shown in Fig. 1-5. The small amount of nitrifying bacteria that is required for the oxidation of low concentrations of  $\text{NH}_4^+\text{-N}$ , is fixed on the membrane surface creating an attached biomass that acts similar to a biofilm. Raw water passes through the biofilm prior to the membrane separation. Thus simultaneously, membrane

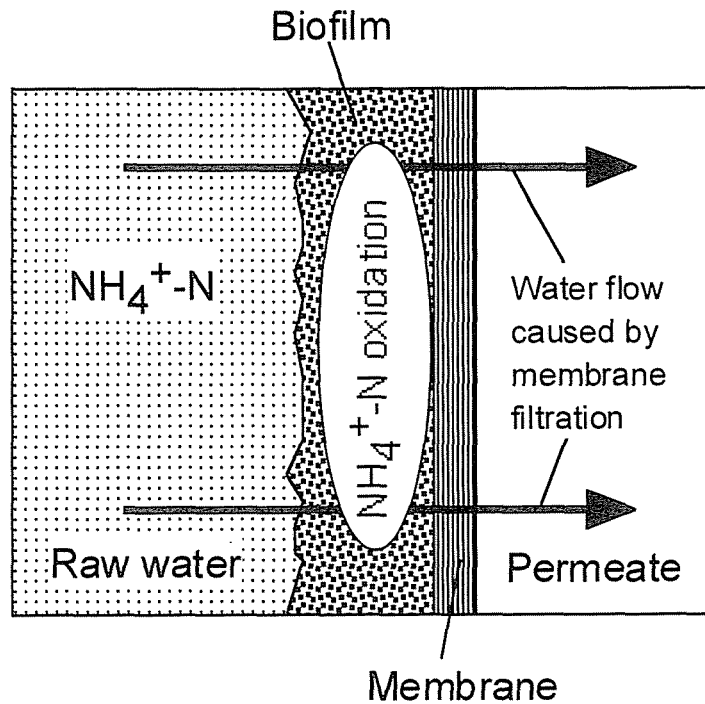


Fig. 1-5. A novel biofilm-membrane process for ammonia oxidation in low concentrations.

filtration and biological oxidation of  $\text{NH}_4^+\text{-N}$  can be performed in one reactor. In this process, nitrifiers can be held inside the reactor even without implementing the dead-end filtration. Consequently, the membrane permeability can be kept higher even when the raw water contains suspended particles. There have been several attempts to fix biofilms on the membrane surface for water or wastewater treatment. However, in all of them, membrane was used only as the substratum through which the liquid or gas required for the bacterial metabolism could be provided (Rothemund *et al.*, 1994; Freitas dos Santos and Livingston, 1995; McCleaf and Schroeder, 1995; Brindle *et al.*, 1998). To the knowledge of this author, the novel process proposed in this thesis is the first attempt to filtrate through both membrane and biofilm fixed on it, and consequently, it is an original water treatment process.

In this doctoral thesis, the performance and feasibility of the novel biofilm-membrane reactor (BMR) is examined through experiments considering the application of this process to drinking water treatment with  $\text{NH}_4^+$ -N problems. This thesis is composed of the chapters listed below;

CHAPTER 2.

AN ANALYSIS OF THE POTENTIAL OF USING THE ROTATING MEMBRANE DISC MODULE AS THE NOVEL BIOFILM-MEMBRANE REACTOR (BMR)

CHAPTER 3.

MEMBRANE FILTRATION RESISTANCE IN THE NOVEL BIOFILM-MEMBRANE REACTOR (BMR)

CHAPTER 4.

EFFICIENT CLEANING METHOD FOR THE NOVEL BIOFILM-MEMBRANE REACTOR (BMR)

CHAPTER 5.

KINETIC ANALYSIS OF NITRIFYING BIOFILM DEVELOPED IN THE NOVEL BIOFILM-MEMBRANE REACTOR (BMR)

CHAPTER 6.

PILOT SCALE STUDY OF THE NOVEL BIOFILM-MEMBRANE REACTOR (BMR)

CHAPTER 7.

SUMMARY AND CONCLUSIONS

REFERENCES

Allen M. J., Taylor R. H. and Geldreich E.E. (1980) The occurrence of microorganisms in water main encrustations. *Jour. AWWA.* 72(11), 614-625.

AWWA Committee Report. (1981) An assessment of microbial activity on GAC. *Jour. AWWA.* 73(8), 447.

Bull R. J., Gerba C. and Trussel R. R. (1990) Evaluation of the

health risks associated with disinfection. *Crit. Rev. Envir. Control* **20**, 77-114.

Bouhablia E. H., Aïm R. B. and Buisson H. (1998) Microfiltration of activated sludge using submerged membrane with air bubbling (application to waste water treatment). *Desalination* **118**, 315-322.

Brindle K., Stephenson T. and Semmens M. J. (1998) Nitrification and oxygen utilization in a membrane aeration bioreactor. *Jour. of Mem. Sci.* **144**, 197-198.

Duddles A. G., Richardson E. S. and Barth I. E. (1974) Plastic medium trickling filters for biological nitrogen control. *J. WPCF.* **46**, 937-946.

Environment Agency, the government of Japan (1999) *Quality of the Environment in Japan 1998* (in Japanese).

Freitas dos Santos L. M. and Livingston A. G. (1995) Novel membrane bioreactor for detoxification of VOC wastewaters: biodegradation of 1,2-dichloroethane. *Wat. Res.* **29**(1), 179-194.

Kayawake E., Narukami Y. and Yamagata M. (1991) Anaerobic digestion by a ceramic membrane enclosed reactor. *Jour. of Fermentation and Bioengineering* **71**, 122-125.

Hayashi M. (1999) High efficient type advanced water treatment system -The effect of suspended solid on granular activated carbon filtration-. Master thesis, Hokkaido University, Sapporo, Japan.

Kitazawa H., Kunigane S. and Magara Y. (1999) Analysis of Cryptosporidium and Giardia surveillance data of water supply sources. *Jour. JWVA*. **68**(4), 22-31 (in Japanese).

Van der Kooij D., Van Lieverloo J. H. M., Schellart J. A. and Hiemstra P. (1999) Distributing drinking water without disinfectant: highest achievement or height of folly? *J. Water SRT - Aqua* **48**(1), 31-37.

Manem J. and Sanderson R. (1996) Membrane bioreactors. in *Water treatment: Membrane process* (Mallevalle J., Odendaal P. E. and Wiesner M. R. eds.), McGraw-Hill, New York

Matsuo T. (eds.) (1999) *Water Environmental Engineering*, Ohmu-sha, Tokyo (in Japanese)

McCleaf P. R. and Schroeder E. D. (1995) Denitrification using a membrane-immobilized biofilm. *Jour. AWWA*. **87**(3), 77-86.

Ministry of construction, the government of Japan (1998) *White paper on Construction 1997* (in Japanese).

Nabeta Y. and Nishikawa M. (1997) A causing substance of chlorious odor and its reduction. *Jour. JWVA*. **66**(4), 16-23 (in Japanese).

Rittman B. E. and Brunner C. W. (1984) The non-steady-state biofilm process for advanced organic removal. *Jour. WPCF*. **56**, 874-880.

Rose J. B. (1990) Occurrence and control of Cryptosporidium in drinking water. in *Drinking Water Microbiology* (McFeters G. A. (eds.)), Springer-Verlag, New York



Rothmund C., Camper A. and Wilderer P. A. (1994) Biofilms growing on gas permeable membranes. *Wat. Sci. Tech.* **29**(10-11), 447-454.

Secretary to the Minister of State for National Land Agency, the government of Japan (1998) *Water resource in Japan* (in Japanese).

Stringfellow W. T., Mallon K. and DiGiano F. A. (1993) Enumerating and disinfecting bacteria associated with particles released from GAC filter- adsorbers. *Jour. AWWA.* **85**(9), 70-80.

Tambo N. (1976) Structures and capacities of water metabolic systems. *Jour. JWWA.* No. 497, 16-34 (in Japanese).

Watanabe Y. (1999) Development of new urban water metabolic system based on quality requirement. *Proceedings of the 1st symposium on "Social Systems for Better Environment Performance" supported by Core Research for Evolutional Science and Technology (CREST) of Japan Science and Technology Corporation (JST)* (in Japanese).

Wilzac A., Jacangelo J. G., Marcinko J. P., Odell L. H., Kimeyer G. J. and Wolfe R. L. (1996) Occurrence of nitrification in chloraminated distribution systems. *Jour. AWWA.* **88**(7), 74-85.

---

# CHAPTER

## 2

---

### **AN ANALYSIS OF THE POTENTIAL OF USING THE ROTATING MEMBRANE DISK MODULE AS THE NOVEL BIOFILM-MEMBRANE REACTOR (BMR)**

In this chapter, the results from some introductory experiments will be given, in which rotating membrane disk module was tested with respect to its applicability as the novel biofilm-membrane reactor (BMR) proposed through this thesis. First, however, the experimental set-up and methods shall be explained.

#### **2.1. THE ROTATING MEMBRANE DISK MODULE**

In this study, a rotating membrane disk module was employed as the BMR described in Chapter 1. Fig. 2-1 shows the water collection mechanism of the rotating membrane disk (Ohkuma et al., 1994). Two membranes covered the surface of a disk and the center of the disk was fastened to the shaft. Raw water was filtered by suction pressure and flowed between the disk and the membranes. The filtrate was collected in the shaft. This

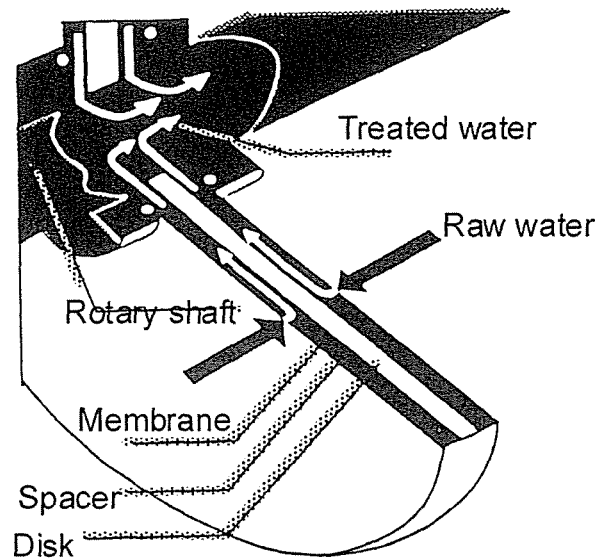


Fig. 2-1. Water collection mechanism in the rotary membrane disk.

type of membrane has been used in several studies recently (Engler and Wiesner, 2000; Dal-Cin *et al.*, 1998; Panham and Davis, 1995; Park *et al.*, 1994) and has already been employed in night soil treatment actually in Japan (Ohkuma *et al.*, 1994).

Crossflow filtration using hollow fiber or tubular membrane is most commonly employed in various types of water and wastewater treatment. In a crossflow filtration system, raw water must be pressured and circulated at high speed in order to produce sufficient velocity along the membrane to prevent accumulation of particles on the membrane surface. This kind of membrane configuration has, however, one distinct drawback, namely that the circulation consumes a lot of energy and requires large space. In the rotating membrane disk module, the fluid velocity along membrane surface is produced by the membrane movement (rotation), which is contrary to the crossflow configuration. Ohkuma *et al.* (1995) confirmed that the energy consumption rate

Table 2-1. Specification of the membrane module.

Volume	10 liters
Diameter of disk	210 mm
Area of membrane	0.3 m <sup>2</sup>
Material of membrane	polysulfone
Cut-off molecular weight of membrane	750000

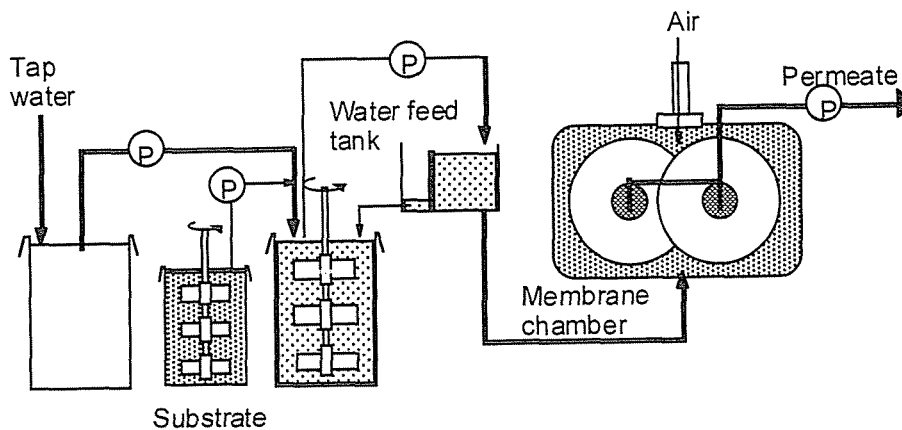


Fig. 2-2. Flow chart of the experimental installation.

of the rotating membrane disk module was low compared with the crossflow tubular module. The rotating membrane disk module does not need the land space for the circulation.

The specifications of the membrane module used in the experiment are shown in Table 2-1. The employed UF membrane is manufactured by Nitto Denko Corp. (Osaka, Japan). The filtration rate (membrane flux) and the rotational speed of the disk can be fixed at arbitrary values.

Table 2-2. Weight ratio of nutrients added to the feed water.

NH <sub>4</sub> Cl	1.0g
NaHCO <sub>3</sub>	7.9g
K <sub>2</sub> HPO <sub>4</sub>	0.9g
MgSO <sub>4</sub> ·7H <sub>2</sub> O	1.3g
NaCl	0.9g

## 2.2. EXPERIMENTAL METHODS

### 2.2.1. Experimental apparatus

Fig. 2-2 shows a flow chart of the experimental installation. Photographs of the used equipment are also shown in Photos 2-1 and 2-2. Tap water was supplemented with NH<sub>4</sub><sup>+</sup>-N and basic minerals. Table 2-2 shows the composition of the nutrients added to tap water. The concentration of suspended solids in the feed water was negligible. Membrane flux was fixed by a microchip computer control. The feed flow rate was always equal to the permeate flow rate; this was achieved by maintaining the liquid level in the water feed tank the same as the level in the membrane chamber. Consequently, there was no overflow from the chamber. In other words, dead-end filtration was implemented. The membrane chamber was aerated to provide oxygen to nitrifiers. This resulted in a dissolved oxygen concentration (DO) in the chamber between 6.8-9.1 mg/L. There were no monitoring of temperature and pH, but in the membrane chamber water temperature varied in the range of 15.0 °C to 25.0 °C and, pH in the range of 6.9 to 7.8.

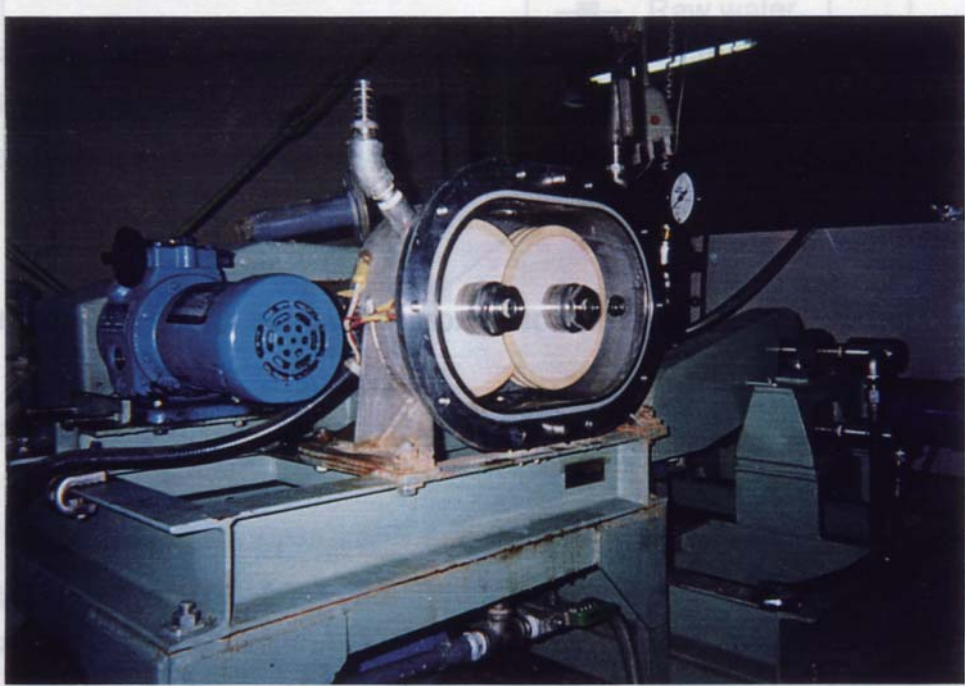


Photo. 2-1. Rotating membrane disk module.



Photo. 2-2. Membrane disk.

### 2.2.2. Analytical methods

The indophenol method (Scheiner, 1976) was applied for analyzing  $\text{NH}_4^+\text{-N}$ . The measurement of suspended solids was carried out following the method recommended by Japan Sewage Works Association (1984).

## 2.3. RESULTS AND DISCUSSION FROM INTRODUCTORY EXPERIMENTS

The experiments were carried out in order to evaluate the following questions:

- a. Evaluation of system applicability
- b. Evaluation of membrane flux on transmembrane pressure
- c. Evaluation of the influence of seeding sludge

### 2.3.1. Evaluation of system applicability (Run 2-1)

The rotating membrane disk module was seeded with activated sludge from a municipal wastewater treatment plant. After the acclimation to the inorganic substrate shown in Table 2-2 for 5 days, the sludge was put into the membrane chamber at the concentration of approx. 1000 mg-SS/L. This sludge was retained inside the membrane chamber due to the sieve effect of the membranes and the employment of the dead-end filtration mode. The membrane flux and the rotational speed of the disk was fixed at 1.0 m/d and 210 rpm, respectively.

After about 200 hours of operation, the transmembrane pressure increased to approx. 40 kPa and the attachment of biomass onto the membrane surface was observed. At this point, the suspended biomass in the reactor was discarded and the continuous

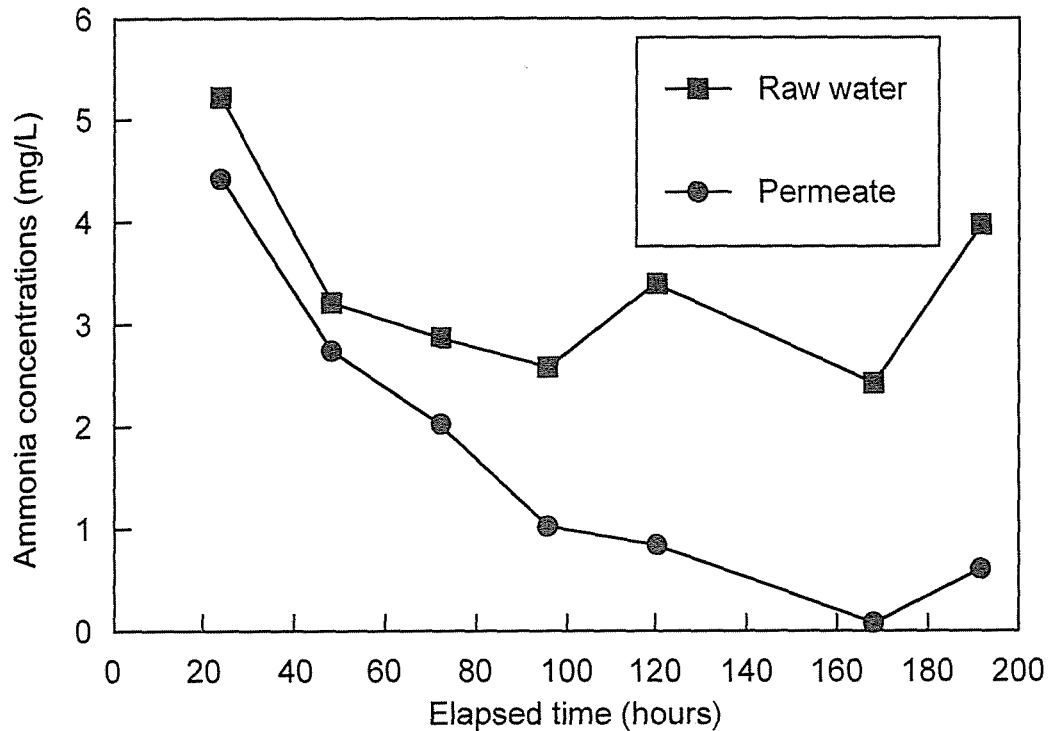


Fig. 2-3. Changes in concentrations of  $\text{NH}_4^+\text{-N}$  in Run 2-1.

operation (Run 2-1), which was aimed for the examination of the oxidation of  $\text{NH}_4^+\text{-N}$  with the fixed biomass on the membrane surface, was started. At the beginning of Run 2-1, the membrane flux and the rotational speed of the disk was re-fixed at 0.5 m/d and 50 rpm, respectively. The rotational speed was reduced in order to prevent detachment of the biomass. The hydraulic retention time (HRT) in the reactor was 100 minutes in Run 2-1.

The changes in the concentrations of  $\text{NH}_4^+\text{-N}$  in Run 2-1 are shown in Fig. 2-3. In the start of the run, only a little nitrification was observed presumably because the population of the nitrifiers in the biofilm was very small. As the operation was continued, the concentration of  $\text{NH}_4^+\text{-N}$  in the permeate decreased from about 5 mg  $\text{NH}_4^+\text{-N/L}$  in the raw water to below 0.1 mg  $\text{NH}_4^+\text{-N/L}$  after 170 operating hours. Fig. 2-4 shows the change in the transmembrane pressure difference in Run 2-1. In this thesis,



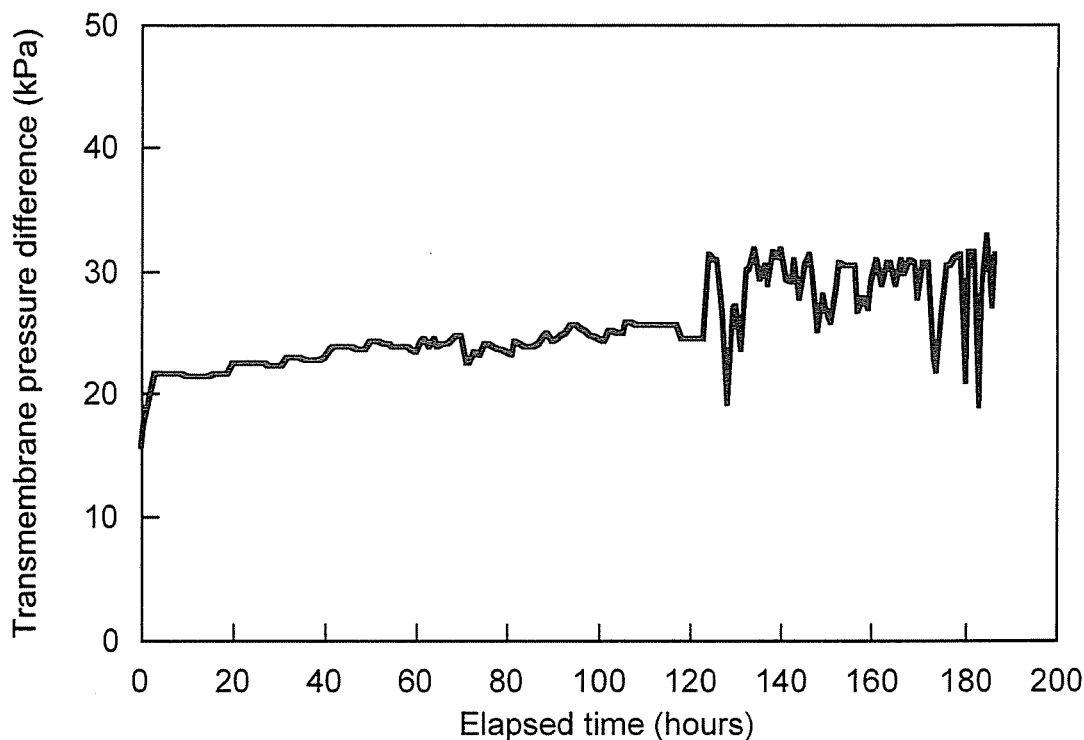


Fig. 2-4. Change in the transmembrane pressure difference in Run 2-1.

all the values of the transmembrane pressure difference are adjusted to the 20 °C equivalent value taking water viscosity into consideration. The filtration rate was set constant in this experiment, and consequently the pressure difference increased with the duration of the run due to the reduction of the membrane permeability caused by the particle build-up on the membrane as well as fouling. At the beginning of Run 2-1, the value of the pressure difference was already slightly higher (approx. 15 kPa.) than it would be after membrane cleaning. This was due to the fact some filtration had been implemented already before Run 2-1 started, as described above. In Run 2-1, the pressure difference increased slowly and the operation could be continued about 200 hours without any membrane cleaning.

This experimental run demonstrated that the system could work (i.e. remove  $\text{NH}_4^+\text{-N}$  in water).

### 2.3.2. Evaluation of membrane flux on transmembrane pressure development (Run 2-2)

At the end of the operation of Run 2-1, chemical cleaning of the membrane using NaClO was carried out. After stopping the suction pump and disk rotation, the membrane chamber was filled with the cleaning solution (500 ppm as free chlorine). The equipment was not touched for 24 hours at room temperature. By this cleaning, the membrane permeability was completely restored and the operation of Run 2-2 was conducted. The membrane flux was increased to 0.8 m/d, resulting in decrease of HRT from 100 minutes to 62.5 minutes. The rotational speed of the disk was maintained (50 rpm). At the beginning of Run 2-2, activated sludge taken from a municipal wastewater treatment plant was again seeded to the membrane chamber. The concentration of the sludge in the chamber was 450 mg-SS/L. The sludge seeded in Run 2-2 was not acclimated to the inorganic substrates.

The changes in the transmembrane pressure difference and the concentration of SS in the membrane chamber are shown in Fig. 2-5 and Fig. 2-6, respectively. With the decrease of SS concentration (mainly due to the attachment of biomass onto the membrane surface), the pressure difference increased. Compared to Run 2-1, the pressure difference increased more rapidly. This was probably due to the increase of the membrane flux from 0.5 m/d to 0.8 m/d. The characteristics of the sludge seeded at the beginning of the operation seemed also, however, to have a significant influence on the membrane fouling (this point will be discussed in detail in the next chapter). Fig. 2-7 shows the changes in the concentration of  $\text{NH}_4^+\text{-N}$  in Run 2-2. The concentration of  $\text{NH}_4^+\text{-N}$  in the feed water was controlled to be around 0.5 mg/L, a level similar to what you may find in Japanese

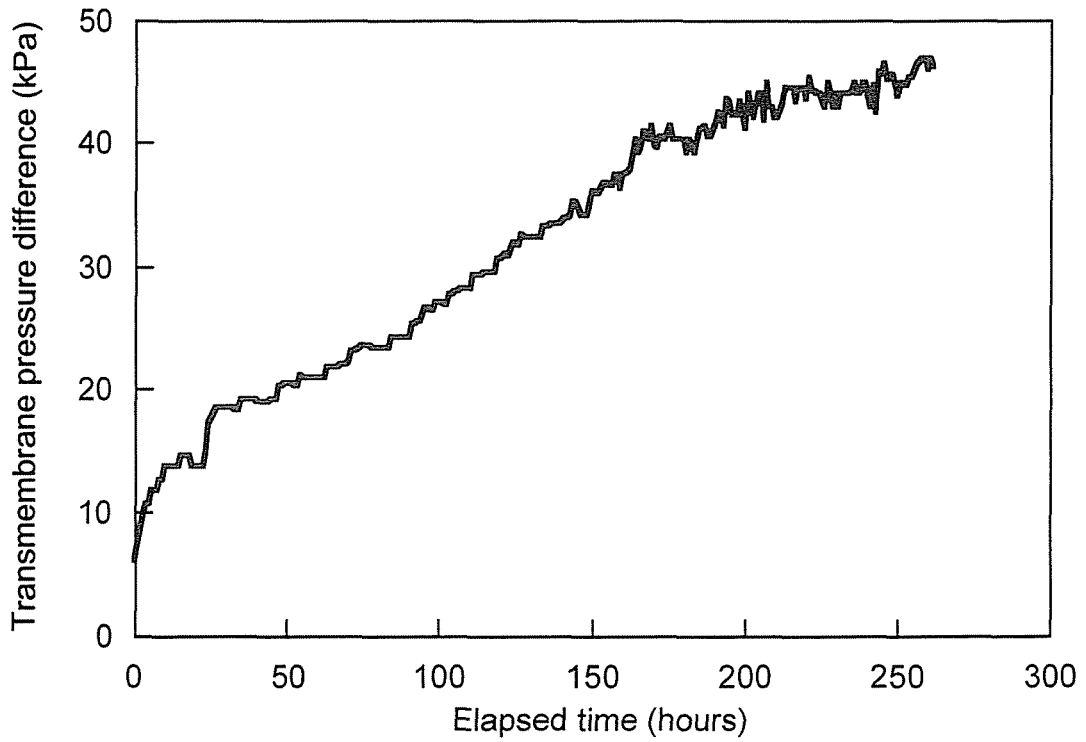


Fig. 2-5. Change in the transmembrane pressure difference in Run 2-2.

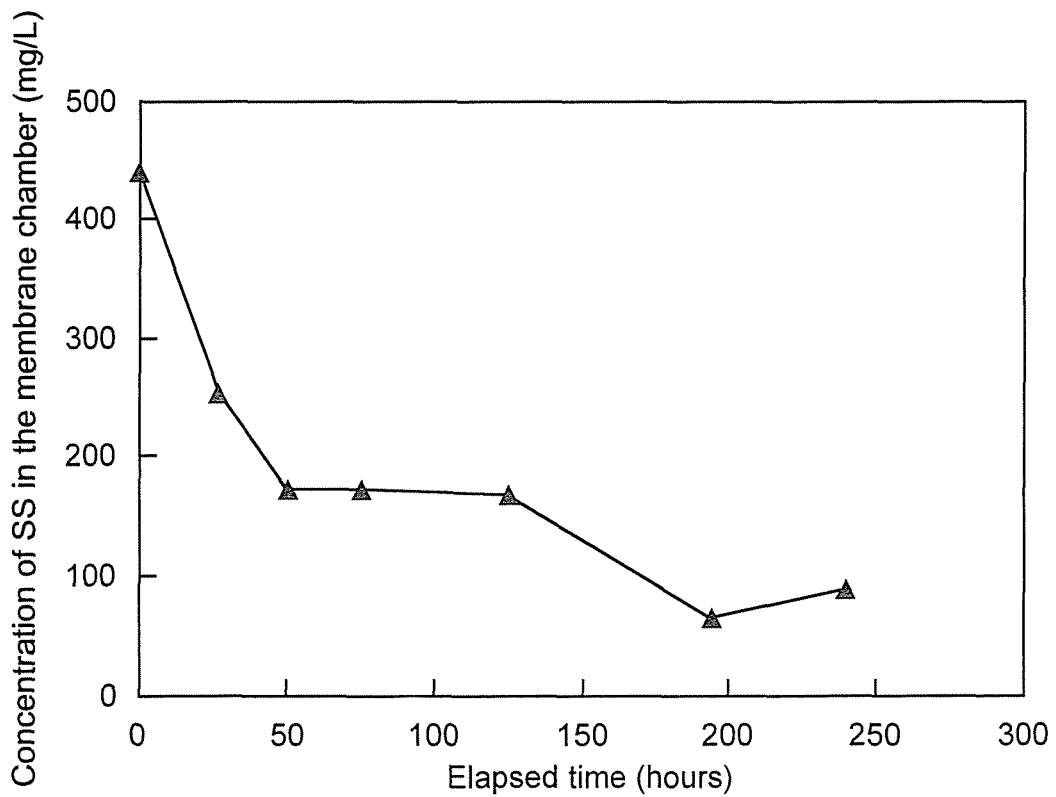


Fig. 2-6. Change in the concentration of SS in the membrane chamber in Run 2-2.

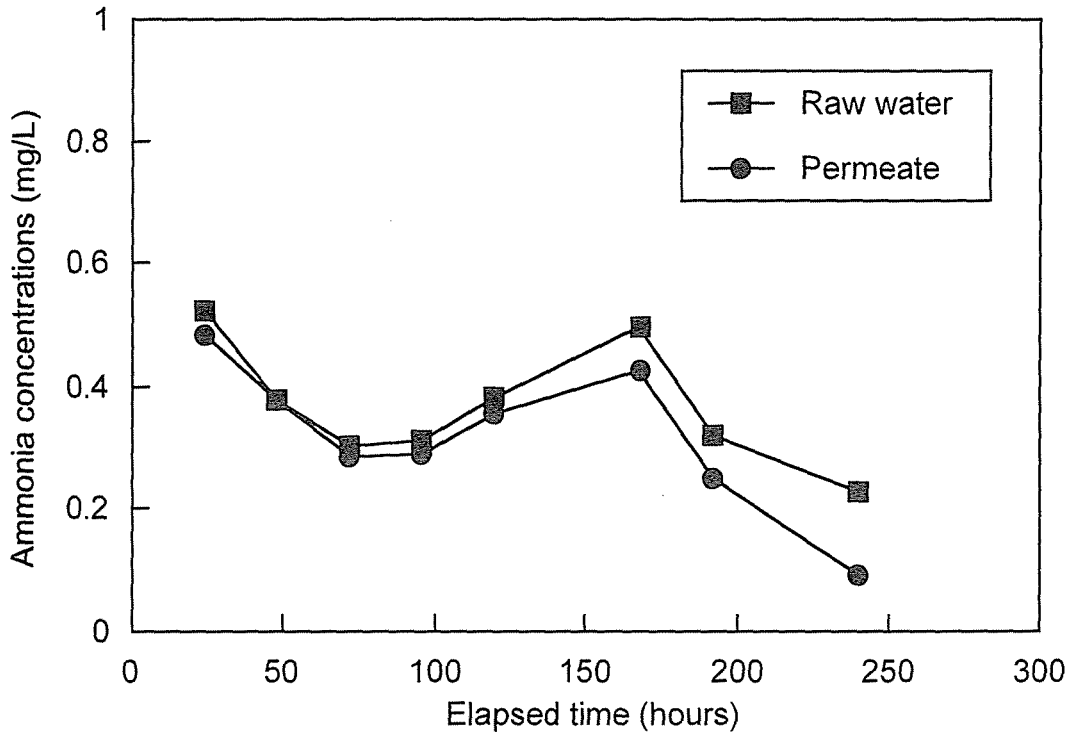


Fig. 2-7. Changes in the concentrations of  $\text{NH}_4^+\text{-N}$  in Run 2-2.

drinking water source that needs treatment. Since the  $\text{NH}_4^+\text{-N}$  loading was low and the duration of the run was shorter than in Run 2-1 (besides the data shown in Fig. 2-3, there was the extra duration for the fixation of biomass in Run 2-1), only an insignificant nitrification was observed during Run 2-2.

### 2.3.3. Evaluation of the influence of seeding sludge mass (Run 2-3)

The concentration of  $\text{NH}_4^+\text{-N}$  in typical polluted Japanese surface water is 0.5-1.0 mg/L. The quantity of nitrifiers required to oxidize such a low concentration of  $\text{NH}_4^+\text{-N}$  can be expected to be small. In the previous experiments, the quantity of the biomass introduced to the membrane chamber (1000 mg-SS/L and 450 mg-SS/L in Runs 2-1 and 2-2, respectively) might have been excessive in comparison to what would have been needed. Thus,

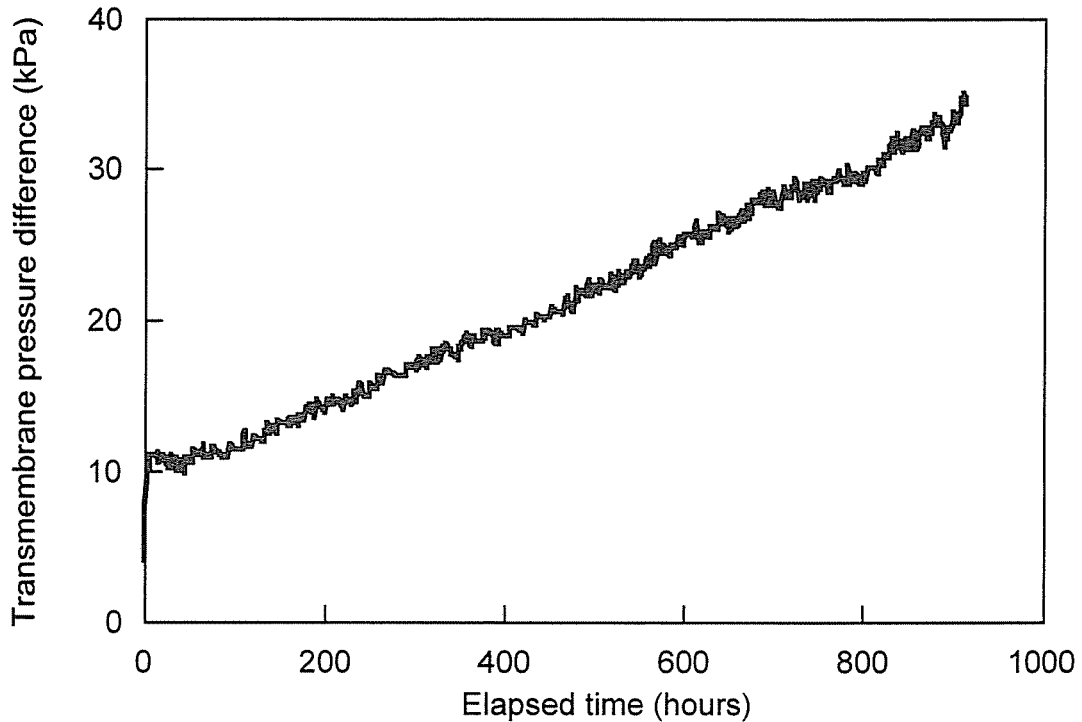


Fig. 2-8. Change in the transmembrane pressure difference in Run 2-3.

in this next experiment (Run 2-3), the quantity of seeding sludge was reduced to 20 mg-SS/L in order to examine that such a small quantity of the seeding sludge was enough for the nitrification. The membrane flux and the rotational speed of the disk were set at the same values as in Run 2-2. Activated sludge from the same municipal wastewater treatment plant as Runs 2-1 and 2-2 was again used for the inoculation. After acclimation of the seeding sludge to the inorganic substrates for 2 days, the sludge was inoculated. Since the quantity of the inoculated biomass was small, the concentration of SS in the membrane chamber decreased to negligible level within 24 hours of the operation.

The changes in the transmembrane pressure difference and the concentration of  $\text{NH}_4^+\text{-N}$  are shown in Fig. 2-8 and Fig. 2-9, respectively. Comparing Fig. 2-8 with Fig. 2-5, it is apparent

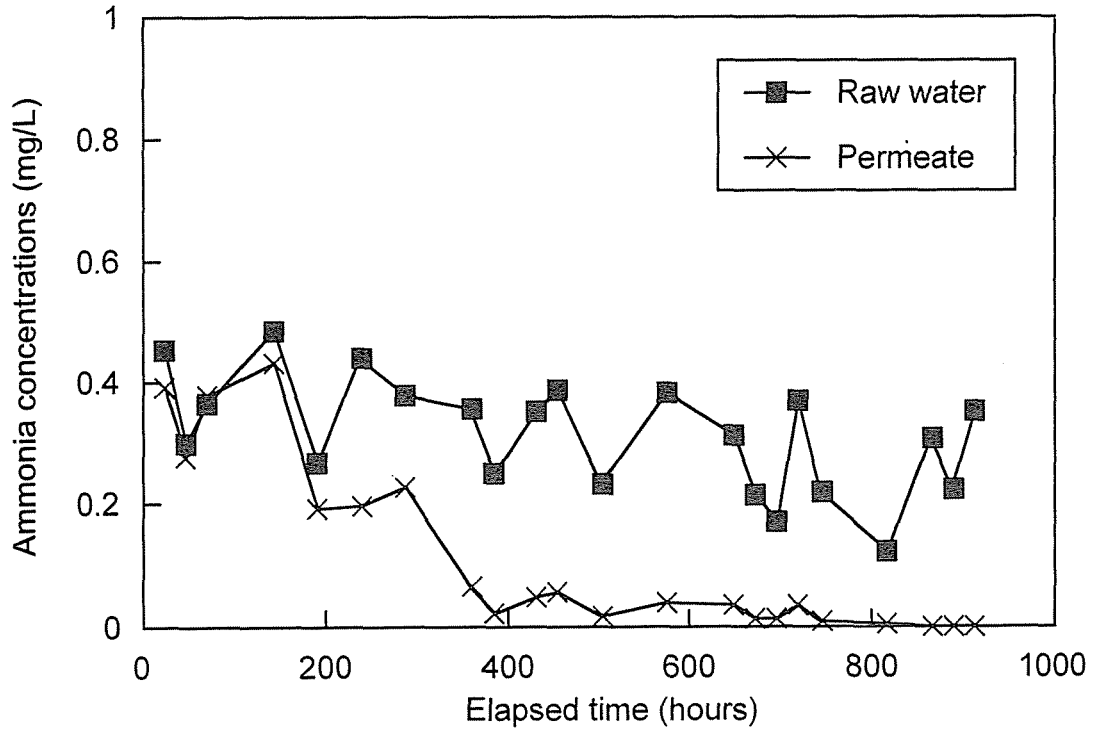


Fig. 2-9. Changes in the concentrations of  $\text{NH}_4^+\text{-N}$  in Run 2-3.

that the pressure difference increased very slowly in Run 2-3 even with the same membrane flux as Run 2-2. This comparison shows that the reduction in inoculation biomass can control the increase of the pressure difference in the subsequent filtration. With respect to the nitrification, it took about 400 hours to observe sufficient nitrification, but stable nitrification occurred after that.

#### 2.4. SUMMARY

In this chapter, the realization of the novel biofilm-membrane reactor (BMR) proposed through this thesis was examined by using the rotating membrane disk module. In addition, the basic performance of BMR for the oxidation of low concentration of  $\text{NH}_4^+\text{-N}$  was surveyed. The experimental results conducted in this chapter can be summarized as follows;

(1) It was possible to perform membrane filtration even though biofilm was attached to the membrane surface. This enables simultaneous membrane filtration and biological oxidation of  $\text{NH}_4^+\text{-N}$  in the BMR.

(2) The quantity of the fixed biomass (corresponding to the biomass quantity in the inoculation) has a significant influence on the increase of transmembrane pressure difference in the subsequent filtration. In order to prevent excess increase of pressure difference, it is desirable to fix only a minimum biomass on the membrane through inoculation.

(3) The required quantity of nitrifiers is small for the oxidation of low concentration of  $\text{NH}_4^+\text{-N}$ . Under the experimental conditions employed in this chapter, sufficient nitrification was achieved when the concentration of the seeding bacteria was 20 mg/L (corresponding to the biofilm density of 0.67 g/m<sup>2</sup>).

#### REFERENCES

Dal-Cin M. M., Lick C. N., Kumar A. and Lealess S. (1998) Dispersed phase back transport during ultrafiltration of cutting oil emulsions with a spinning membrane disk geometry. *J. Membrane Sci.* **141**, 165-181

Engler J. and Wiesner M. R. (2000) Particle fouling of a rotating membrane disk. *Wat. Res.* **34**(2), 557-565

Japan Sewage Works Association (1984) *Standard methods for wastewater analysis.*

Ohkuma N., Shinoda T., Aoi T., Okaniwa Y. and Magara Y. (1994)

Performance of rotating disk modules in a collected human excreta treatment plant. *Wat. Sci. Tech.* **30**(4), 141-149

Ohkuma N., Hotta M. and Okuno Y. (1995) Application of the rotating membrane disk module to wastewater treatment. *Membrane* **20**(5), 346-354 (in Japanese)

Park J. Y., Choi C. K. and Kim J. J. (1994) A study on dynamic separation of silica slurry using a rotating disk filter 1. Experiments and filtrate fluxes. *J. Membrane. Sci.* **97**, 263-273

Panham C. S. and Davis R. H. (1995) Protein recovery from cell debris using rotating and tangential crossflow microfiltration. *Biotechnol. Bioeng.* **47**, 155-164

Scheiner D. (1976) Determination of ammonia and Kjeldahl nitrogen by indophenol method. *Wat. Res.* **10**(1), 31-36



---

# CHAPTER

## 3

---

### MEMBRANE FILTRATION RESISTANCE IN THE NOVEL BIOFILM-MEMBRANE REACTOR (BMR)

Long term membrane filtration is inevitably associated with an increase in the membrane filtration resistance (the reduction of membrane permeability). This is one of the most important issues to be addressed in the application of membrane technology to water treatment. In order to prevent the increase of membrane filtration resistance and to carry out the efficient operation for a long period, it is necessary to collect information on the substances which cause membrane fouling and to investigate the fouling mechanism. This also applies to the novel biofilm-membrane reactor (BMR) proposed through this thesis. As pointed out already in Chapter 2, the type and the quantity of seeding bacteria seem to have a significant influence on the filtration resistance in the subsequent filtration.

In this chapter, membrane filtration resistances of the BMR, developed for the oxidation of low concentrations of  $\text{NH}_4^+\text{-N}$ , will be discussed based on experimental results obtained in six long term (approx. 1000-3000 hours) operations.

### 3.1. EXPERIMENTAL METHOD

#### 3.1.1. Experimental apparatus

Continuous membrane filtration was carried out with the same experimental apparatus as described in Chapter 2. The water temperature varied in the range of 14.2 C° to 28.8 C° and pH in the range of 7.1 to 7.9 in the membrane chamber. In all the experiments, the membrane flux and the rotational speed of the disks were fixed at 0.8 m/d and 50 rpm, respectively. Prior to each continuous operation, seeding bacteria for the oxidation of  $\text{NH}_4^+\text{-N}$  were placed in the membrane chamber at very low concentrations compared to those used in the experiments described in Chapter 2 (details will be described later). These bacteria were retained inside the membrane chamber due to the sieve effect of the membranes and the implementation of the dead-end filtration. Since the quantity of the seeding bacteria was very small, almost all of the bacteria were fixed on the membrane surface within a few hours of filtration. When each run was finished, chemical membrane washing using  $\text{NaClO}$  was implemented following the same procedure as described in Chapter 2. All chemical washing worked well and the permeability of the membrane was almost completely restored. Next run was started after completion of such a chemical washing.

#### 3.1.2. Analytical methods

The indophenol method (Scheiner, 1976) was applied for analyzing  $\text{NH}_4^+\text{-N}$ . At the end of the operations, the cake accumulated on the membrane surface was removed and the composition of the cake was investigated. The removed cake was examined with respect to total solids (TS), volatile solids (VS), protein, carbohydrate and metals. TS and VS were determined by

drying samples at 110 C° and 600 C°, respectively. The Lowry method (Lowry et al., 1951) was applied for protein determination and the phenol-sulphuric method of Dubois et al. (1956) was used for carbohydrate determination. Fluorescent X-ray analysis (HORIBA MESA-500) was performed on the residue at 600 C°, and the inorganic elemental contents in the cake were determined. The analyses of total organic carbon (TOC) and Fourier-translated infrared (FT-IR) spectrum were implemented with SHIMAZU TOC-5000 and HORIBA FT-530, respectively. At the end of the fourth operation (Run 3-4), a part of membrane was cut and taken out for the scanning electron microscope (SEM) observation. The procedure of the sample preparation for the SEM observation is shown in Table 3-1.

### 3.1.3. Division of the total membrane filtration resistance

Membrane flux ( $J$ ,  $\text{m}^3/\text{m}^2/\text{s}$ ) is often described by Darcy's law:

$$J = \frac{\Delta p}{\mu R_t} \quad (3.1)$$

where  $\Delta p$  is the transmembrane pressure difference (Pa),  $\mu$  is the viscosity of filtered water (Pa·s) and  $R_t$  is the total membrane filtration resistance ( $\text{m}^{-1}$ ).  $R_t$  is produced by both the membrane and materials accumulated on and in the membranes over time. With respect to the division of the  $R_t$ , various definitions have been proposed so far (Aimar et al. (1988); Labbe et al. (1990); Chiemchaisri and Yamamoto (1994); Choo and Lee (1996, 1998); Shimizu et al. (1996); Bouhablia E. H. et al. (1998); Huang and Morrissey (1998)). In this study,  $R_t$  is simply divided as below:

$$R_t = R_m + R_c + R_{irr} \quad (3.2)$$

$$J = \frac{\Delta p}{\mu R_t} = \frac{\Delta p}{\mu(R_m + R_c + R_{irr})} \quad (3.3)$$

where  $R_m$  is the intrinsic membrane resistance ( $m^{-1}$ ),  $R_c$  is the accumulated cake resistance ( $m^{-1}$ ) and  $R_{irr}$  is the resistance due to the irreversible membrane fouling ( $m^{-1}$ ). Using these equations,  $R_c$  and  $R_{irr}$  at the end of each filter run were determined. From the water flux and the pressure difference at the end of a filter run,  $R_t$  was calculated using Eq. (3.1). When a filter run was terminated, all membrane disks were taken out from the membrane chamber. The accumulated cake was removed from the membrane surface by cleaning it with a sponge. All the membrane disks were cleaned in this way and placed back into the membrane chamber. Following cleaning, the suction pressure decreased due to the removal of the cake. From the water flux and the pressure difference at this time,  $(R_m + R_{irr})$  could be calculated with Eq. (3.3) assuming  $R_c=0$ . When  $(R_m + R_{irr})$  was determined in this way,  $R_c$  at the end of a filter run could be determined using Eq. (3.2). Thus  $R_c$  was considered to be a reversible resistance in this study.  $R_{irr}$  at the end of a operation was determined by the subtraction of  $R_m$  from the resistance that remained after the removal of the cake.

### 3.2. RESULTS AND DISCUSSION FROM THE SIX LONG TERM EXPERIMENTS

#### 3.2.1. Experiment using pure cultures of the nitrifiers (Run 3-1)

Pure cultures of the nitrifiers (*Nitrosomonas europaea*-IFO14298 and *Nitrobacter winogradskyi*-IFO14297) were employed as the seeding bacteria in the first long term operation (Run 3-1). At the beginning of Run 3-1, the populations of these nitrifiers were controlled to the level around  $10^5$  cells/ml in

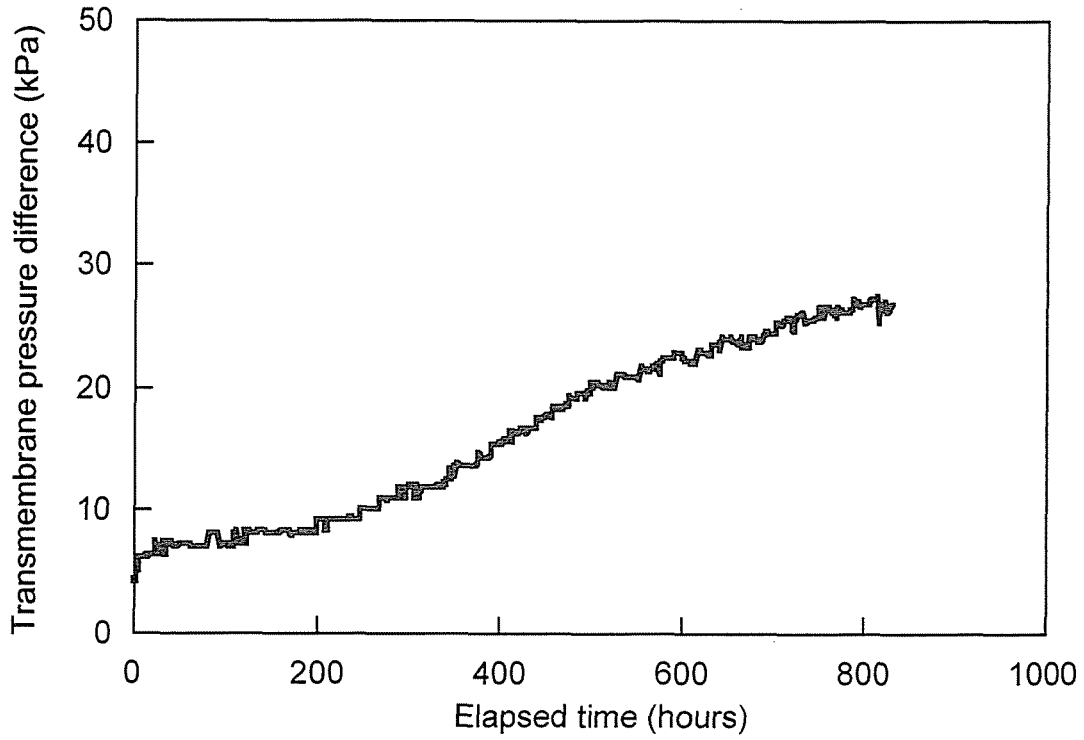


Fig. 3-1. Change in the transmembrane pressure difference in Run 3-1.

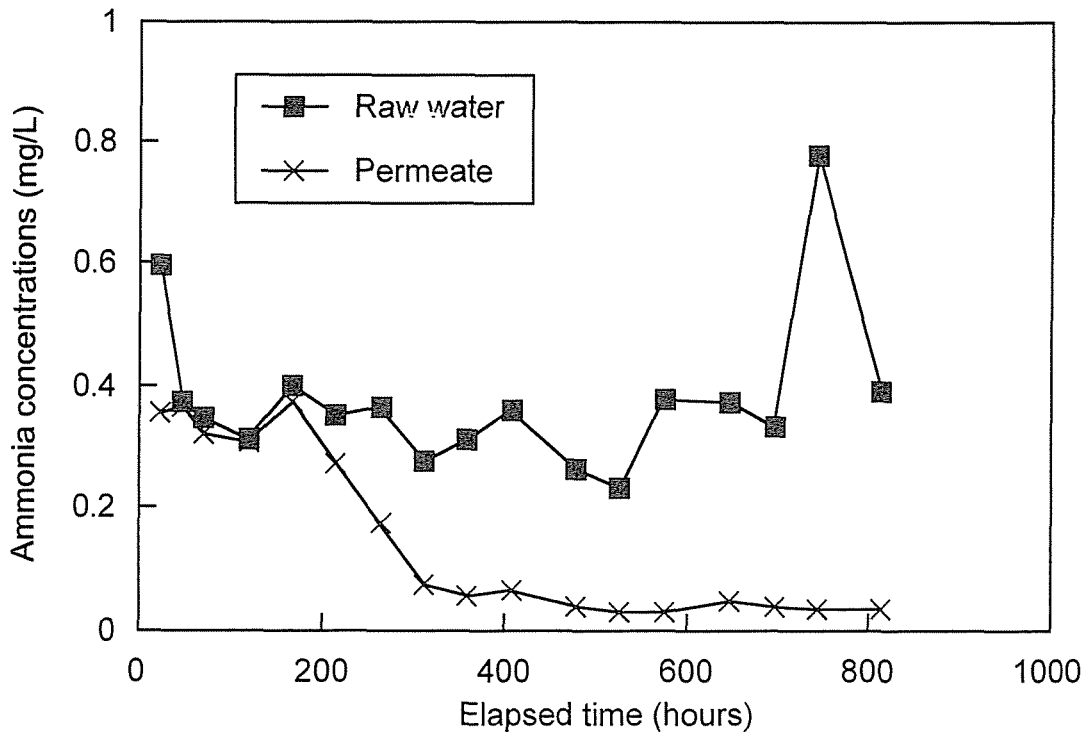


Fig. 3-2. Changes in the concentrations of  $\text{NH}_4^+$ -N in Run 3-1.

the chamber. Cell numbers were enumerated with the acridine orange method (Hobbie et al., 1977). Changes in the transmembrane pressure difference and the  $\text{NH}_4^+\text{-N}$  concentrations are shown in Figs. 3-1 and 3-2, respectively. Although no membrane cleaning was implemented during the continuous operation of Run 3-1, the required pressure difference for the membrane filtration was low (approx. 25 kPa) at the end of this operation. Compared to the experiment in which activated sludge acclimated to the inorganic substrates was employed as the seeding bacteria (see Run 2-3 in Chapter 2), the rate of increase in the required pressure difference was significantly lower in Run 3-1. Even though the activated sludge was acclimated to the inorganic substrates, heterotrophs and various organic substances would still remain in the sludge. They were probably the cause for the rapid increase of the transmembrane pressure difference in Run 2-3. Even though it took about 300 hours before good nitrification occurred (see Fig. 3-2), it was very stable and almost complete after that.

### 3.2.2. Experiments using bacteria acclimated to the inorganic substrates (Runs 3-2 and 3-3)

It was possible to retard the increase of the pressure difference by employing the pure cultures of the nitrifiers as the seeding bacteria, as compared to that experienced with the inoculation of activated sludge. However, it is not easy in practice to obtain and keep pure cultures. In addition, pure cultures are more sensitive to the growing environments (e.g. water temperature) compared with mixed cultures such as activated sludge. This may lead to operation failure such as no nitrification. In this section, therefore, a method to minimize the rate of the pressure difference increase, other than using the pure cultures was investigated.

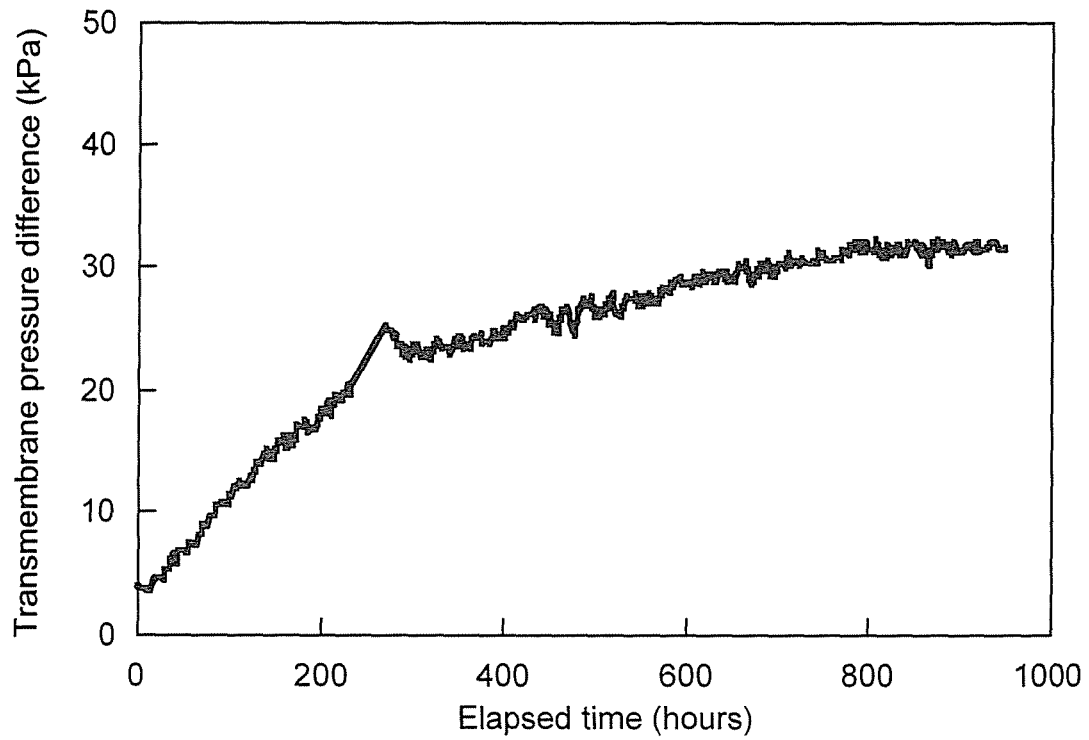


Fig. 3-3. Change in the transmembrane pressure difference in Run 3-2.

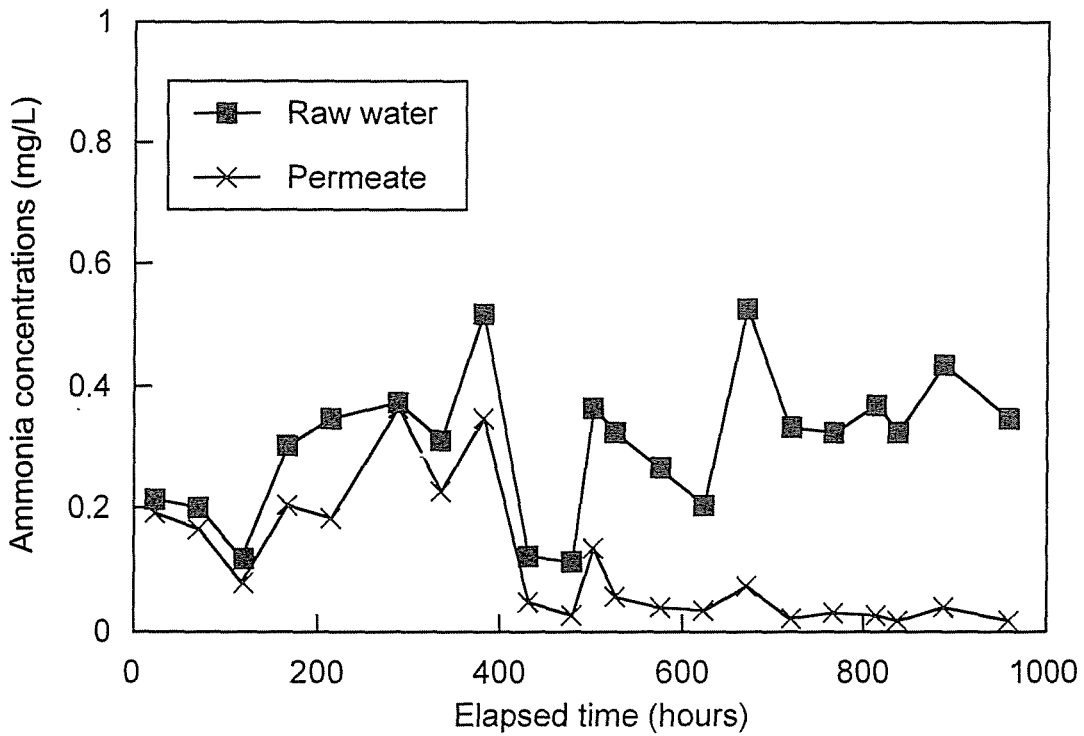


Fig. 3-4. Changes in the ammonia concentrations in Run 3-2.

Firstly, activated sludge from a municipal wastewater treatment plant was acclimated to the inorganic substrates in the same manner as in the experiments described in Chapter 2. This sludge was used as the seeding bacteria in Run 3-2. The concentration of the bacteria in the membrane chamber was 8 mg-SS/L. Changes in the transmembrane pressure difference and the  $\text{NH}_4^+\text{-N}$  concentrations in Run 3-2 are shown in Figs. 3-3 and 3-4, respectively. By comparing Runs 3-1 and 3-2, it was found that the increase rate of the pressure difference was higher in Run 3-2, especially in the early stage of the operation.

During the operation of Run 3-2, organic substrate available for heterotrophs was limited. Therefore, the microbial population in the accumulated cake would be acclimated with less organic substrate. Consequently the cake should be expected to develop a culture that was rich in nitrifiers and have less heterotrophs toward the end of Run 3-2. By comparing the seeding sludge and the cake accumulated through Run 3-2, relative amount of the heterotrophs to that of the nitrifiers (mass of the heterotrophs/mass of the nitrifiers) would be expected to be lower in the cake accumulated through Run 3-2. These considerations derived a hypothesis that using this accumulated cake as the seed in the next operation would minimize the increase of the pressure difference.

When the operation of Run 3-2 was finished, a part of the cake accumulated on the membrane was removed, and used as the seeding bacteria in the next operation (Run 3-3). The concentration of the bacteria at the beginning of Run 3-3 was 5 mg-SS/L. Changes in the transmembrane pressure difference and the  $\text{NH}_4^+\text{-N}$  concentrations in Run 3-3 are shown in Figs. 3-5 and 3-6, respectively. The increase of the pressure difference in Run 3-3 was as low as that in Run 3-1 where the pure cultures of



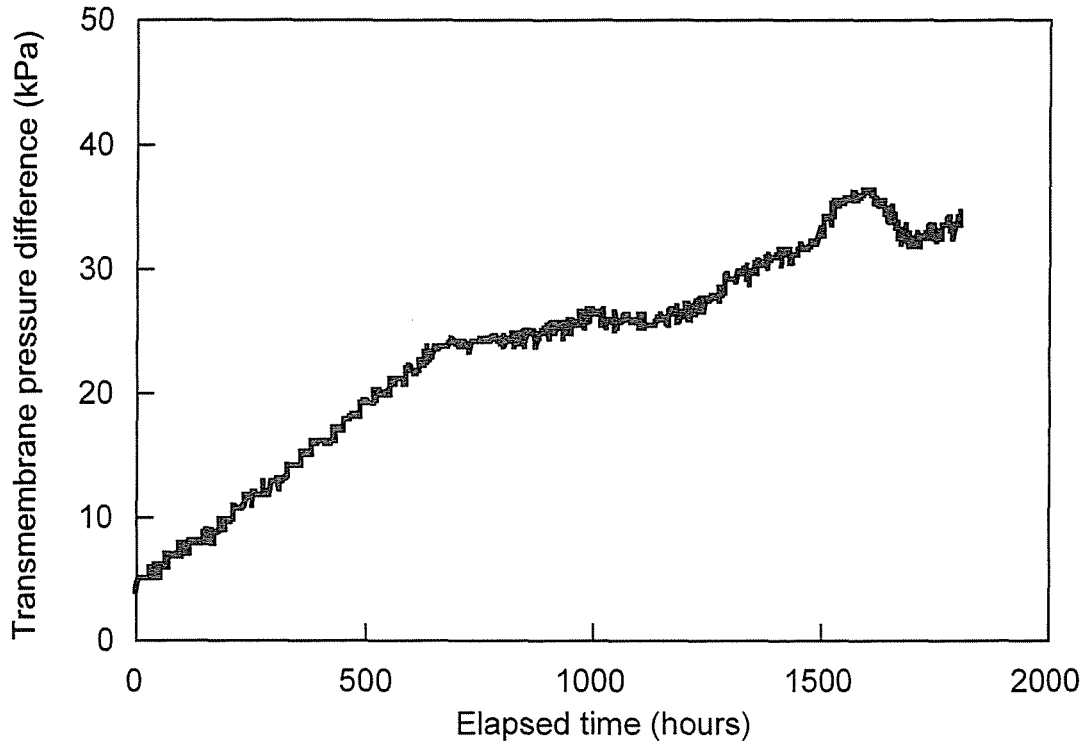


Fig. 3-5. Change in the transmembrane pressure difference in Run 3-3.

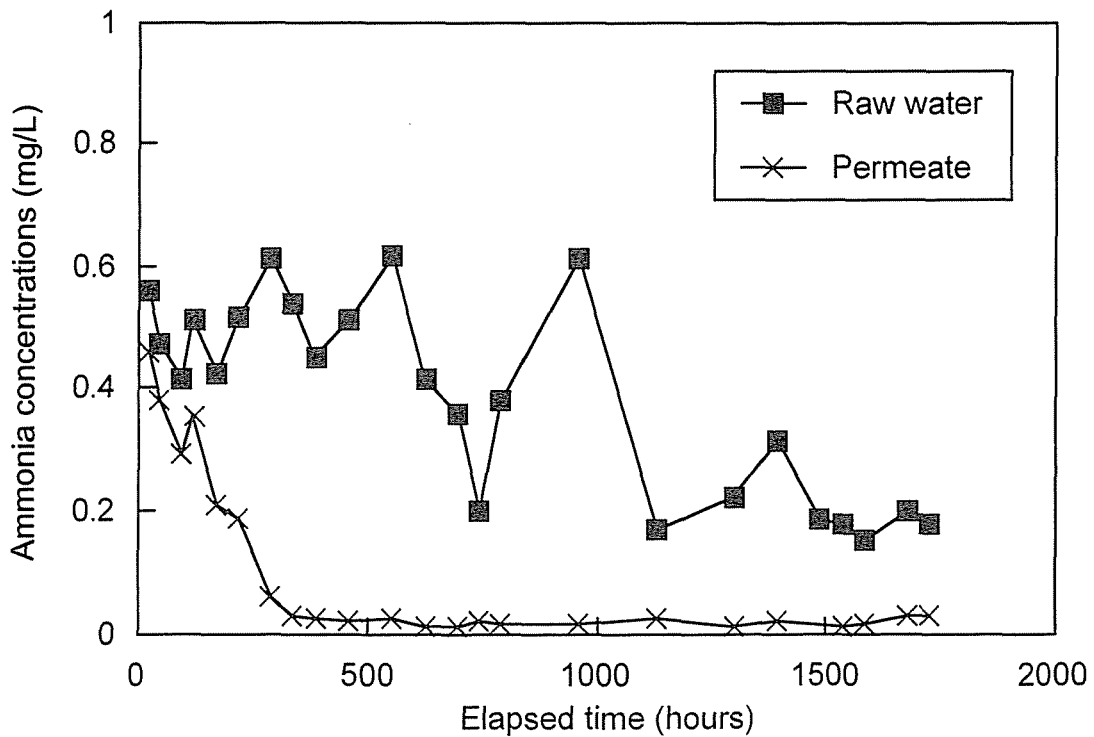


Fig. 3-6. Changes in the concentrations of  $\text{NH}_4^+\text{-N}$  in Run 3-3.

the nitrifiers were used as seeding bacteria. The filter run could be continued more than 1800 hours without any membrane cleaning.

### 3.2.3. Distribution of the membrane filtration resistances and analysis of the deposit cake on the membrane

After the operation of Run 3-3, the membranes were cleaned step-by-step in the manner described in 3.1.3, in order to estimate the magnitude of the cake filtration resistance ( $R_c$ ) and the irreversible filtration resistance ( $R_{irr}$ ). Fig. 3-7 shows the magnitude of  $R_c$  and  $R_{irr}$  developed in Run 3-3. Obviously,  $R_c$  was dominant in Run 3-3. The simplified composition of the cake accumulated in Run 3-3 is shown in Fig. 3-8. The difference between total solids (TS) and volatile solids (VS) represents the quantity of inorganic substances, while VS represents the quantity of organic substances. Protein and carbohydrate are assumed to represent the quantity of microorganisms and extracellular polymeric substances (EPS), respectively. The quantity of inorganic substances was higher than that of the organic substances in Run 3-3, and the former accounted for 65 % of the total accumulated material. Iron, silicon, phosphorus, zinc and aluminum were the major elements determined. Iron, silicon, zinc and aluminum came from tap water that contained these elements at concentrations smaller than 0.1 mg/L. With respect to phosphorus,  $K_2HPO_4$  added in the feed water as the substrate for nitrifiers, seemed to be adsorbed by the iron that had previously accumulated on the membrane. Microorganisms accounted for only 10 % of the total cake, which suggests that the microorganisms themselves did not create a lot of the filtration resistance in Run 3-3. The presence of organic substance other than protein and carbohydrates (see Fig. 3-8), could probably be explained by the humic substances

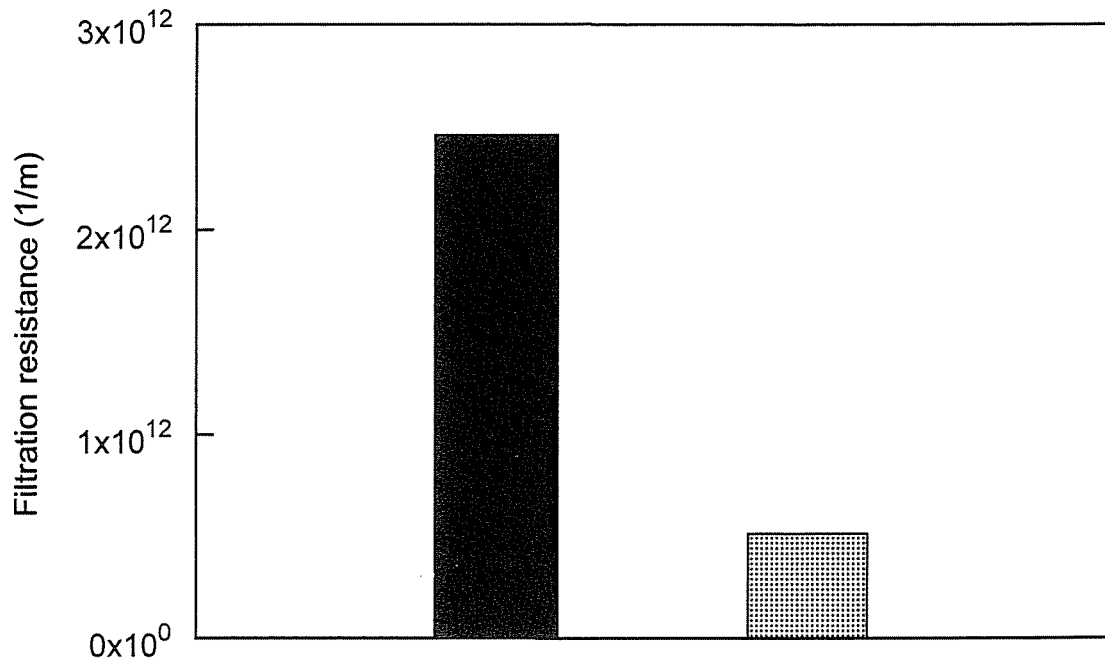


Fig. 3-7. Distribution of the filtration resistance in Run 3-3.

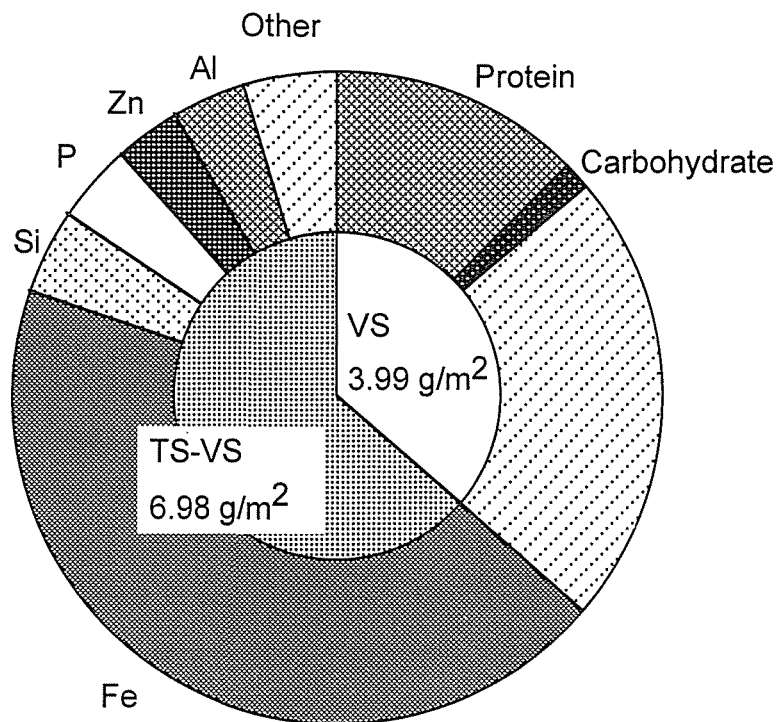


Fig. 3-8. Composition of the cake accumulated on the membrane surface in Run 3-3.

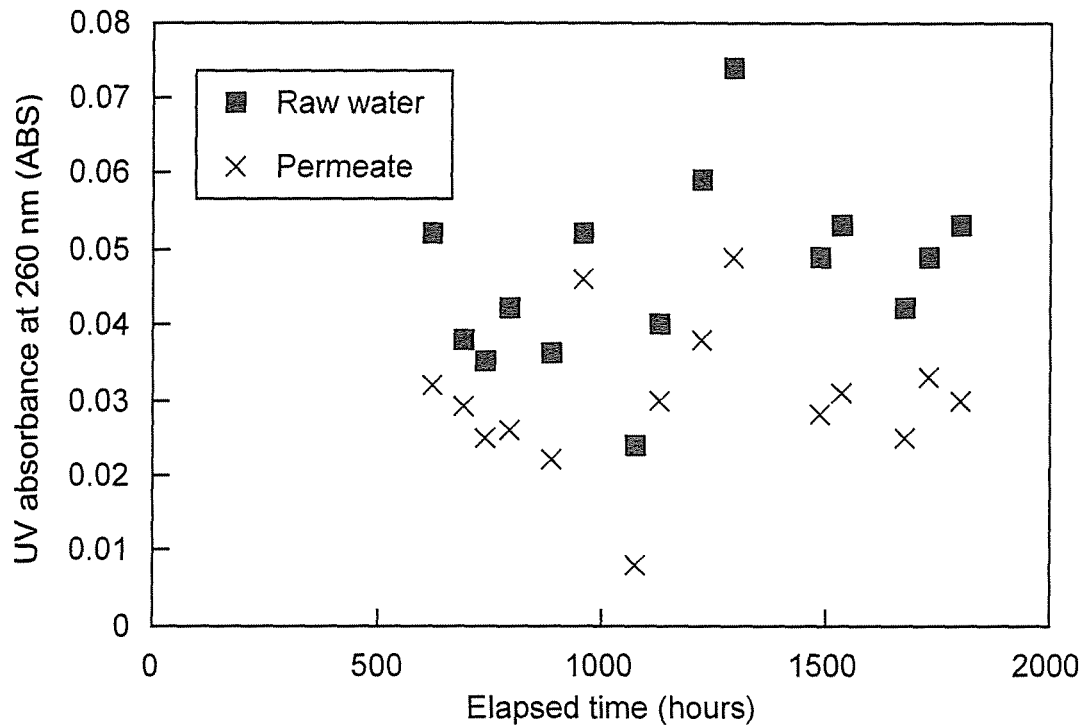


Fig. 3-9. Changes in the concentrations of humic substances (5 cm cell was used in the measurement).

contained in tap water. Fig. 3-9 shows the changes in the concentration of humic substance in Run 3-3. The UV absorbance at 260 nm was used as the indicator of the humic content in this study. It is shown that 30-40 % of the humic substance contained in the feed water was removed with the BMR.

Chemical cleaning using NaClO worked well and the membrane permeability was completely restored. This suggests that  $R_{irr}$  was caused by some organic substances because inorganic substances could not usually be dissolved by oxidation reagents such as NaClO.

#### 3.2.4. Longer operation with periodical cleaning (Run 3-4)

The experiences from the experiments described in previous sections were as follows;

(1) Use of the seeding sludge in which the quantity of unnecessary bacteria (e.g. heterotrophs) and organic substances were reduced, was effective in controlling the increase of the transmembrane pressure difference.

(2) Accumulated cake resistance ( $R_c$ ), which could be reduced without chemical reagents, was the dominating type of resistance.

(3) Most of the accumulated cake was composed of the materials contained in the feed water (in this case tap water) and retained by the membranes.

In addition, the amount of nitrifiers required for the oxidation of such low concentrations of  $\text{NH}_4^+\text{-N}$ , as one is dealt with in this study, is expected to be very small.

Based on these results and assumptions, it was summarized that the efficient way of BMR operation is as follows. Microorganisms acclimated to the actual condition should be used as the seeding bacteria and the accumulated cake should be removed from the membrane at an appropriate interval. This can lead to long filter runs with slow development of pressure difference. The next experiment (Run 3-4) was conducted in order to examine such a long term operation with periodical membrane cleaning. Periodical cleaning in BMR operation should not be chemical one but physical one. This is because the dominating resistance in BMR operation can be cancelled without chemical reagents as described before and because use of chemicals would cause damage to nitrifiers.

The tubular or hollow-fiber membranes can effectively be backwashed to remove the accumulated cake. The membrane used

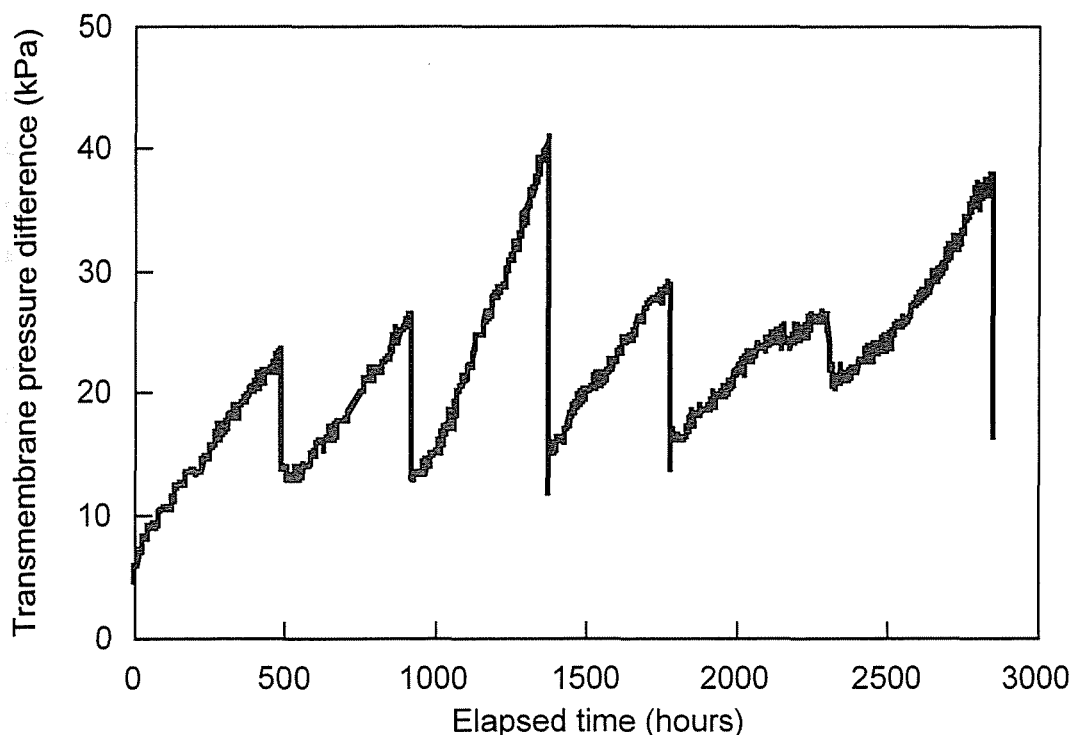


Fig. 3-10. Change in the transmembrane pressure difference in Run 3-4.

in this study was a kind of plate and frame type and therefore backwashing could not be applied. It was therefore investigated whether or not the shear stress induced by increasing the rotational speed of the disks could remove the accumulated cake. After stopping the suction pump, the rotational speed was increased and cleaning was continued for 15 minutes. The rotational speed was increased from 50 rpm, the normal operation speed, to 400 rpm. This cleaning method will be called as "shear cleaning" hereafter. After shear cleaning, the detached cake in the membrane chamber was discarded and continuous operation was restarted.

Prior to the continuous operation of Run 3-4, the acclimated bacteria were seeded at the concentration of 4 mg/L in the chamber. The change in the transmembrane pressure difference in Run 3-4 is shown in Fig. 3-10. Shear cleaning was implemented

at intervals of about 500 hours. Comparing the increase of the pressure difference observed during the first 500 hours in Run 3-4 with that of Runs 3-1, 3-2 and 3-3, it can be seen that the increase in Run 3-4 was faster than Runs 3-1 and 3-3 but was slower than Run 3-2. In the latter unacclimated bacteria (activated sludge from a municipal wastewater treatment plant) had been used as the seeding bacteria. Based on Fig. 3-10, it can be concluded that the "shear" cleaning procedure described above was very effective. After shear cleaning, the pressure difference decreased to around 10 kPa and then increased slowly again. After the second shear cleaning, the pressure difference increased rapidly. This was probably due to the experimental mistake that the discard of the detached cake was insufficient at the second cleaning. Only the fifth cleaning did not work well. There was no apparent reason for this difference, however, the mode of operation of the permeate valve might be the reason. The valve was closed during the fifth cleaning while it was open during the others. In the sixth cleaning, the operation had been continued for more than 2900 hours; nevertheless the transmembrane pressure difference decreased to about 15 kPa after shear cleaning. This suggested that much longer operation could be possible.

Accumulated cake was removed and discarded every 500 hours during Run 3-4, which meant that nitrifiers contained in the cake were also discarded. Consequently, it might be expected that the nitrification rate would decrease after shear cleaning. Fig. 3-11 shows the variations in the concentrations of  $\text{NH}_4^+\text{-N}$  in Run 3-4. It took only 100 hours to observe good nitrification in Run 3-4 since bacteria acclimated to the experimental condition were used as the seed. The  $\text{NH}_4^+\text{-N}$  concentrations in the permeate temporarily increased just after cleaning and 40-50 hours were required in order to reach the same nitrification

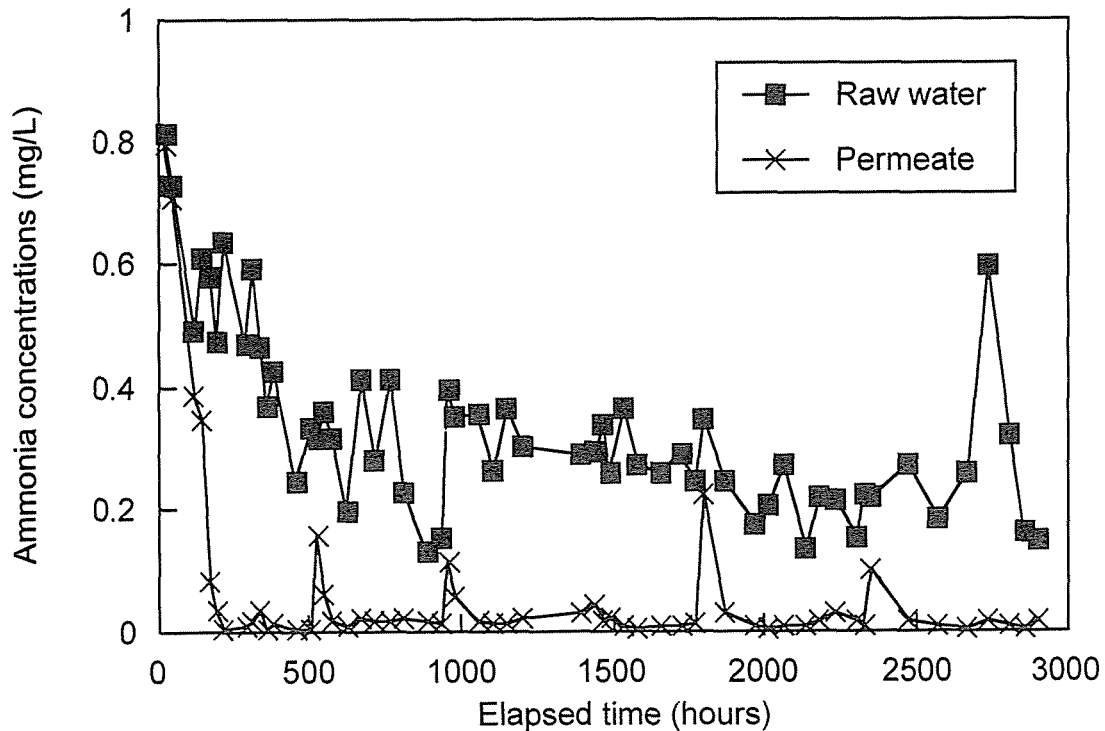


Fig. 3-11. Changes in the concentrations on  $\text{NH}_4^+\text{-N}$  in Run 3-4.

rate as the one before shear cleaning. A small quantity of the accumulated cake remained on the membrane surface even after shear cleaning. This grew rapidly, however, and was probably the explanation for the rapid recovery of the nitrification capacity.

The minimum amount of the microorganisms for this experimental condition can be determined as the amount that was present at the time when recovery of the nitrification rate was observed after shear cleaning. The amount of microorganisms remained on the membrane after the sixth cleaning was measured to be  $0.04 \text{ g-protein/m}^2$ . The doubling time of the nitrifiers is reported to be in the range of 3 to 10 days (Schönborn, 1986) and consequently one can expect that the increase of the nitrifiers within 40-50 hours after cleaning would be insignificant. The actual amount of microorganisms accumulated on the membrane



Table 3-2. Estimated protein amount on the membrane just before cleaning.

Cleaning No.	Protein on the membrane (g/m <sup>2</sup> ).
1	0.75
2	0.66
3	1.07
4	0.82
5	0.44
6	0.99

just before cleaning was estimated from the concentration of the protein in the membrane chamber just after cleaning. Table 3-2 shows the estimated values at each cleaning. From Table 3-2, the actual amount of microorganisms was found to be excessive to the minimum value by one order, which suggests that more efficient operation than Run 3-4 could be possible.

Fig. 3-12 shows  $R_c$  and  $R_{irr}$  estimated at the end of Run 3-4.  $R_c$  was dominant in Run 3-4, in accordance with that found in other experiments.  $R_{irr}$  was, however, notably higher in Run 3-4, probably due to the longer operation period.

### 3.2.5. Substances causing the irreversible membrane fouling in the operation of the BMR

As pointed out in the previous section,  $R_{irr}$  seemed to be caused by some organic substances under the actual experimental condition. When the operation of Run 3-4 was finished, the membrane cleaned with a sponge was observed with scanning electron microscope (SEM). Some deposits which could not be removed with sponge cleaning was found on the membrane surface

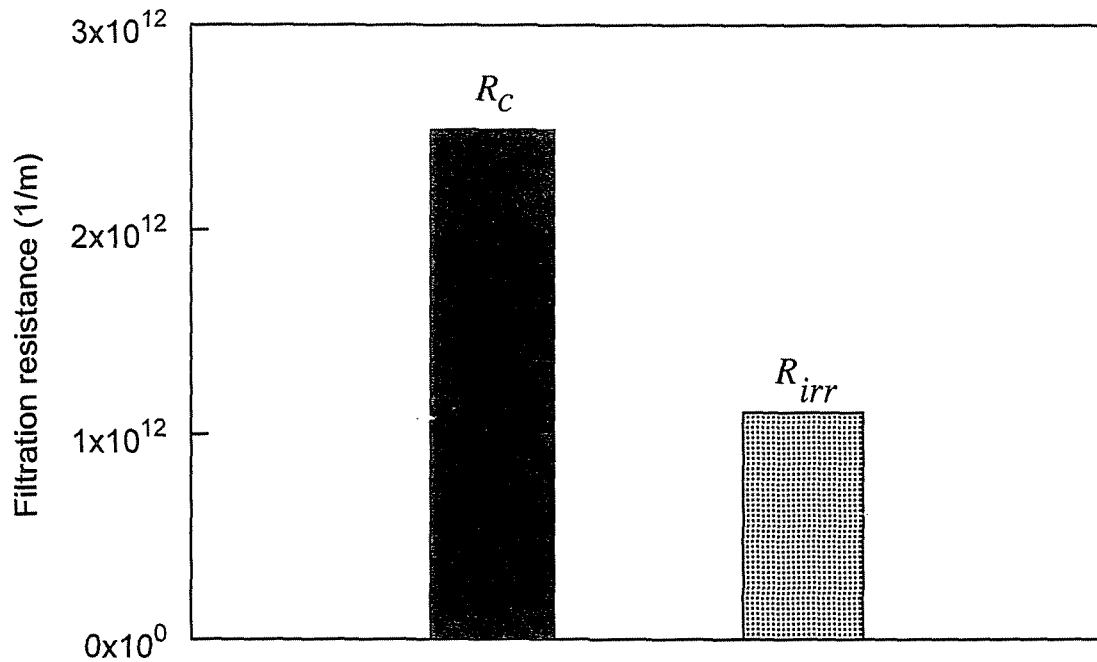


Fig. 3-12. Distribution of the filtration resistance in Run 3-4.

and the micropores of the membrane was hidden by the deposit. This could account for  $R_{irr}$ . The elemental analysis accompanied with the SEM observation could only detect elements with element number greater than Na. No such elements were detected. This observation revealed that the deposits were organic substances.

During the SEM observation, the irradiation of the electron beam caused a crack in the deposit, through which micropores of the membrane could be seen (Photo 3-1). Photo 3-1 suggests that plugging of the micropores did not occur in the operation of BMR.

Besides the SEM observation, extraction of the organic substances from the membrane after sponge cleaning and simple analysis were attempted in order to obtain information about the substances that were causing  $R_{irr}$ . The extraction was



Photo. 3-1. SEM observation of the membrane used in RUN 3-4.

Table 3-3. Extraction of organic substances from the membranes.

	Membrane used in Run 3-4	Virgin membrane
TOC (mg/L)	17.6	15.9
UV absorbance (ABS)	0.316	0.108
Protein (mg/L)	ND	_____*
Carbohydrate (mg/L)	7.3	ND
Membrane area used for the extraction (cm <sup>2</sup> )	156	51.9
Volume of the extraction liquid (ml)	90	30

\*not analyzed

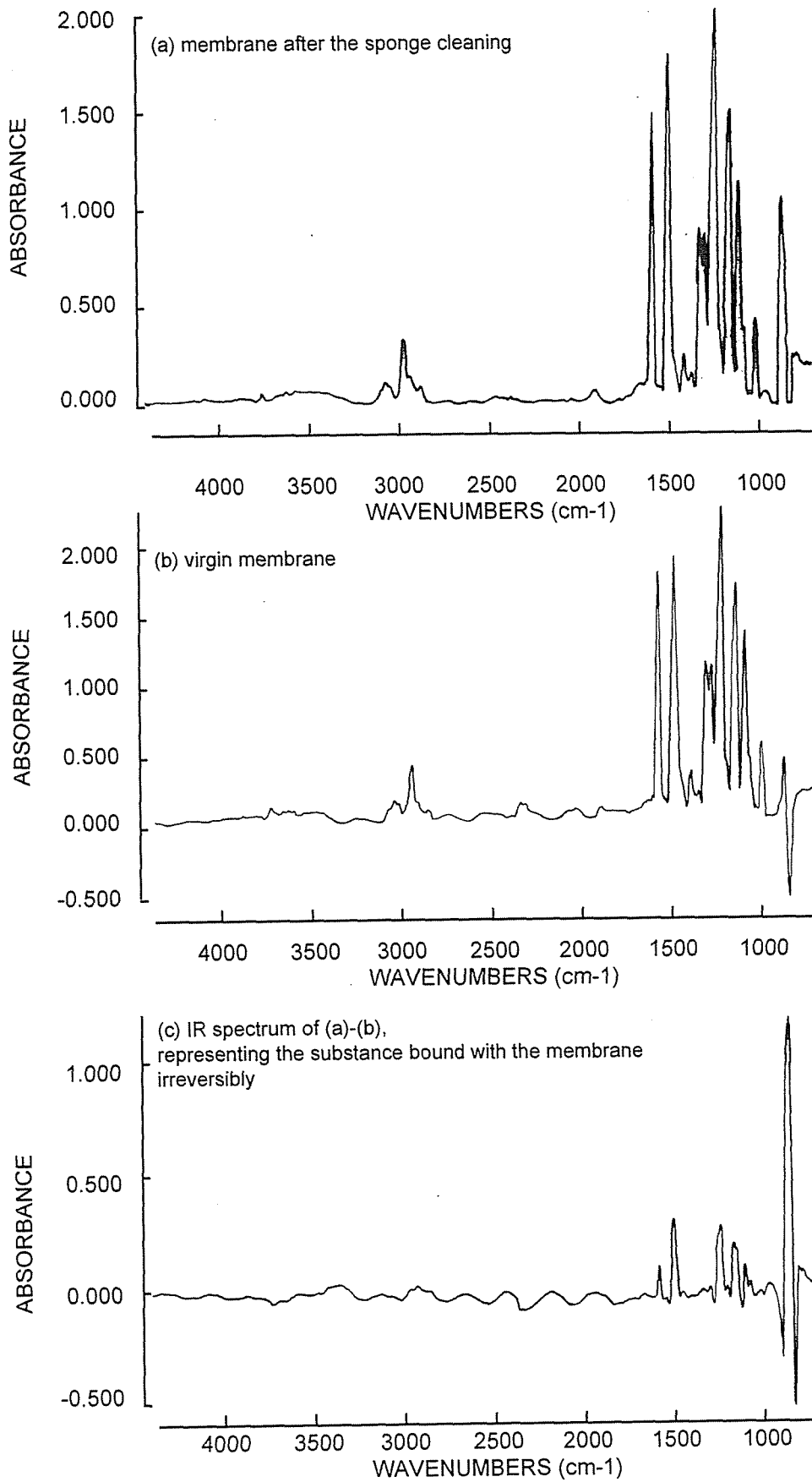


Fig. 3-13. IR spectra of membranes.

Table 3-4. Compounds suggested their existence by the IR spectrum (Silverstein et al., 1991).

Compounds	Wavenumber (cm <sup>-1</sup> )
Monocyclic aromatic compounds	Around 1500 and around 1100
Aliphatic nitro compounds	Around 1600 and around 1400
Aromatic nitro compounds	Around 1500, around 1300 and around 880
Nitrate esters	Around 1600, around 1250 and around 880
Nitroso compounds (RNO)	1150-1600
Aliphatic esters	1100-1180
Aliphatic SiO compounds	1000-1150

implemented by submerging the membrane into alkaline solution (NaOH, pH 12, for 24 hours, at room temperature). The extracted liquid was filtered with 0.45  $\mu\text{m}$  PTFE membrane filter and then analyzed for TOC, UV absorbance at 260 nm, protein and carbohydrate. This extraction and analysis were performed also with a virgin membrane. Table 3-3 shows the results of the analysis. With respect to TOC, there was not a significant difference between the two membranes. A substantial amount of organic carbon eluted from even the virgin membrane probably due to the hydrolysis of the membrane supporting material. Compared to the virgin membrane, a higher amount of humic substances (indicated by UV absorbance) and carbohydrates eluted from the membrane used in Run 3-4. This shows that these components play an important role in creating  $R_{irr}$ . Fig. 3-13 shows the IR spectra of the membrane cleaned with a sponge after Run 3-4 (Fig. 3-13 (a)), the virgin membrane (Fig. 3-13 (b)) and the difference between them (Fig. 3-13 (c)). The spectrum shown in Fig. 3-13 (c) should, therefore, represent the

compounds causing the  $R_{irr}$ . From Fig. 3-13 (c), the absorbance peaks are found at the wave numbers of 1581, 1498, 1238, 1166, 1153, 1103 and 856  $\text{cm}^{-1}$ , which suggest the presence of the compounds listed in Table 3-4. In addition to the humic substances and carbohydrates, organic compound that have been bound to nitrate produced as the end product of nitrification, may also have an impact on the  $R_{irr}$ .

### 3.2.6. Estimation of the magnitude and the type of the filtration resistance induced by nitrifiers (Run 3-5)

Figs. 3-14 and 3-15 shows the changes in the transmembrane pressure difference and the concentrations of  $\text{NH}_4^+$ -N respectively, in an experiment (Run 3-5) where pure cultures of the nitrifiers were used as the seeding bacteria and no nitrification was observed. Prior to the operation of Run 3-5, the pure cultures were inoculated at the same concentration as in Run 3-1 where good nitrification was observed (seeding:  $10^5$  cells/mL in the membrane chamber). Nevertheless, one can see from Fig. 3-14 that no nitrification occurred in Run 3-5. A possible explanation for this was that the water temperature was low and the fluctuation of it was substantial. Fig. 3-16 shows the changes in the water temperature measured in Run 3-1 and Run 3-5. Generally, pure cultures are supposed to be sensitive to the environment such as water temperature and therefore the pure cultures of the nitrifiers used in Run 3-5 could not show their function either.

Even though no nitrification occurred, the transmembrane pressure difference in Run 3-5 increased substantially. The increase of the population of the nitrifiers and the secretion of EPS by the nitrifiers were expected to be negligible in Run

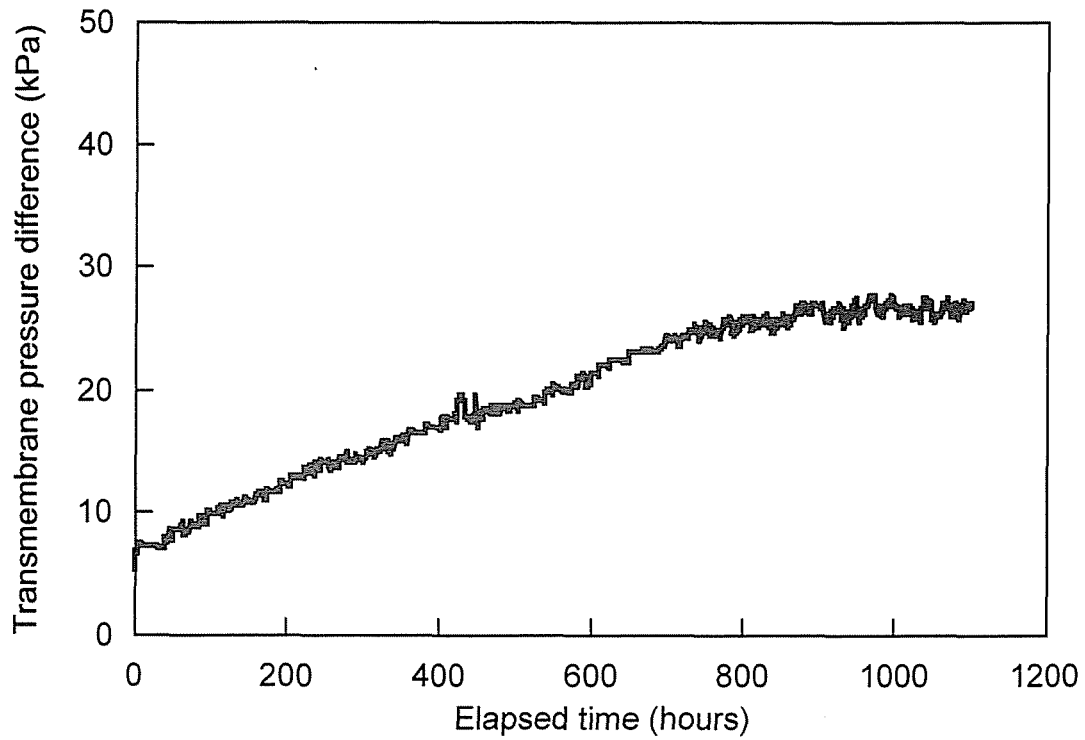


Fig. 3-14. Change in the transmembrane pressure difference in Run 3-5.

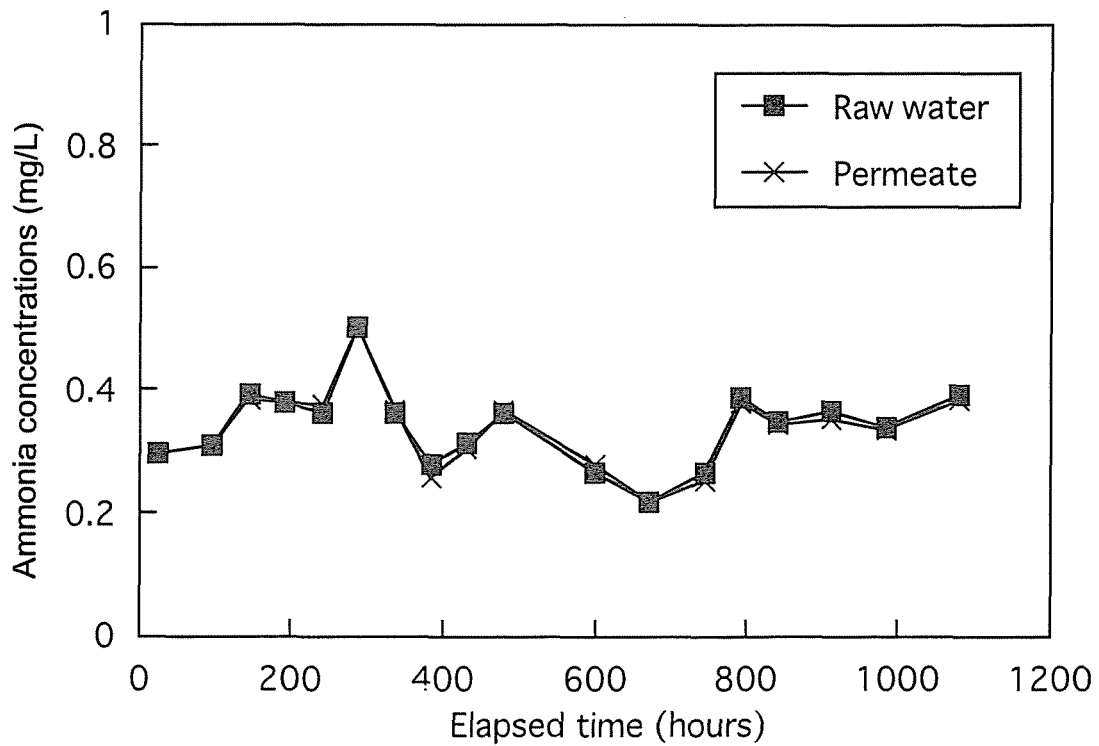


Fig. 3-15. Changes in the concentrations of  $\text{NH}_4^+\text{-N}$  in Run 3-5.

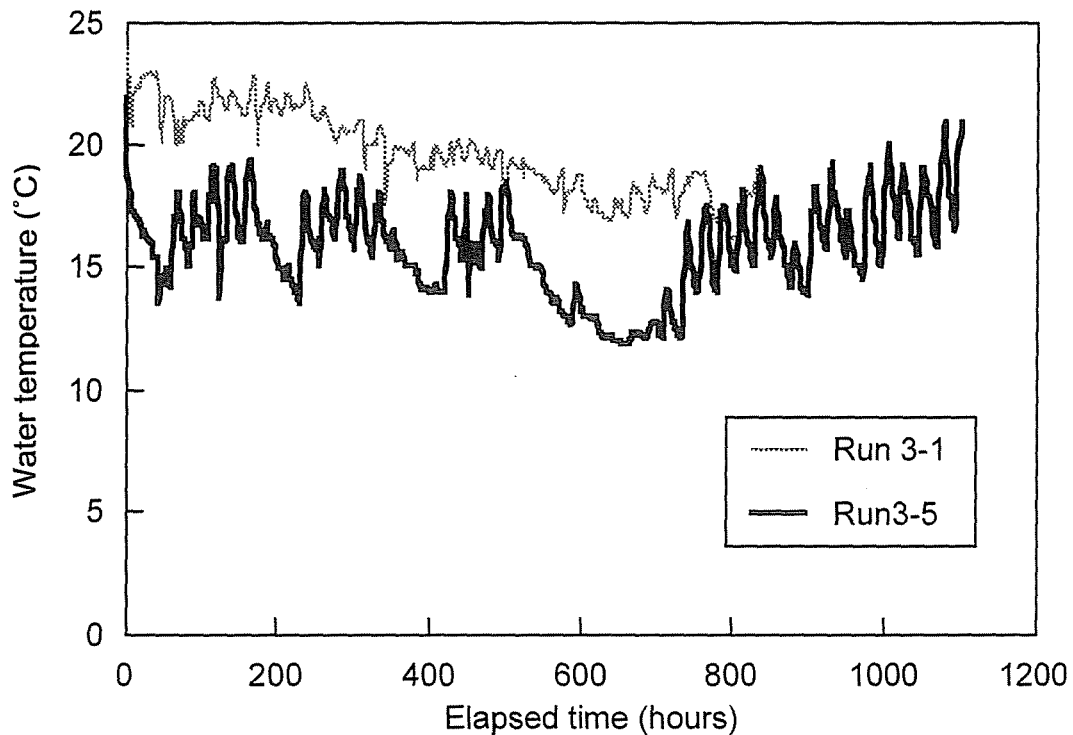


Fig. 3-16. Changes in the water temperature in Runs 3-1 and 3-5.

3-5 because the oxidation of  $\text{NH}_4^+\text{-N}$  was not observed. Additionally, the mass of the nitrifiers introduced into the membrane chamber at the beginning of the operation of Run 3-5 was quite small. The suspended solids (SS) concentration in the membrane chamber was close to zero even after the inoculation. Consequently, the increase of the pressure difference in Run 3-5 can be attributed to the organic and inorganic substances contained in the feed water (in this case tap water). Comparing the increase of the pressure difference in Runs 3-1 and 3-5 (Figs. 3-1 and 3-14), one can see that the increase in Run 3-1 was similar to the one in Run 3-5, which indicates the filtration resistance induced by the nitrifiers was insignificant.

Fig. 3-17 shows the divided filtration resistances estimated at the end of Runs 3-1 and 3-5. As mentioned above, the filtration



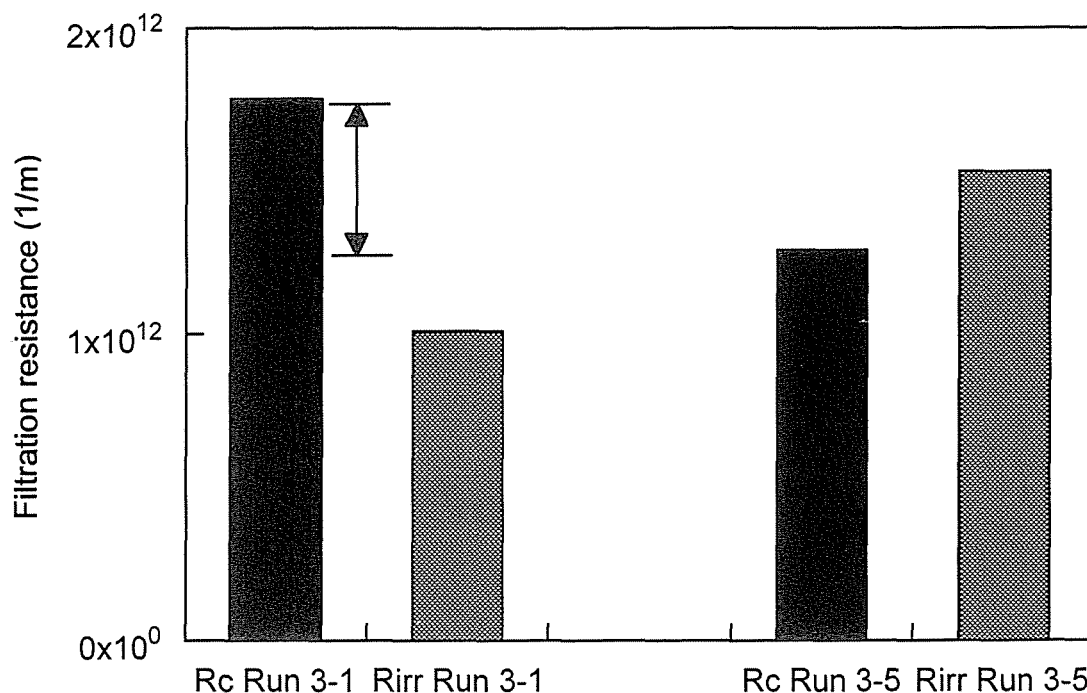


Fig. 3-17. Divided filtration resistances in Runs 3-1 and 3-5.

resistance observed in Run 3-5 could be attributed to the substances contained in tap water.  $R_c$  was created by the accumulation of the organic and inorganic particles in tap water with larger sizes than the micropore size of the used membrane.  $R_c$  eventually accounted for almost half of the total filtration resistance in Run 3-5. The composition of the cake accumulated in Runs 3-1 and 3-5 was simply analyzed and the results are shown in Table 3-5. Both cakes contained more inorganic substances (TS-VS) than organic substances (VS). The compositions of the inorganic elements in both cakes were quite similar. Namely, iron, silicon, aluminum were the major elements and they accounted for 85 % of the inorganic fraction. Especially, the iron contents of both cakes were high (70 % of the inorganic fraction). These elements were contained at higher concentrations in tap water than the other metal elements and they accumulated on the membrane surface with the filtration. The tendency for inorganic elements to accumulate on the

Table 3-5. Composition of the cakes accumulated in Runs 3-1 and 3-5.

	Run 3-1	Run 3-5
VS	1.025	0.745
TS-VS	2.145	1.545
Protein		0.06
Carbohydrate		0.03

all values are expressed as g/m<sup>2</sup>.

membrane seen in Runs 3-1 and 3-5, was similar to the one seen in Run 3-3 as described before.

When the operation of Run 3-5 was finished, the protein and carbohydrates contents of the accumulated cake were analyzed. Almost no protein and carbohydrates were detected in the analysis, which was consistent with the experimental result that no nitrification occurred in Run 3-5. It was reasonable to conclude, therefore, that the organic substances accumulated on the membrane in Run 3-5 were humic substances contained in tap water. Judging from these results, inorganic and organic substances contained in tap water could create substantial cake filtration resistance ( $R_c$ ) irrespective of the activity of the nitrifiers. However, it was still unclear which fraction played a more important role in creating  $R_c$ , inorganic (mainly iron) or organic (mainly humic) substances.

In Run 3-1,  $R_c$  was dominant. Comparing the magnitudes of  $R_c$  in Runs 3-1 and 3-5, the former was greater although the operation period of Run 3-1 was shorter. Since good nitrification was observed in Run 3-1, the difference between these two  $R_c$ s

(indicated by the arrow in Fig. 3-17) might be attributed to the nitrifiers.

In Run 3-5,  $R_{irr}$  was slightly greater than  $R_c$ . As discussed in the previous section,  $R_{irr}$  was probably created by humic substances or carbohydrates.  $R_{irr}$  in Run 3-5 could be attributed to the humic substances in tap water because no nitrification occurred in that operation. However, in Run 3-1, EPS secreted by the nitrifiers possibly cause some  $R_{irr}$  in addition to that created by the humic substances.

Assuming that  $R_{irr}$  in Run 3-1 was caused mainly by the EPS secreted from the nitrifiers, the magnitude of  $R_{irr}$  in Run 3-5 should be considerably smaller because the population of nitrifiers was scarce. The actual magnitude of  $R_{irr}$  in Run 3-5, however, was not that small and was in contradiction to the assumption. Inversely, assuming that  $R_{irr}$  in Run 3-1 was caused mainly by the humic substance in tap water, the magnitude of  $R_{irr}$  in Run 3-5 should be larger corresponding to the length of the operation. The data shown in Fig. 3-17 supports this assumption. From these considerations, it should be reasonable to presume that  $R_{irr}$  in this membrane process was caused mainly by the humic substances contained in the feed water (in this case tap water).

#### 3.2.7. Experiment using the feed water pre-treated with the same membrane (Run 3-6)

In the previous section, it was experimentally shown that the fixation of the nitrifiers on the membrane hardly created additional filtration resistance. The magnitude and the type of the filtration resistance that the nitrifiers caused were also discussed. In order to obtain more in-depth information on these subjects, the next experiment using pre-treated feed

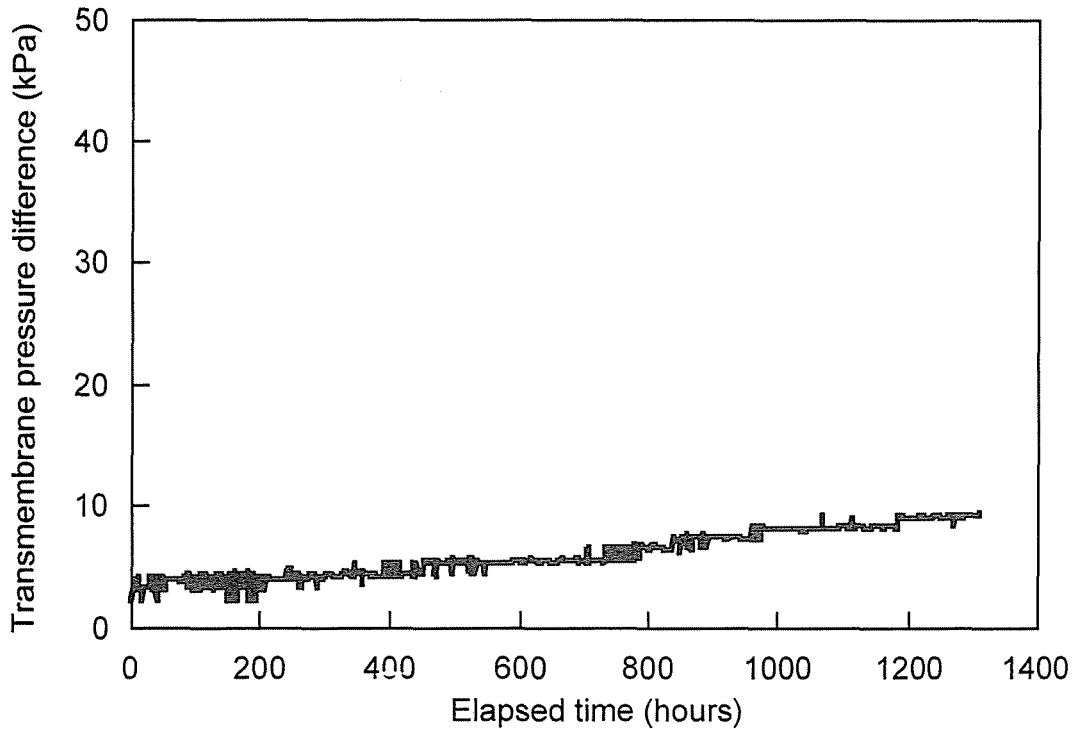


Fig. 3-18. Change in the transmembrane pressure difference in Run 3-6.

water (Run 3-6) was conducted.

The pre-treatment of the feed water was implemented by using the same membranes as the ones used in the previous operations. Run 3-6 was conducted using a feed water from which the substances, that could be cut off by the membranes, were removed. Therefore, in Run 3-6, the increase of the filtration resistance due to the feed water (tap water) could be diminished and all of the increase could be attributed to the nitrifiers.

The bacteria acclimated to the experimental condition were seeded in the membrane chamber at the beginning of Run 3-6. The concentration of the bacteria was 6 mg-SS/L. In Run 3-6, the concentration of  $\text{NH}_4^+\text{-N}$  in the feed water was maintained at a higher level compared to the previous operations (around 1.0 mg/L) in order to estimate the maximum filtration resistance

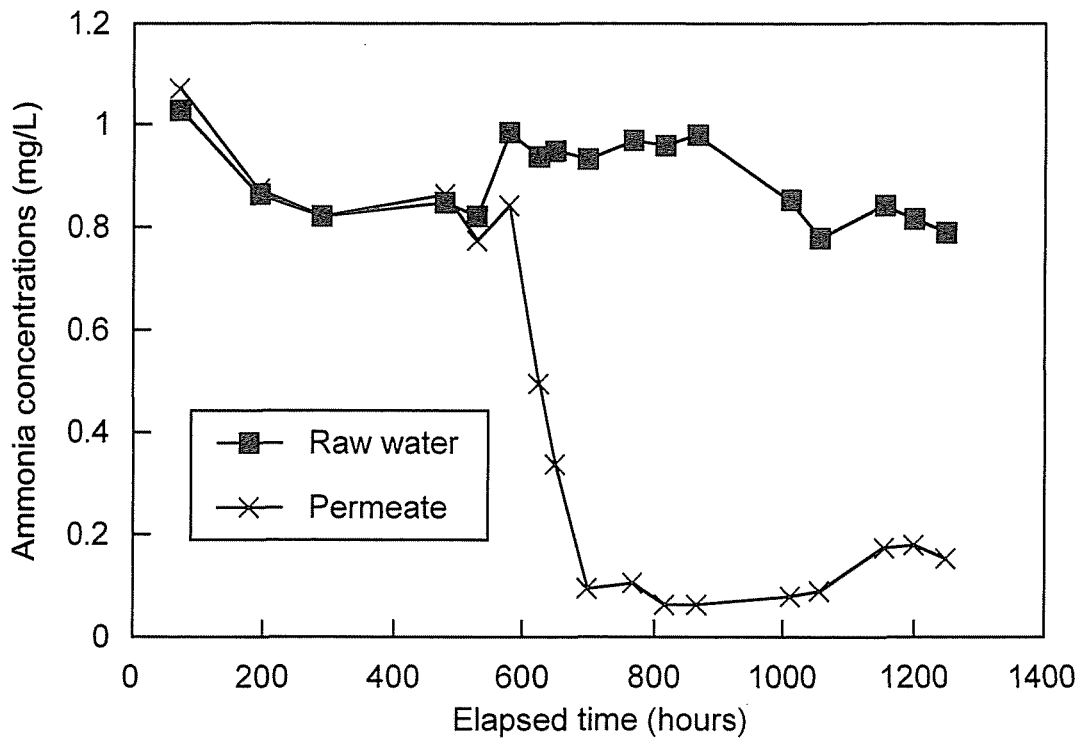


Fig. 3-19. Changes in the concentrations of  $\text{NH}_4^+\text{-N}$  in Run 3-6.

caused by the nitrifiers. Figs. 3-18 and 3-19 show the changes in the transmembrane pressure difference and the concentrations of  $\text{NH}_4^+\text{-N}$  in Run 3-6, respectively. It took 500 hours to observe good nitrification in Run 3-6 in spite of the inoculation of the accumulated bacteria. A possible explanation for this may be that some  $\text{NaClO}$  used in the chemical washing carried out just before the continuous operation may have remained in the pipes and damaged the bacteria. By the pre-treatment, substances in tap water that could deteriorate the membrane permeability were removed and consequently the increase of the pressure difference was significantly lower than in the previous runs. The required pressure difference was less than 10 kPa even after 1300 hours of the operation.

Fig. 3-20 shows the distribution of the filtration resistance in Run 3-6. As previously described, the fixed nitrifiers seemed

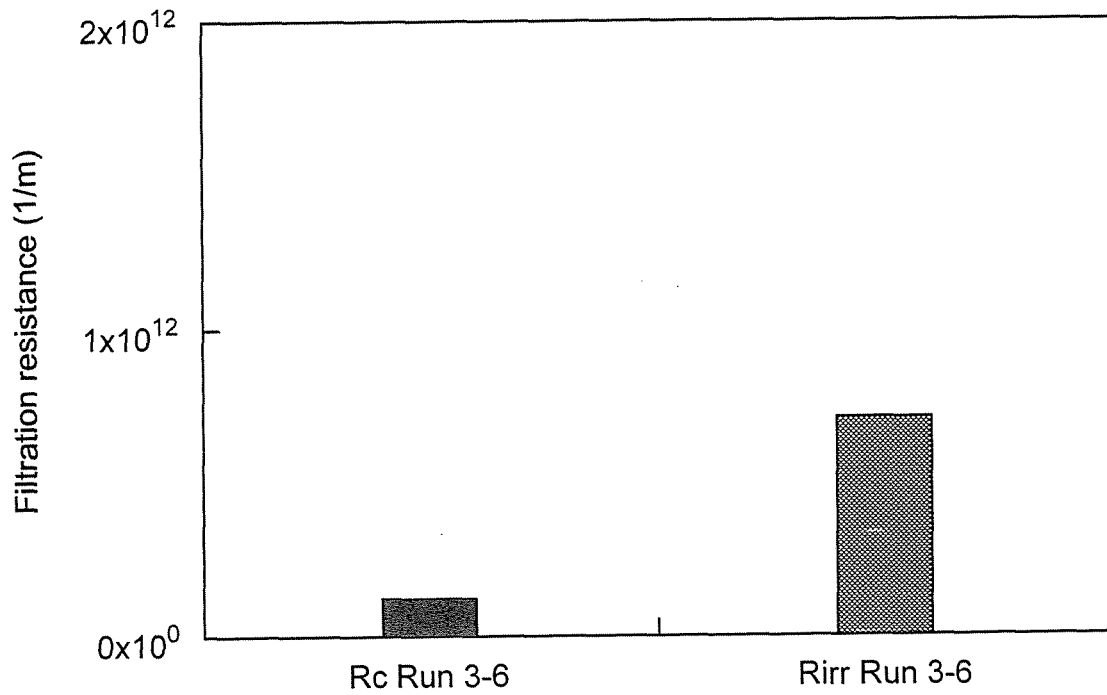


Fig. 3-20. Distribution of the filtration resistance in Run 3-6.

Table 3-6. Composition of the cake accumulated in Run 3-6.

VS	0.312
TS-VS	0.177
Protein	0.148
Carbohydrate	0.049

all values are indicated as g/m<sup>2</sup>.

to increase some cake resistance ( $R_c$ ), which was indicated by the difference between  $R_c$ s observed in Run 3-1 and 3-5 (Fig. 3-17). However, the magnitude of  $R_c$  observed in Run 3-6 was quite small. Table 3-6 shows the composition of the cake accumulated in Run 3-6. The amounts of both inorganic (TS-VS) and organic (VS) substances were considerably smaller compared to those of Runs 3-1 and 3-5. This was because the particles with larger sizes than the micropore size were removed by the pre-treatment. The inorganic fraction of the cake in Run 3-6 was reduced significantly. Although the amount of the microorganisms (indicated by protein) was also small, this amount was sufficient for the oxidation of low concentration of  $\text{NH}_4^+\text{-N}$ . It was found that the fixation of such a small quantity of microorganisms on the membrane increased  $R_c$  insignificantly. The magnitude of  $R_c$  caused by the nitrifiers that was estimated previously (the arrow in Fig. 3-17), was significantly bigger than the  $R_c$  in Run 3-6. The nitrifiers might, however show higher  $R_c$  value when existing with the other cake components (e.g. iron or humic substances) through some interactions.

In Run 3-6,  $R_{irr}$  was dominant. It was reasonable to consider that this  $R_{irr}$  was caused by EPS secreted by the nitrifiers in Run 3-6 since the pre-treatment was implemented. Comparing the magnitude of the  $R_{irr}$ s in Runs 3-1, 3-5 and 3-6, the magnitude in Run 3-6 was the smallest. It amounted to 70 % of that of Run 3-1 and 46 % of that of 3-5. This is, however, in contradiction to the assumption made in the previous section (3.2.6), that the nitrifiers hardly caused  $R_{irr}$ . Fig. 3-21 shows the changes in the UV-absorbance in Run 3-6. The UV-absorbance indicates the quantity of humic substances. Because of the pre-treatment, it was expected that the reduction of the UV-absorbance (humic concentration) did not occur in Run 3-6. From Fig. 3-21, however, one can see that some fraction of the humic substance was still

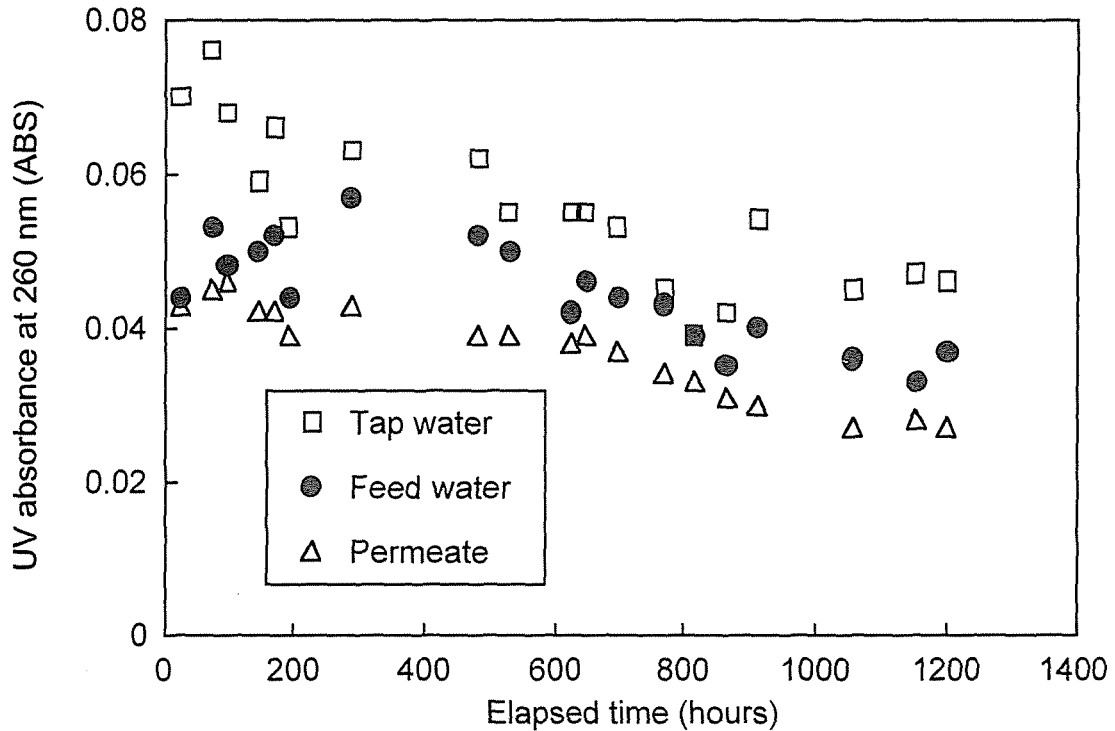


Fig. 3-21. Changes in the UV absorbance (the measurements were implemented with the 5 cm cells).

removed in Run 3-6. This removed humic substance should create some filtration resistance in Run 3-6. In Run 3-6, the feed water should only contain the humic substances with the molecular sizes that were smaller than the sizes of the membrane micropores. Humic substances with the low molecular weight tend to cause irreversible membrane fouling (Bian *et al.*, 1998). Most of the  $R_{irr}$  in Run 3-6 might be attributed to such small sized humic substances, too.

### 3.3. SUMMARY

Through this chapter, the filtration resistances created in the novel biofilm-membrane reactor (BMR) used for oxidation of low concentration of  $\text{NH}_4^+\text{-N}$ , were investigated. The experimental results and discussions conducted in this chapter can be



summarized as follows;

(1) The type of seeding has a significant influence on the increase of transmembrane pressure difference. If the seeding contain a lot of organic substances and heterotrophs, as it would when using seeding from a activated sludge plant, the increase of the pressure difference will be more rapid. The use of pure cultures of nitrifiers results in much lower increase of the pressure difference. A similar effect can be obtained by using the bacteria acclimated to the operating conditions, i.e. bacteria taken from biomass retained on the membrane.

(2) Most of the filtration resistance developed in the operation of the BMR can be explained by the reversible cake resistance. Therefore, the filter runs can be continued for a long time without the need for chemical membrane washing when an efficient physical membrane cleaning is applied.

(3) Increasing the rotational speed of the disks was found to be a very efficient membrane cleaning method (shear cleaning). When this procedure was applied every 500 hours, the filter run could be continuously operated and maintaining a good nitrification rate for approx. 3000 hours without any chemical membrane cleaning.

(4) Irreversible membrane fouling in the operation of the BMR is caused by some organic substances, most probably humic substances and carbohydrates. The produced nitrate may have an impact on the formation of this kind of membrane fouling by its interactions with organic substances.

(5) The fixation of the nitrifiers on the membrane surface for the oxidation of low concentrations of  $\text{NH}_4^+$ -N hardly increases

the filtration resistance.

#### REFERENCES

Aimer P., Taddei C., Lafaille J.-P. and Sanchez V. (1988) Mass transfer limitations during ultrafiltration of cheese whey with inorganic membranes. *Jour. of Mem. Sci.* **38**, 203-221

Bian R., Watanabe Y., Ozawa G. and Tambo N. (1998) Membrane fouling in ultrafiltration -Evaluation with batch filtration tests using surface river water-. *Jour. of Japanese Waterworks Association* **67**(1), 16-24 (in Japanese)

Bouhablia E. H., Aim R. B. and Buisson H. (1998) Microfiltration of activated sludge using submerged membrane with air bubbling (application to wastewater treatment). *Desalination* **118**, 315-322

Chiemchaisri C. and Yamamoto K. (1994) Performance of membrane separation bioreactor at various temperature for domestic wastewater treatment. *Jour. of Mem. Sci.* **87**, 119-129

Choo K.-H. and Lee C.-H. (1996) Membrane fouling mechanisms in the membrane-coupled anaerobic bioreactor. *Wat. Res.* **30**(8), 1771-1780

Choo K.-H. and Lee C.-H. (1998) Hydrodynamic behavior of anaerobic biosolids during crossflow filtration in the membrane anaerobic bioreactor. *Wat. Res.* **32**(11), 3387-3397

Dubois M., Gillers K. A., Hamilton J. K., Robers P. A. and Smith F. (1956) Colorimetric method for determination of sugars and related substances. *Analyt. Chem.* **28**, 350-356

Hobbie J. E., Daley R. J. and Jasper S. (1977) Use of nuclepore filters for counting bacteria by fluorescence microscopy. *Appl. Environ. Microbiol.* **33**, 1225-1228

Huang L. and Morrissey M. T. (1998) Fouling of membranes during microfiltration of surimi wash water: Role of pore blocking and surface cake formation. *Jour. of Mem. Sci.* **144**, 113-123

Labbe J.-P., Quemerais A., Michel F. and Daufin G. (1990) Fouling of inorganic membranes during whey ultrafiltration: Analytical methodology. *Jour. of Mem. Sci.* **51**, 293-307

Lowry O. H., Rosebrough N. J., Farr A. L. and Randall R. J. (1951) Protein measurement with the Folin phenol reagent. *J. biol. Chem.* **193**, 265-275

Schönborn W. (1986) *Biotechnology-vol. 8*, p.69, VCH Publishers, Weinheim

Scheiner D. (1976) Determination of ammonia and Kjeldahl nitrogen by indophenol method. *Wat. Res.* **10** (1), 31-36

Silverstein R. M., Bassler G. C. and Morrill T. C. (1991) *Spectrometric identification of organic compounds (5th edition)* Wiley, New York

Shimizu Y., Okuno Y., Uryu K., Ohtsubo S. and Watanabe A. (1996) Filtration characteristics of hollow fiber microfiltration membranes used in membrane bioreactor for domestic wastewater treatment. *Wat. Res.* **30**(10), 2385-2392

---

# CHAPTER

## 4

---

### **EFFICIENT CLEANING METHOD FOR THE NOVEL BIOFILM-MEMBRANE REACTOR (BMR)**

All the experiments shown in the previous chapters were conducted using feed water that contained almost no suspended solids. In practical applications of the BMR, the feed water that the BMR deals with will contain some suspended particles, even if some pre-treatments are implemented. In this chapter, the performance of the BMR in simultaneous oxidation of  $\text{NH}_4^+\text{-N}$  and removal of suspended solids will be examined and an efficient membrane cleaning method for the BMR will be demonstrated.

#### **4.1. SIMULTANEOUS OXIDATION OF $\text{NH}_4^+\text{-N}$ AND REMOVAL OF SUSPENDED SOLIDS EMPLOYING THE DEAD-END FILTRATION MODE (Run 4-1)**

The data shown in Chapters 2 and 3 were obtained with the experimental apparatus employing the dead-end filtration mode (see Fig. 2-2). Simultaneous oxidation of  $\text{NH}_4^+\text{-N}$  and removal of suspended solids was attempted with this dead-end filtration apparatus.

Kaolin (Wako Pure Chemical, Japan) was used as the suspended

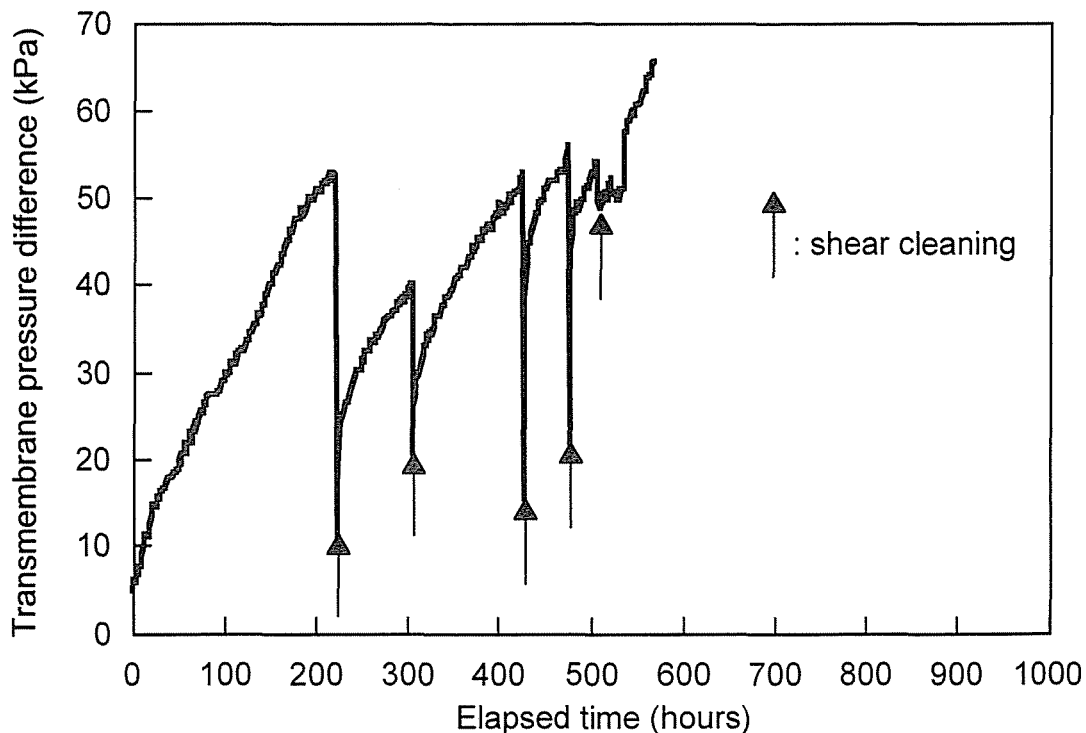


Fig. 4-1. Change in the transmembrane pressure difference in the operation where the feed water contained turbidity (Run 4-1).

solids and added to the feed water. The concentration of kaolin in the feed water was controlled to be around 5 turbidity units (TU). Turbidity was measured by using a turbidity meter (Mitsubishi-Kasei TR-35, Japan). The membrane flux and the rotational speed of the disks were fixed at 0.8 m/d and 50 rpm respectively, which was the same as in the previous experiments. Prior to the continuous operation, the bacteria acclimated to the experimental conditions were seeded in the membrane chamber at concentration of 100 mg-SS/L.

Fig. 4-1 shows the change in the transmembrane pressure difference in the filter run where the feed water contained turbidity (Run 4-1). The increase of the pressure difference was quite rapid. The required pressure difference reached 50 kPa within 200 hours of the operation in spite of the inoculation of acclimated bacteria. The amount of bacteria seeded in this

experiment was certainly bigger than the ones in the experiments discussed in Chapter 3. However, the influence of the amount of seeded bacteria was assumed to be small because the bacteria were previously acclimated to the experimental conditions, as discussed earlier.

Compared to the result from the experiments in the previous chapters, the accumulated cake resistance ( $R_c$ ) should be more significant in Run 4-1. This was apparently due to the turbidity added to the feed water. As described in Chapter 3, increasing the rotational speed of the disks was found to be an efficient cleaning method (shear cleaning) for reduction of  $R_c$ . Although shear cleaning was implemented many times (at the points indicated by arrows in Fig. 4-1) and in the same manner as Chapter 3, the efficiency of shear cleaning in this experiment was not found to be sufficiently effective. At about 600 hours of the operation, the membrane filtration could not be continued any more.

When dead-end filtration is carried out, all suspended particles contained in the feed water will be retained inside the membrane chamber. If these retained particles are dispersed and suspended, the filtration resistance should not increase so much. In Run 4-1, however, almost all of the suspended particles contained in the feed water were found to be fixed on the membrane surface. This was revealed by the measurement of suspended solids concentration in the chamber. If suspended solids (kaolin) are kept inside the chamber for a long period, they probably tend to fix on the membrane surface for some reasons, for example by interactions with extracellular polymeric substances (EPS) matrixes.

One possible measure for the prevention of particle

accumulation on the membrane, is to apply high shear stress continuously. This type of approach has been employed in many installed membrane systems. However, it certainly requires high energy consumption and does not suit to the BMR where microorganisms are to be fixed on the membrane. Another approach is continuous discharge of particles from the membrane chamber. This would mean that dead-end filtration is given up.

#### **4.2. MODIFICATION OF THE OPERATING METHOD FOR SIMULTANEOUS OXIDATION OF $\text{NH}_4^+$ -N AND REMOVAL OF SUSPENDED SOLIDS**

As described in the previous section, the dead-end filtration mode is not suitable for the BMR if both oxidation of  $\text{NH}_4^+$ -N and removal of suspended solids are required simultaneously. It was expected that a continuous overflow from the membrane chamber would be effective in preventing the accumulation of particles on the membrane. The BMR can successfully be operated in this manner without wash-out of nitrifiers, because they are fixed on the membrane. This is a significant advantage that the BMR has over other membrane bioreactors. Based on this, a modified membrane unit was assembled and the next experiment was conducted using this new unit.

Fig. 4-2 shows the flow chart of the modified experimental installation and Table 4-1 shows the characteristics of the new membrane unit. Inside the new unit, two membrane shafts were vertically mounted and the upper membrane disks were partially submerged in the water. Although no aeration equipment was used, the DO concentration in the chamber was always above 7 mg/l. This is because oxygen was induced by the air contact of the rotating upper disks. Overflow from the membrane chamber was controlled by the feed water pump. The overflow rate was maintained appropriately so that the water recovery defined as

Table 4-1. Specification of the membrane module.

Volume	10 liters
Diameter of disk	210 mm
Area of membrane	0.3 m <sup>2</sup>
Material of membrane	polysulfone
Cut-off molecular weight of membrane	750000

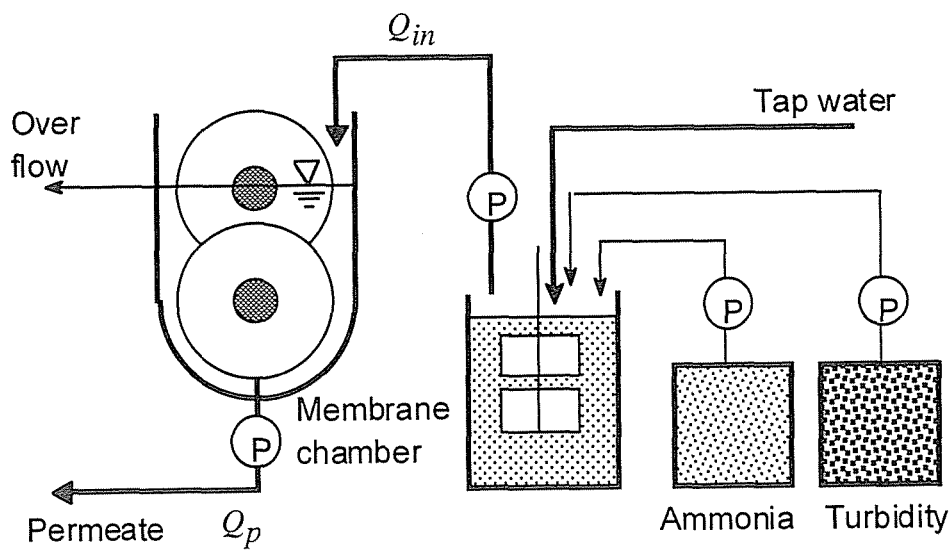


Fig. 4-2. Flow chart of the modified experimental installation for the simultaneous performance of the oxidation of ammonia and the removal of suspended solids.



$Q_p/Q_{in}$  was in the range of 0.9-0.95. In addition to establishing the overflow from the chamber, intermittent operation (15 minutes operation and 1 minute pause) was implemented in order to minimize the membrane fouling. The membrane flux and the rotational speed of the disks were fixed at 0.8 m/d and 50 rpm respectively, the same as in the previous experiments.

#### **4.3. SIMULTANEOUS OXIDATION OF $\text{NH}_4^+$ -N AND REMOVAL OF SUSPENDED SOLIDS WITH THE MODIFIED OPERATION (Run 4-2)**

Prior to the continuous operation, the acclimated bacteria were seeded in the membrane chamber. Dead-end filtration (i.e.  $Q_p/Q_{in}=1$ ) with tap water was carried out for 30 minutes in order to fix the biomass on the membrane surface. The membrane flux was 0.8 m/d even during this dead-end filtration period. At the beginning of the dead-end filtration period, the suspended solids concentration was 48 mg/l. Then it decreased to 16 mg/l after 30 minutes of operation. This means that the suspended solids were fixed on the membrane at the density of 1.06 g/m<sup>2</sup>. After the 30 minutes of dead-end filtration, the remaining suspension in the chamber was drained and the continuous operation with overflow from the membrane chamber (Run 4-2) was started. In the feed water, kaolin was added to a concentration of about 10 of the turbidity units. Figs. 4-3 and 4-4 show the changes in the transmembrane pressure difference and the concentration of  $\text{NH}_4^+$ -N, respectively. The  $\text{NH}_4^+$ -N concentration in the permeate gradually decreased and ample nitrification was observed after 400 hours of operation. Turbidity particles were completely removed over the duration of Run 4-2. Although turbidity was contained in the feed water, the increase rate of the transmembrane pressure difference remained moderate. The accumulation of suspended particles on the membrane surface was

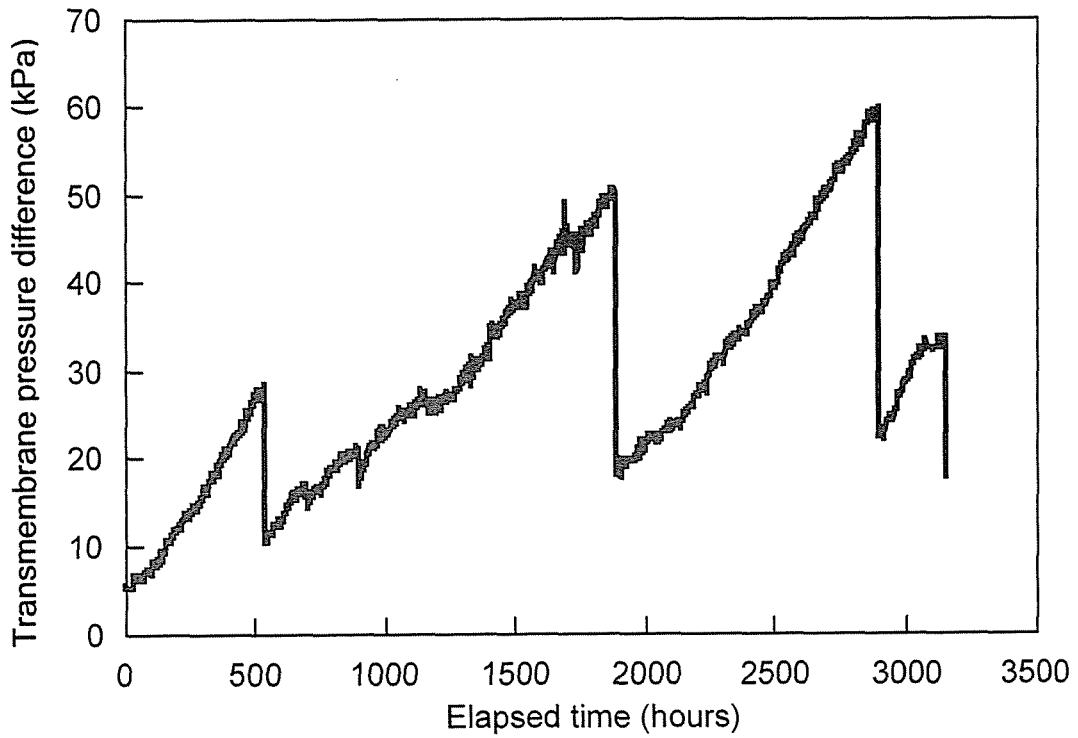


Fig. 4-3. Change in the transmembrane pressure difference in the modified operation (Run 4-2).

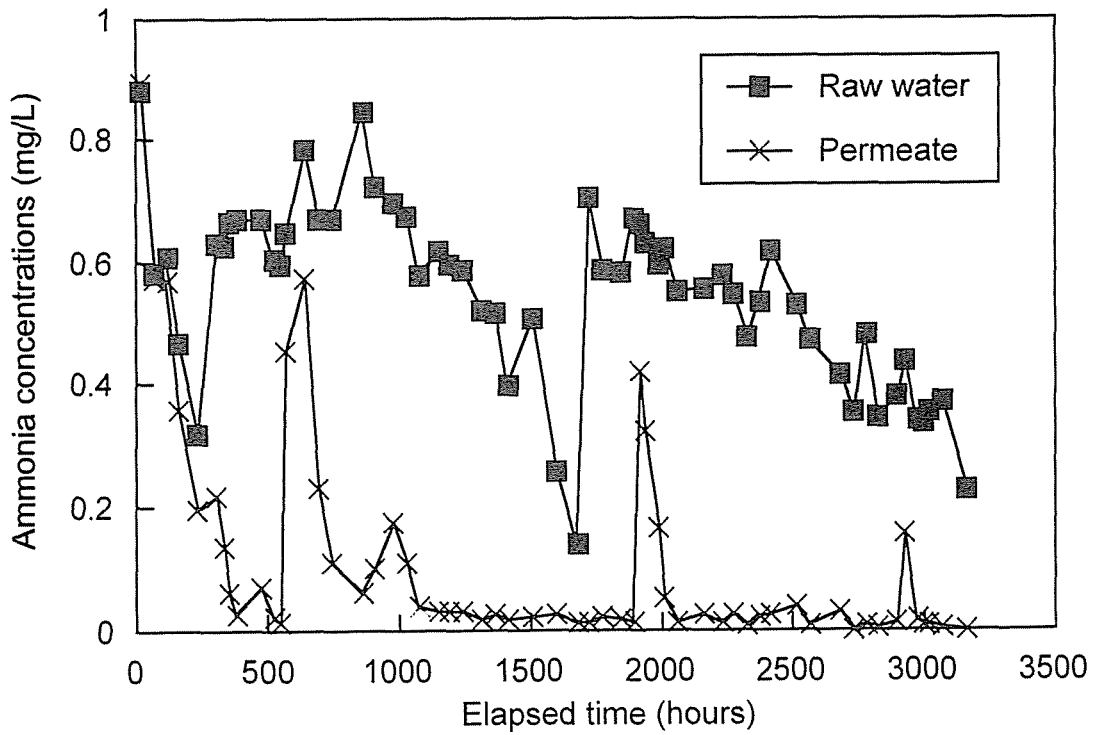


Fig. 4-4. Changes in the concentrations of NH<sub>4</sub><sup>+</sup>-N in Run 4-2.

controlled by the overflow from the chamber and the intermittent operation. On the upper disks (partially submerged), less suspended particle accumulation was observed. A possible explanation for this is that the fluid turbulence might be more intensive near the half-submerged disks compared to that of the fully-submerged disks. The first cleaning of the membranes was conducted after 500 hours when the value of the suction pressure was still low (i.e. 30 kPa). It was considered that cleaning of the membranes would be more effective if it was carried out before the pressure difference showed a dramatic increase. The procedure of membrane cleaning was the same as in Run 4-1 except for the rotational speeds. The rotational speeds of the upper shaft and the lower shaft were set at 50 rpm and 500 rpm, respectively.

Even though cleaning was implemented for 15 minutes, no recovery of membrane permeability was observed. The accumulated cake did not detach from the membrane surface what so ever. Turbidity particles seemed to fill the inside of the cake and reinforce its structure, which made it difficult to be removed.

In order to enhance the efficiency of the membrane cleaning, sponge particles cut randomly with scissors as shown in Photo. 4-1, were introduced into the membrane chamber and the rotational speed was again increased. The quantity of the sponge particles was small and their total dry volume was only about 60 ml. The rotational speeds and the duration of cleaning were the same as the ones without sponge particles. The cleaning of the membranes with sponge particles (called "sponge cleaning" hereafter) proved to be very effective in removing the attached cake. The water in the membrane chamber was mixed vigorously by the use of high rotational speed. The sponge particles were



Photo. 4-1. Sponge particles utilized in "sponge cleaning".

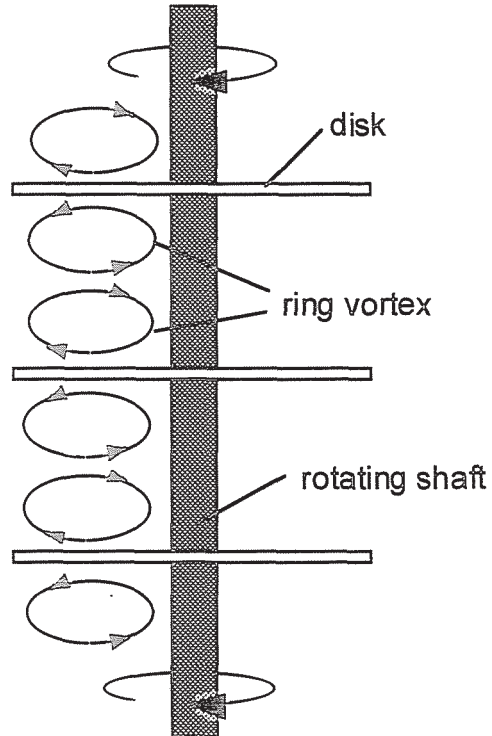


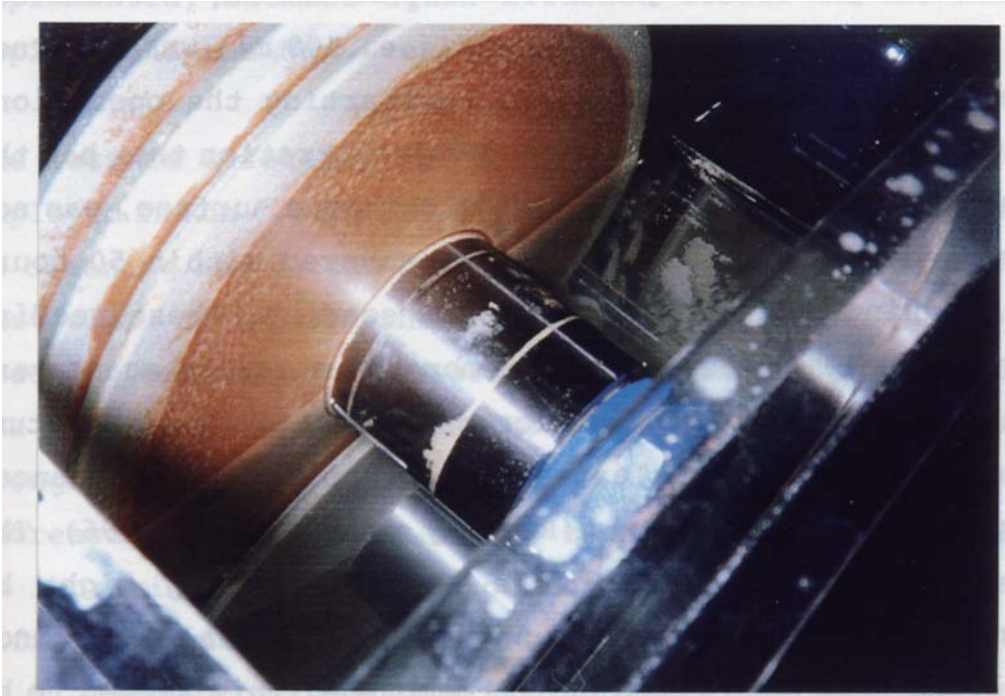
Fig. 4-5. Ring vortexes formed between the rotating disks (Ito *et al.*).

transported to the space between the membrane disks by the fluid motion. Ito *et al.* (1990) demonstrated that ring vortexes were formed between the rotating disks as described in Fig. 4-5. It was observed in the experiments presented here, that such vortexes introduced the sponge particles between the disks. This can be assumed to have caused the enhanced cake removal efficiency. After the sponge cleaning, most of the accumulated cake was removed from the membrane surface as seen in Photo. 4-2. The suspension containing the removed cake and the sponge particles were drained from the chamber and operation was restarted. The pressure difference decreased to about 10 kPa. Thereafter it started to increase slowly again.

The  $\text{NH}_4^+$ -N oxidation rate decreased to about 20 % after cleaning while almost complete nitrification was observed before cleaning. This was due to the removal of most of the nitrifiers attached to the membrane by cleaning and draining. For the rapid recovery of the  $\text{NH}_4^+$ -N oxidation rate, a part of the removed cake should be fixed on the membrane again and the necessary amount of the nitrifiers should be kept.

A second sponge cleaning was implemented at 1900 hours of operation in the same manner as the first cleaning with the sponge particles. As seen in Fig. 4-3, the suction pressure just previous to the second cleaning was almost twice as high as the one just previous to the first cleaning. This was probably because more suspended particles accumulated on the membrane and because compaction of the cake occurred. In the second cleaning, therefore, the cleaning efficiency was expected to decrease. However, the accumulated cake was easily removed again and consequently the pressure difference decreased considerably. The suspension containing the removed cake and

Before cleaning



After cleaning

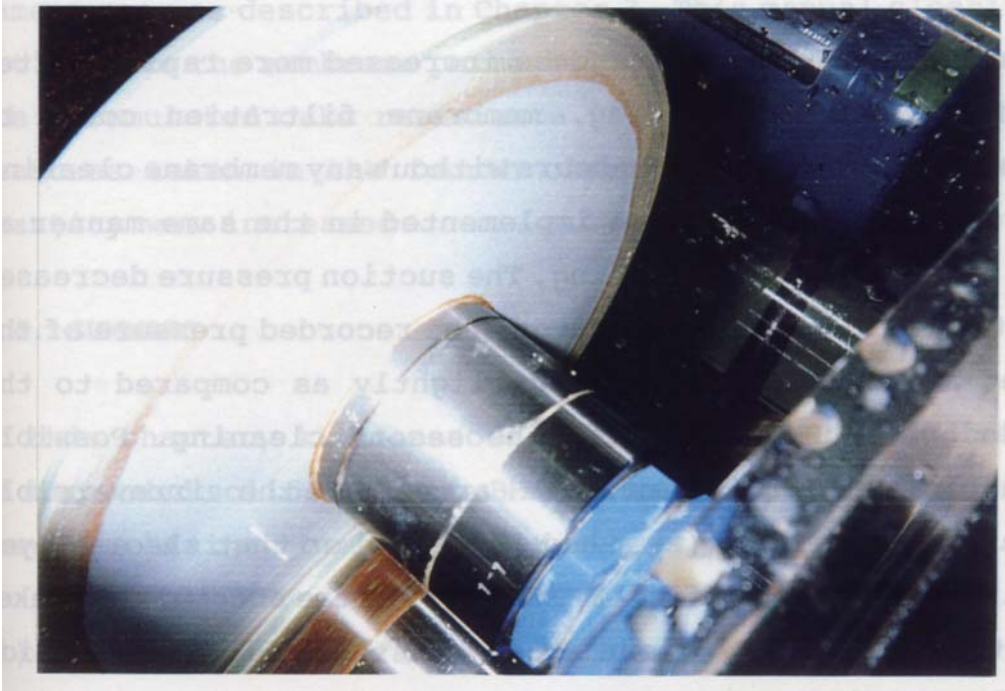


Photo. 4-2. Effect of "sponge cleaning".

the sponge particles was drained in the same manner as in the first cleaning. For the quick recovery of the  $\text{NH}_4^+$ -N oxidation rate, 5 % of the drained suspension (i.e. 500 ml) was returned to the membrane chamber prior to re-starting the operation. After the second cleaning, the dead-end filtration that had the purpose of fixing the biomass on the membrane surface, was not implemented.  $\text{NH}_4^+$ -N oxidation rate recovered within 50 hours after cleaning due to the additional seeding. These seeding bacteria, just removed from the membrane, attached again very quickly. For the attachment of microorganisms to the substratum, microbial "glue" such as extracellular polymeric substances (EPS) plays an important role (Ridgway and Flemming, 1996). The microorganisms seeded after the second cleaning might be covered with a substantial amount of the microbial glue since they already had been fixed on the membrane. This seemed to be the reason for the rapid attachment of the seeded bacteria and the quick recovery of the  $\text{NH}_4^+$ -N oxidation rate.

Although the pressure difference increased more rapidly after the second sponge cleaning, membrane filtration could be continued for more than 1000 hours without any membrane cleaning. A third sponge cleaning was implemented in the same manner as in the first and second cleaning. The suction pressure decreased after the third cleaning. However, the recorded pressure of the cleaned membrane had increased slightly as compared to the recorded pressure just after the second cleaning. Possible explanations of this increase are that the irreversible filtration resistance ( $R_{irr}$ ) had increased or that the employed cleaning method had difficulty in removing the accumulated cake. After the third sponge cleaning, 2 % of the drained suspension (200 ml) containing the removed cake that had just been detached from the membrane, was seeded in the chamber. Even though a

dead-end filtration period for the fixation of biomass was not implemented, biomass again attached itself on the membrane rapidly and the  $\text{NH}_4^+$ -N oxidation rate recovered.

The factors affecting the efficiency of the cleaning method employed in Run 4-2 are: a) the rotational speed, b) the duration of cleaning and c) the size, shape and quantity of the sponge particles. Optimizing these factors was expected to improve the cleaning efficiency. Therefore, the sponge particle quantity was increased to 400 ml of the total dry volume and a fourth sponge cleaning was conducted at 3100 hours of operation. Increasing the quantity of the sponge proved to be effective in improving cleaning efficiency and the required pressure difference was decreased to 18 kPa, which was almost the same as in the second cleaning. After the fourth sponge cleaning, the membranes were taken out of the membrane chamber and the membrane surfaces were manually cleaned with a sponge in the same manner as described in Chapter 3. This manual cleaning did not improve the membrane permeability, which means that all of the accumulated cake resistance ( $R_c$ ) could be removed by the measures taken in the fourth cleaning, in which the sponge quantity was increased.

#### 4.4. SUMMARY

In this chapter, simultaneous oxidation of  $\text{NH}_4^+$ -N and removal of suspended solids with the BMR was examined. The experimental results obtained can be summarized as follows;

(1) The dead-end filtration mode shown in Fig. 2-2 was found to be unsuitable for treating suspended solids due to the intensive accumulation of suspended particles on the membrane



surface, which caused a very rapid increase of the filtration resistance.

(2) Continuous overflow from the membrane chamber and intermittent operation proved to be effective in preventing the excess accumulation of the suspended particles.

(3) Shear cleaning utilizing the shear stress induced by the increased rotational speed did not work well in removing the accumulated cake when feed water contained turbidity.

(4) Sponge cleaning utilizing a small quantity of sponge particles, considerably improved the cleaning efficiency. Even when feed water contained turbidity, the accumulated cake resistance ( $R_c$ ) was completely cancelled by this modified cleaning method. When implementing sponge cleaning once every 1000-1500 hours, more than 3000 hours of operation could be carried out.

(5) For the quick recovery of the  $\text{NH}_4^+$ -N oxidation rate, a part of the removed cake should be returned to the membrane chamber after cleaning the membrane with sponge particles. It was found that, 200 ml of suspension containing the removed cake (equivalent to 2 % of the whole-accumulated cake) was enough to recover the nitrification capacity within 50 hours.

#### REFERENCES

Ito R., Hirata Y. and Ohshio A. (1990) Characteristics of flow and intermixing in ring vortexes induced by rotating multistage disks. *Kagaku Kougaku Ronbunshu* 16(5), 1013-1019 (in Japanese)

Ridgway H. F. and Flemming H.-C. (1996) Membrane biofouling. in *Water treatment: Membrane Process* (Mallevalle J., Odendaal P. E. and Wiesner M. R., editors) McGraw-Hill, New York.

---

# CHAPTER

## 5

---

### KINETIC ANALYSIS OF NITRIFYING BIOFILM DEVELOPED IN THE NOVEL BIOFILM-MEMBRANE REACTOR (BMR)

The proposed novel biofilm-membrane reactor (BMR) is quite analogous to the conventional biofilm process called Rotating Biological Contactor (RBC), invented about 100 years ago (Huang and Bates, 1980). The RBC has been mainly used for the treatment of wastewater. Many mathematical models have already been formulated for the prediction of performance of the RBC as well as for the reactor design (Famularo *et al.*, 1978; Mueller *et al.*, 1980; Gönenç and Harremöes, 1985; Watanabe *et al.*, 1989, 1990; etc.). When the RBC is applied for the oxidation of low concentrations of  $\text{NH}_4^+\text{-N}$ , nitrification rate should be limited by mass transport of  $\text{NH}_4^+\text{-N}$  to the biofilm (i.e. molecular diffusion of  $\text{NH}_4^+\text{-N}$  through the diffusion layer). When a comparison is made between the conventional RBC and the proposed process, it can be expected that the latter has an advantage especially in oxidation of low concentrations of  $\text{NH}_4^+\text{-N}$ . The reason for this is that mass transport to the biofilm would overwhelmingly be due to the advection flow created by the membrane filtration in the BMR while the mass transport due to

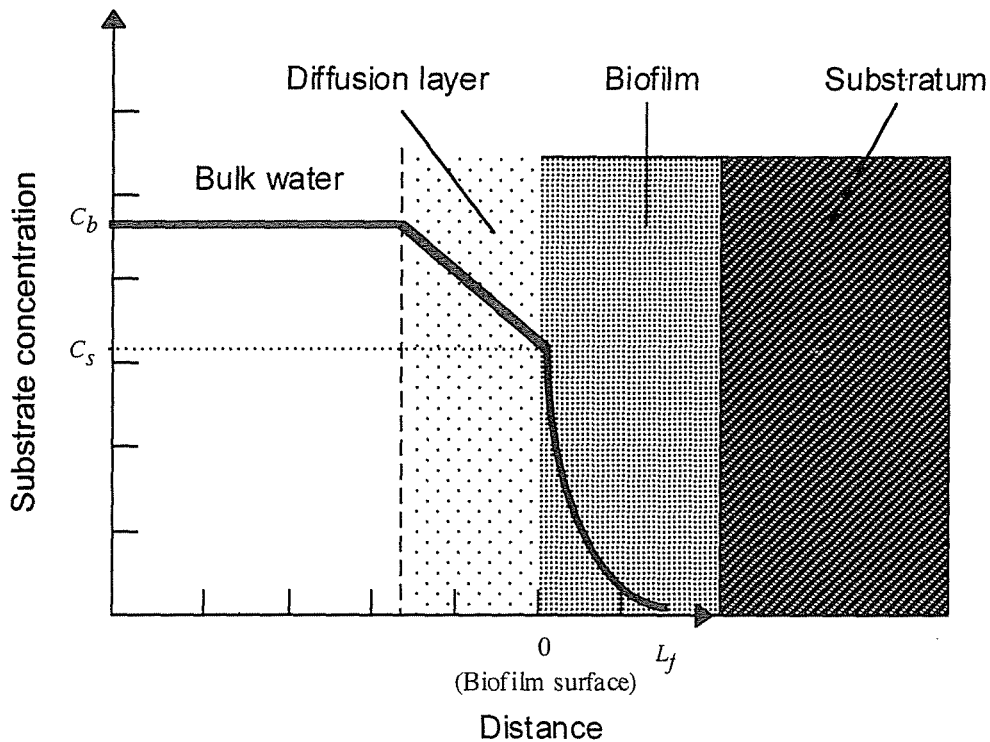


Fig. 5-1. Biofilm system for kinetic analysis.

molecular diffusion can be expected to be about the same in the two systems.

In this chapter, the advantages that BMR may have will be examined by using the conventional biofilm model (i.e. one dimensional, zero-order kinetics, assuming flat, homogeneous and continuous biofilm). It is often argued, however, that this kind of model does not describe practical conditions well. Thus the feasibility of applying the conventional biofilm model to the analysis of the BMR will also be discussed.

### 5.1. THE CONVENTIONAL BIOFILM MODEL

Watanabe *et al.* (1989, 1990) investigated a mathematical model dealing with the nitrification performance of the RBC in wastewater treatment. In their model, the reactor is assumed to be divided into three parts (i.e. bulk liquid, biofilm, and

diffusion layer adjacent to the biofilm) as shown in Fig. 5-1. They took molecular diffusion through the diffusion layer, diffusion in the biofilm and biological oxidation in the biofilm into consideration and formulated the relationship between bulk  $\text{NH}_4^+$ -N concentrations and  $\text{NH}_4^+$ -N flux to the biofilm.

Considering the mass balance at the biofilm surface at steady state, the following equation was derived by Watanabe *et al.* (1989,1990):

$$D_f \frac{d^2 C}{dz^2} = r \dots (5-1)$$

where  $D_f$  is the  $\text{NH}_4^+$ -N diffusivity in the biofilm ( $\text{m}^2\text{h}^{-1}$ ),  $C$  is the  $\text{NH}_4^+$ -N concentration in the biofilm ( $\text{gm}^{-3}$ ),  $z$  is the biofilm depth measured from the interface between liquid and biofilm (m) and  $r$  is the volumetric zero-order  $\text{NH}_4^+$ -N consumption rate within the biofilm ( $\text{gm}^{-3}\text{h}^{-1}$ ). Eq. (5-1) can be solved with the boundary conditions as below:

$$C = C_s \text{ at } z = 0 \dots (5-2)$$

$$\frac{dC}{dz} = 0 \text{ at } z = L_f \dots (5-3)$$

where  $C_s$  is the  $\text{NH}_4^+$ -N concentration at the surface of the biofilm ( $\text{gm}^{-3}$ ) and  $L_f$  is the depth, to which  $\text{NH}_4^+$ -N penetrates into the biofilm. The biofilm that will develop in the proposed process is expected to be sufficiently thin for  $\text{NH}_4^+$ -N to penetrate the whole depth of the biofilm. Thus in this study the boundary conditions expressed with Eq. (5-3) can be slightly modified as shown below:

$$\frac{dC}{dz} = 0 \text{ at } z = L \dots (5-4)$$

where  $L$  is the thickness of the biofilm (m). Solving Eq. (5-1) with the previously stated boundary conditions yields:

$$C = \frac{r}{2D_f} z^2 - \frac{rL}{D_f} z + C_s \dots (5-5)$$

The  $\text{NH}_4^+$ -N flux through the diffusion layer at steady state is given (Watanabe *et al.*, 1989,1990):

$$F_b = \frac{D_w}{L_d} (C_b - C_s) \dots (5-6)$$

where  $F_b$  is the  $\text{NH}_4^+$ -N flux through the diffusion layer at steady state ( $\text{gm}^{-2}\text{h}^{-1}$ ),  $D_w$  is the  $\text{NH}_4^+$ -N diffusion coefficient in the water ( $\text{m}^2\text{h}^{-1}$ ),  $C_b$  is the  $\text{NH}_4^+$ -N concentration in the bulk water ( $\text{gm}^{-3}$ ) and  $L_d$  is the thickness of the external diffusion layer (m).  $L_d$  can be calculated by the equation that Levich (1962) showed for the submerged rotating disk:

$$L_d = 1.16 \left( \frac{D_w}{\nu} \right)^{\frac{1}{3}} \left( \frac{\nu}{2\pi N_r} \right)^{\frac{1}{2}} \dots (5-7)$$

where  $\nu$  is the kinematic viscosity of water ( $\text{m}^2\text{sec}^{-1}$ ) and  $N_r$  is the rotating speed of the disk (rps). At steady state, the  $\text{NH}_4^+$ -N flux outside the diffusion layer and the flux at the biofilm surface should be identical. Therefore, the following equation can be formulated (Watanabe *et al.*, 1989,1990):

$$\frac{D_w}{L_d}(C_b - C_s) = -D_f \left( \frac{dC}{dz} \right)_{z=0} \dots (5-8)$$

Derivation of Eq. (5-5) gives:

$$\frac{dC}{dz} = \frac{r}{D_f} z - \frac{r}{D_f} L \dots (5-9)$$

By substituting Eq. (5-9) into Eq. (5-8),  $C_s$  can be determined as follows:

$$C_s = C_b + \lambda - (\lambda^2 + 2\lambda C_b)^{1/2} \dots (5-10)$$

$$\lambda \equiv \frac{D_f}{D_w} r \frac{L_d^2}{D_w} \dots (5-11)$$

According to Williamson and McCarty (1976) and Horn and Hempel (1997),  $D_f$  was considered to be  $0.8 D_w$  in this study. By the use of Eqs. (5-6), (5-10) and (5-11), one can calculate the  $\text{NH}_4^+$ -N flux to the biofilm at various bulk  $\text{NH}_4^+$ -N concentrations.

## 5.2. VERIFICATION OF THE FEASIBILITY OF THE CONVENTIONAL BIOFILM MODEL

### 5.2.1. Limitations with the conventional model

In the last decade, some new techniques have provided interesting information about the biofilm structure. Especially, application of confocal scanning laser microscopy (CSLM) has shown that the structure of the actual biofilm is quite heterogeneous and not homogenous and continuous as many model assume (Massol-Deya *et al.*, 1995, Okabe *et al.*, 1998). In addition, the presence of highly permeable water channels within the biofilm, which is supposed to influence on the mass

transport, has clearly been demonstrated (de Beer, 1994). The conventional biofilm model described before assumes, however, that the biofilm is homogeneous and continuous. Therefore, the conventional model may be inadequate for describing the phenomena occurring in biofilms.

In the BMR, however, the advection flow caused by the membrane filtration holds the biofilm "artificially" on the membrane surface, and the biofilm structure may, therefore, be more homogeneous and continuous, than in biofilms formed in conventional biofilm reactors, such as the RBC. This may indicate that the conventional biofilm model might still be feasible to the analysis of the biofilm in a BMR.

#### 5.2.2. Materials and methods

In order to examine the feasibility of applying the conventional biofilm model to analysis of the biofilm in the proposed process, some experiments and calculations were implemented. Firstly, the structure of the biofilm developing on the membrane was investigated by cryosectioning the biofilm. Secondly, the  $\text{NH}_4^+$ -N concentration profile within the biofilm was measured with microelectrode in order to compare it with the calculated profile. Finally, a comparison was carried out between the model calculations and the experimental results obtained in the long-term filter run leading to discussions about reaction kinetics. Fig. 5-2 shows the flow chart of the experimental installation. The same membrane unit as the one described in Chapter 4 was used. However, the membranes were not mounted on the upper shaft for the reasons of simplification. The membrane flux and the rotational speed of the disks were fixed at 0.8 m/d and 50 rpm respectively, which was the same as in the previous experiments. Overflow from the membrane chamber was always



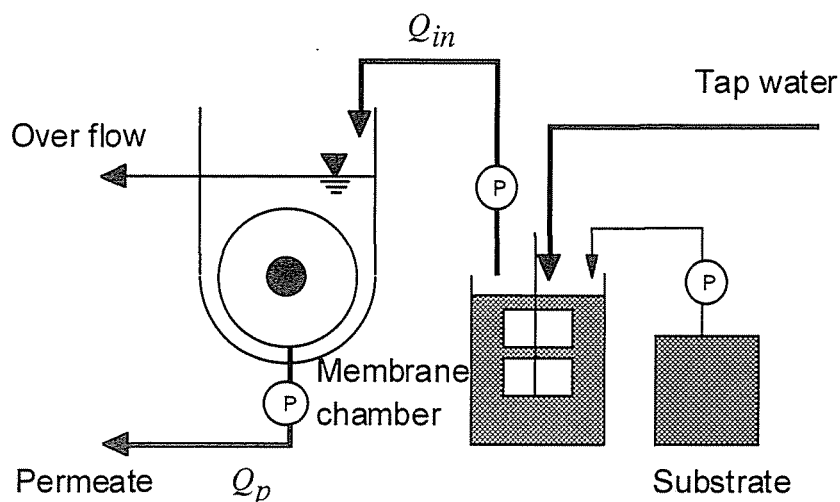


Fig. 5-2. Flow chart of the continuous filter run.

produced, resulting in a water recovery ratio, defined as  $Q_p/Q_{in}$ , in the range of 0.9-0.95. Tap water was supplemented with ammonia ( $\text{NH}_4\text{Cl}$ ), inorganic carbon ( $\text{NaHCO}_3$ ) and basic minerals ( $\text{KH}_2\text{PO}_4$ ,  $\text{MgSO}_4 \cdot 7\text{H}_2\text{O}$  and  $\text{NaCl}$ ). The concentration of  $\text{NH}_4^+\text{-N}$  in the feed water was maintained around 1.0 mg/L. The water temperature and pH were not continuously controlled, but they varied in the membrane chamber between 15.2-23.0 °C and 7.0-7.5, respectively. No aeration was attempted in this experiment, however, the dissolved oxygen (DO) concentration in the membrane chamber was always above 7 mg/L. This ensured that nitrification was not limited by oxygen supply.

Employing the experimental conditions as described above, a long-term filter run (about 850 hours) was carried out in order to grow an active, nitrifying biofilm. Prior to the continuous operation, a small quantity of the activated sludge, previously acclimated to the autotrophic environment, was fixed on the membrane surface. The fixation of the microorganisms was implemented by 2 hours dead-end filtration (i.e. no overflow from the membrane chamber) of microorganisms suspension. The mass per area of the fixed microorganisms was 0.61 g/m<sup>2</sup>.

After finishing the continuous filter run, several biofilm samples were cut out with the membrane for cryosectioning and microelectrode measurements. The preparation of the specimen for cryosectioning was implemented following the procedure described by Okabe *et al.* (1998). The cut out biofilm samples (attached on the membrane) were embedded with Tissue-Tek<sup>®</sup> OCT-compound (Miles, Elkhart, IN) and rapidly frozen. The frozen samples were cut into 30 micron-thick vertical sections with a cryostat (Reichert-Jung Cryocut 1800, LEICA) at -20 °C. The sectioned specimen was fixed on a glass slide (Cell-line, USA), and allowed to air dry. The specimen was examined with a normal light microscopy. The determination of the biofilm thickness was carried out with image analysis software provided by Zeiss. The microelectrode was used to determine the  $\text{NH}_4^+$ -N concentration profile in the biofilm. The measurement with the microelectrode was implemented just after finishing the continuous filter run. The protocol of the preparation of the microelectrode for  $\text{NH}_4^+$ -N measurement was obtained from de Beer *et al.* (1997).

In the determination of  $\text{NH}_4^+$ -N concentration, the indophenol method (Scheiner, 1976) was used for the low concentration range and ion chromatography (DIONEX DX-100, column; DIONEX CS3) was used for the high concentration range.

### 5.2.3. Comparison between the model calculation and the microelectrode measurement

The changes in the transmembrane pressure difference and  $\text{NH}_4^+$ -N concentration in the continuous filter run are shown in Figs. 5-3 and 5-4, respectively. Since the constant flow rate operation was employed, the pressure difference needed increased slowly. Sufficient  $\text{NH}_4^+$ -N oxidation was observed

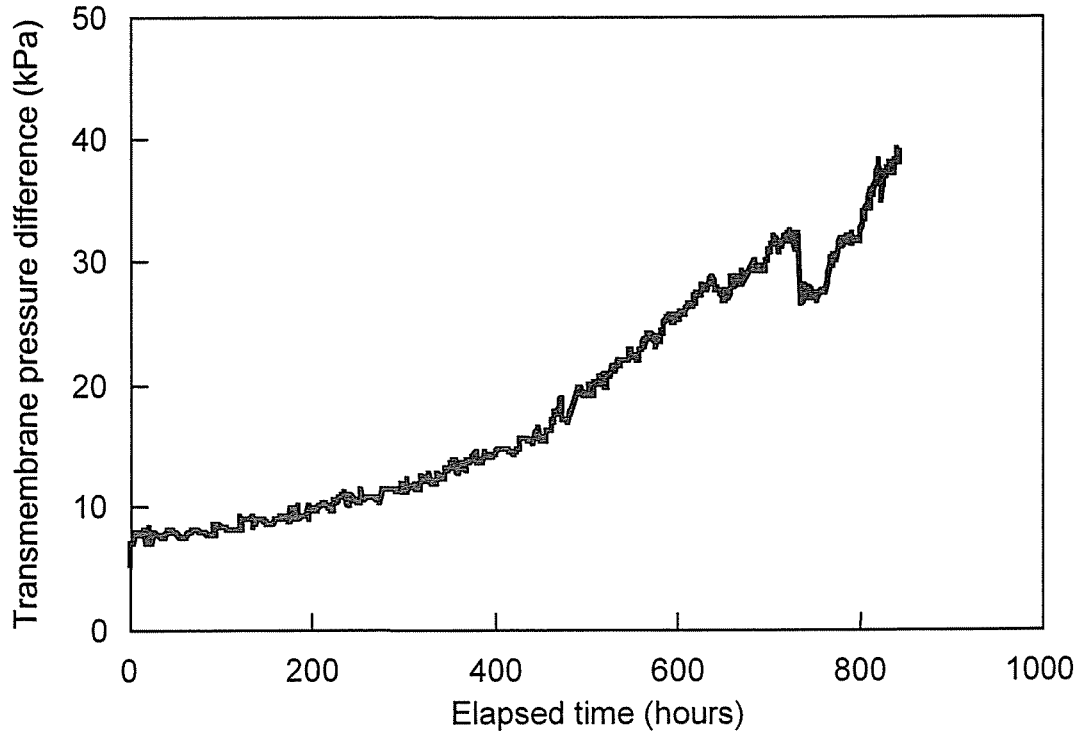


Fig. 5-3. Change in the transmembrane pressure difference.

after 300 hours of operation. At the end of the continuous filter run, a cross-section view of the biofilm attached on the membrane (Photo. 5-1) was obtained by the means described above. From Photo. 5-1, it can be seen that the biofilm formed had a very dense and homogeneous structure, which was quite different from the ones seen in the biofilms grown in wastewater (Okabe *et al.*, 1998). The dense structure demonstrated in Photo 5-1 was probably caused by the fact that the biofilm studied had been under influence of suction pressure. The picture analysis of the biofilm, seems to support the view that the "conventional" biofilm model, that assumes a flat, continuous and homogeneous structure of the biofilm, is reasonable to use for this kind of biofilm.

Obviously, the reaction rate within the biofilm is of significant importance when calculating results based on biofilm models. In previously published biofilm models,

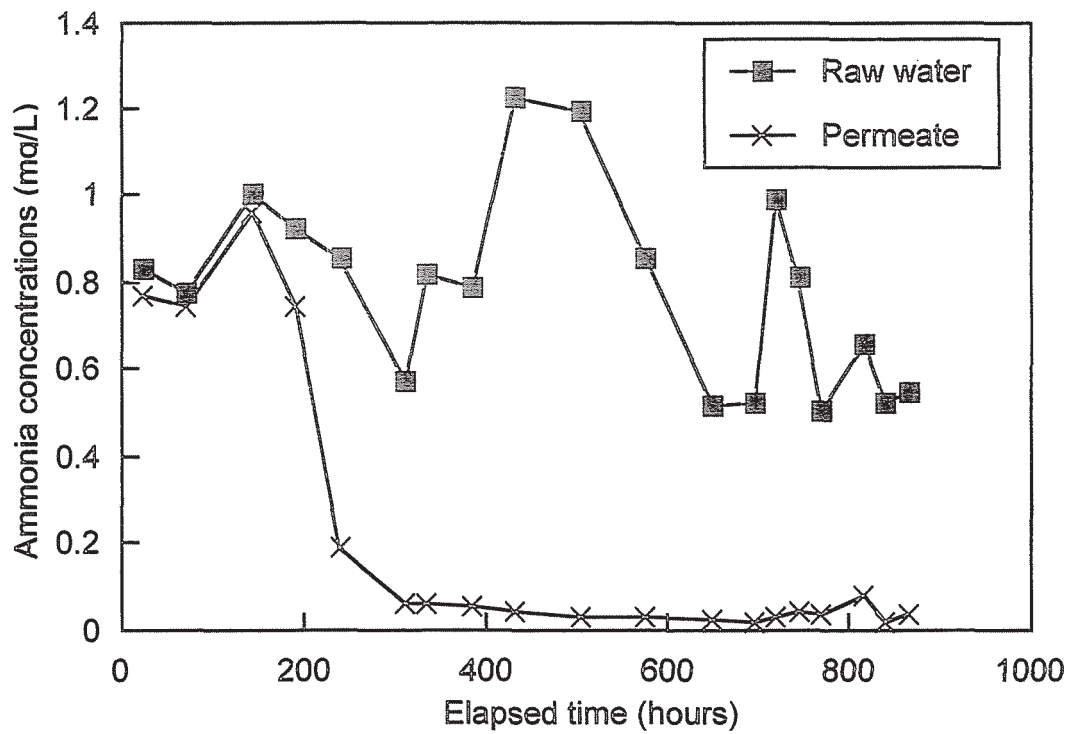


Fig. 5-4. Changes in the  $\text{NH}_4^+$ -N concentrations.

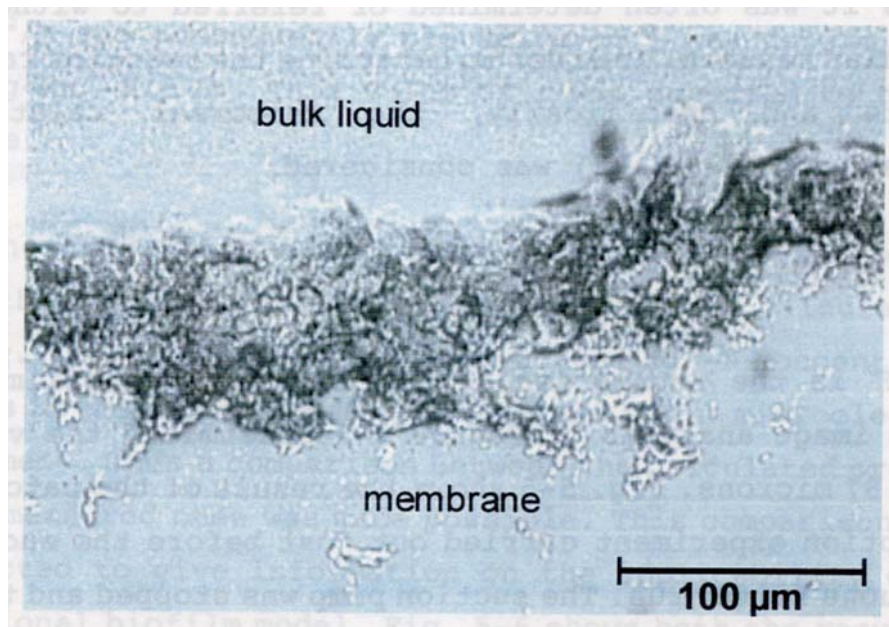


Photo. 5-1. Cross-section view of the biofilm attached on the membrane.

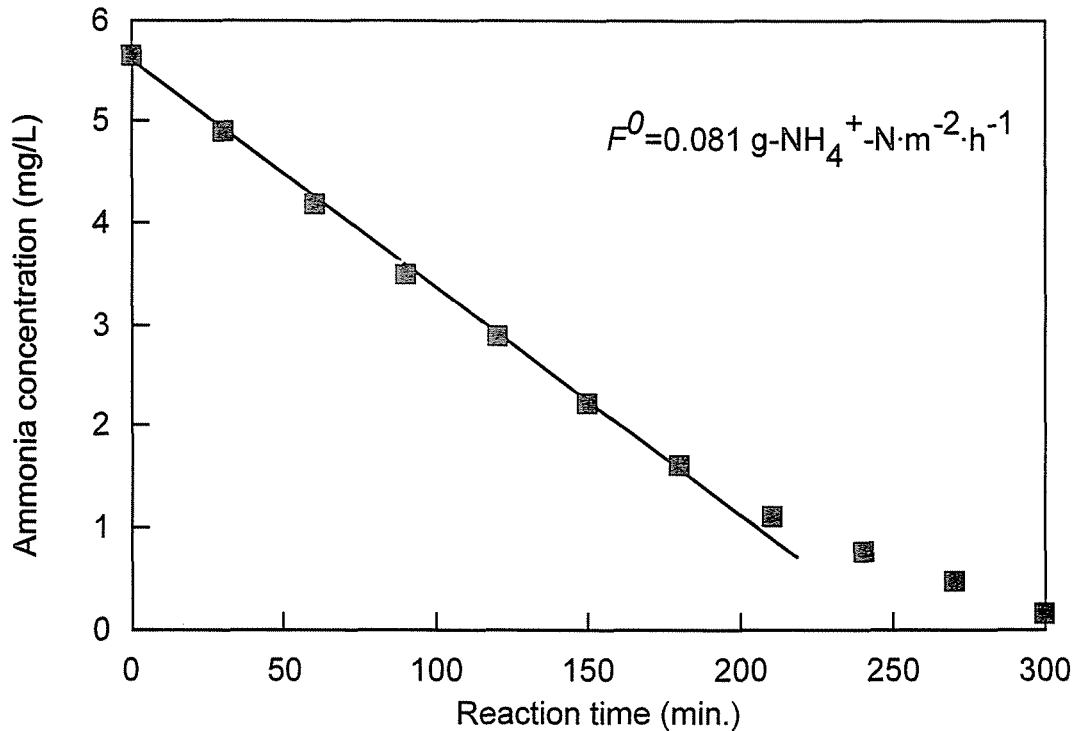


Fig. 5-5. Batch experiment for determination of the reaction rate.

however, the value of the reaction rate might not be appropriate because it was often determined or referred to without any particular reasons. In order to determine the reaction rate more accurate and specifically, the universal relationship expressed as Eq. (5-12) was considered:

$$F^0 = rL \dots (5-12)$$

where  $F^0$  is the zero-order  $\text{NH}_4^+\text{-N}$  flux to the biofilm ( $\text{gm}^{-2}\text{h}^{-1}$ ). The image analysis of Photo. 5-1 determined the value of  $L$  to be 87 microns. Fig. 5-5 shows the result of the batch  $\text{NH}_4^+\text{-N}$  consumption experiment carried out just before the end of the continuous filter run. The suction pump was stopped and the disk rotational speed was decreased to 15 rpm in the batch experiment. Also, aeration in the chamber with air pump was implemented in order to ensure sufficient DO level. From the linear slope drawn

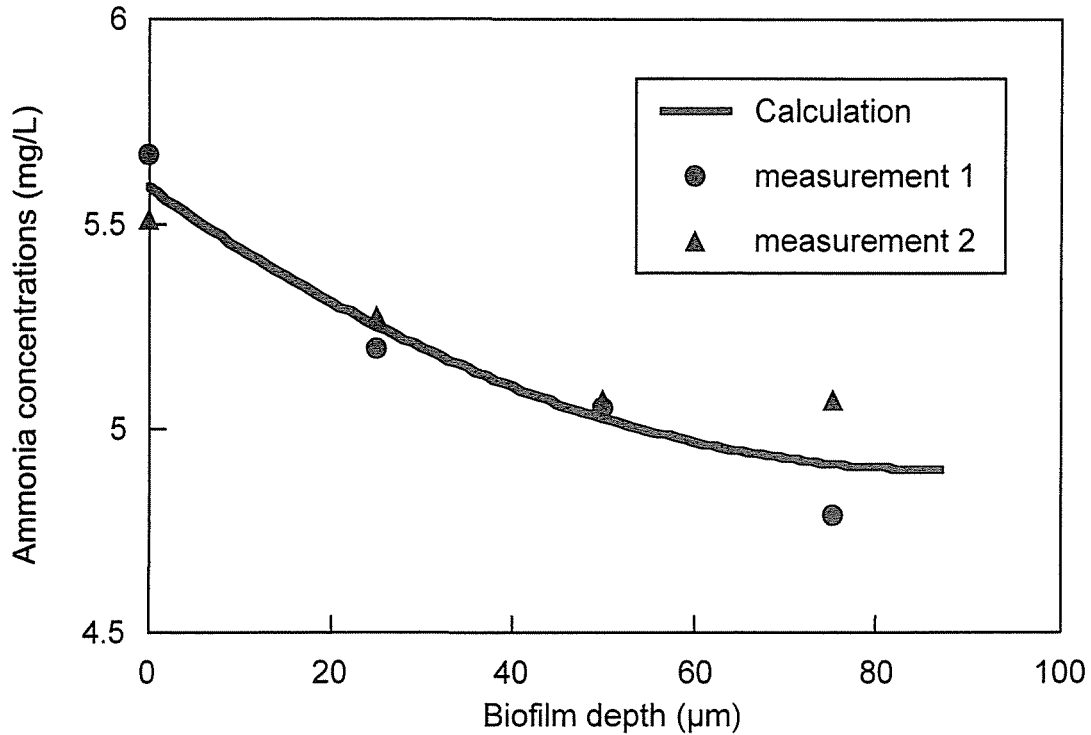


Fig. 5-6. Comparison between the calculated  $\text{NH}_4^+$ -N profile in the biofilm and the measured ones.

in Fig. 5-5, the value of  $F^0$  was determined to be  $0.081 \text{ g-NH}_4^+\text{-N/m}^2\text{/h}$  and consequently the value of  $r$  was determined to be  $930 \text{ g-NH}_4^+\text{-N/m}^3\text{/h}$ . This value of  $r$  was supposed to be very accurate.

Utilizing this value of  $r$ , the  $\text{NH}_4^+$ -N concentration profile within the biofilm attached on the membrane was calculated by using Eq. (5-5). In this study, the actual  $\text{NH}_4^+$ -N concentration profiles in the biofilm were also obtained by the microelectrode measurement. Thus a comparison between the calculated profiles and the measured ones was made possible. This comparison would be expected to give information on the applicability of the conventional biofilm model. Fig. 5-6 shows both the results of the calculation and the microelectrode measurements. The microelectrode measurements were carried out on biofilms operated at the bulk concentration of  $6.1 \text{ mg-NH}_4^+\text{-N/L}$ , which

was similar to the one in the batch experiment (Fig. 5-5). The value  $1.53 \text{ cm}^2/\text{d}$  was used for  $D_w$  (Lide, 1998) and the mean value of the microelectrode measurements was used for  $C_s$ . The values of  $r$  and  $L$  were determined previously. As demonstrated in Fig. 5-6, the model calculation proved to be very close to the measured profile.

There are some researches that have notified the importance of the heterogeneity of the biofilm structure in the model calculation. For instance, Horn and Hempel (1997) reported that only taking into account the porosity inside the biofilm could explain the experimental results. However, considering the accuracy of the value of  $r$  determined in this study, the conventional and simple biofilm model (assuming flat, homogeneous and continuous structure) was still useful and accurate in the analysis of the biofilm grown in the proposed process. One can assume that this was so because the studied biofilm actually had a simple structure.

#### 5.2.4. Analysis of data obtained in the continuous filter run

In the previous section, the feasibility of the conventional biofilm model to analysis of the nitrifying biofilm in BMR was demonstrated. In this section, analysis of data obtained in continuous operation will be examined based on the conventional model.

As described before, the  $\text{NH}_4^+\text{-N}$  flux at arbitrary bulk  $\text{NH}_4^+\text{-N}$  concentration can be calculated with Eqs. (5-6), (5-10) and (5-11). The  $\text{NH}_4^+\text{-N}$  flux calculated with these equations was compared with the fluxes observed during continuous operation. The latter was expected to be higher, because the advection flow toward the biofilm caused by the membrane filtration would

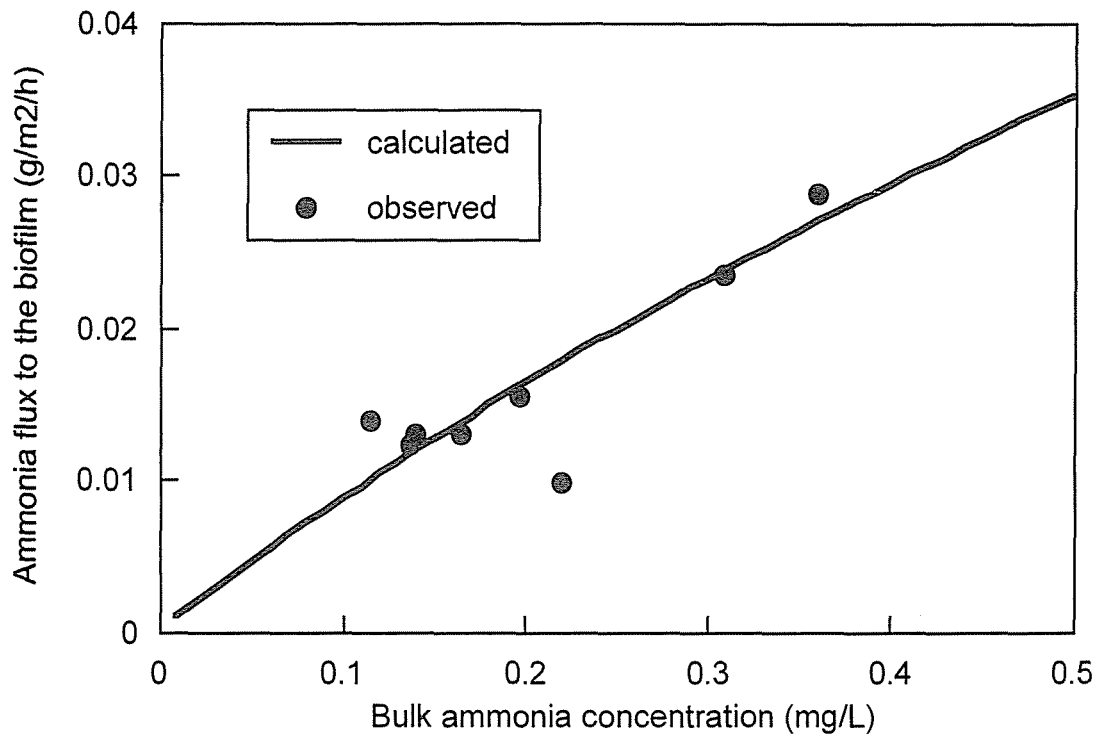


Fig. 5-7. Comparison between the calculated ammonia flux and the measured ones (zero-order).

increase the  $\text{NH}_4^+\text{-N}$  flux. The value of  $r$  was determined in the previous section ( $930 \text{ g-NH}_4^+\text{-N/m}^2\text{/h}$ ) and used in this calculation again.  $L_d$  was calculated with Eq. (5-7). The calculation determined the  $L_d$  to be  $67 \mu\text{m}$  when the disk rotates at 50 rpm.

Fig. 5-7 shows the comparison of the observed  $\text{NH}_4^+\text{-N}$  fluxes in the continuous filter run and the calculated  $\text{NH}_4^+\text{-N}$  flux. The data observed after 300 hours, when the steady state was achieved, were plotted in Fig. 5-7. The observed fluxes were almost the same as the calculated one, which was different from the expectation. However, this result does not mean that the employed model is inadequate for the analysis or that the determination of the magnitude of  $r$  was wrong. This discrepancy is assumed to reflect that  $\text{NH}_4^+\text{-N}$  oxidation does not proceed in zero-order kinetics in the low concentration range such as



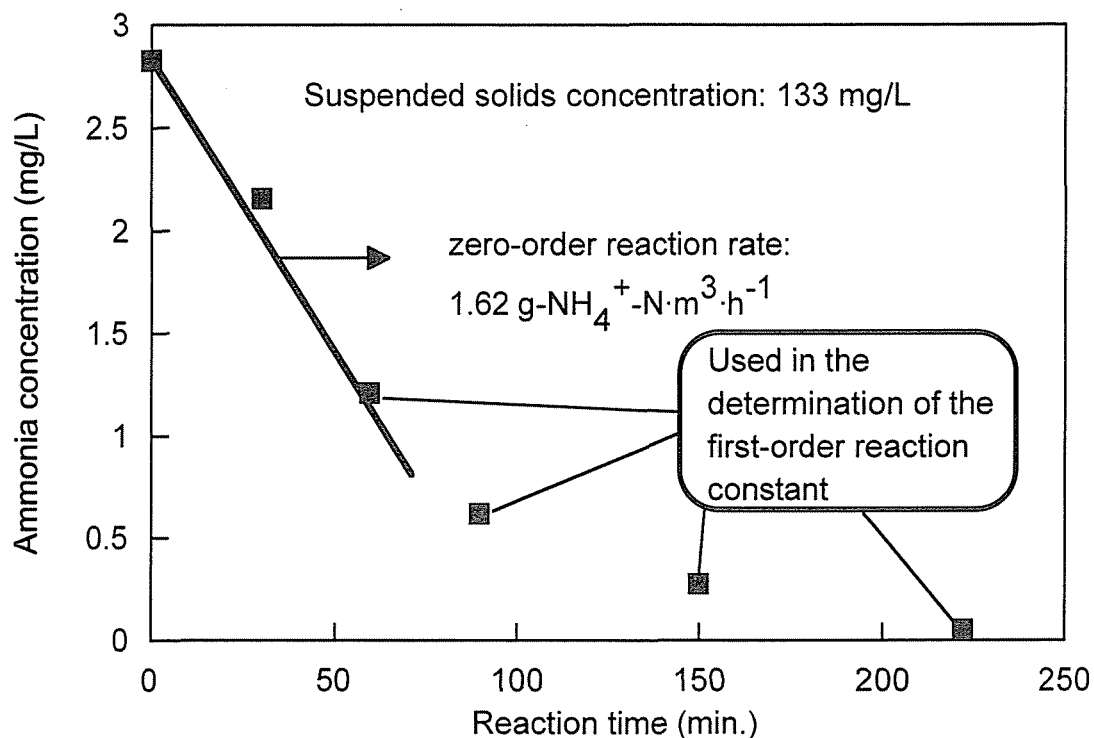


Fig. 5-8 Batch experiment with the biomass removed from the membrane.

below 1.0 mg/L.

A portion of the biofilm was removed and collected at the end of the continuous filter run. The collected biomass was homogenized in the substrate solution and then a batch  $\text{NH}_4^+-\text{N}$  consumption experiment was carried out with the suspended biomass. Fig. 5-8 shows the result of the batch experiment. Obviously, zero-order kinetics did not apply in the whole range of bulk concentrations that was examined in the continuous filter run. In the low concentration range,  $\text{NH}_4^+-\text{N}$  oxidation was found to proceed according to first-order kinetics, and the first-order reaction constant in the batch experiment was determined to be 1.15 (1/h). This reaction constant, however, cannot immediately be used for the analysis of the continuous filter run.

Usually, the reaction rate increases with increase of biomass. Therefore, the first-order reaction constant in the continuous filter run was estimated from the difference in biomass concentration between the batch experiment and the continuous filter run. In the batch experiment, the biomass concentration was 133 g-SS/m<sup>3</sup>. At the end of the continuous filter run, the biomass concentration in the biofilm was 93.4 kg-SS/m<sup>3</sup>. Compared to the batch experiment condition, the biomass concentration in the biofilm was about 700 times higher in the biofilm of the continuous filter run. Consequently, the first-order reaction constant in the continuous operation ( $k$ ) was assumed to be 808 (1/h). This assumption of  $k$  was reasonable because the zero-order reaction rate obtained from Fig. 5-8 (=1.62 g-NH<sub>4</sub><sup>+</sup>-N/m<sup>3</sup>/h) was fairly close to  $r/700$  (=1.33 g-NH<sub>4</sub><sup>+</sup>-N/m<sup>3</sup>/h).

The first-order reaction model is described by:

$$D_f \frac{d^2C}{dz^2} = kC \dots (5-13)$$

The boundary conditions are that  $C=C_s$  at  $z=0$ , and  $dC/dz=0$  at  $z=L$ . Solving Eq. (5-13) with the boundary conditions yields (Melcer *et al.*, 1995):

$$C = C_s \frac{\cosh(r_1(L-z))}{\cosh(r_1L)} \dots (5-14)$$

$$\cosh(u) = 0.5(e^u + e^{-u}) \dots (5-15)$$

$$r_1 = \sqrt{\frac{k}{D_f}} \dots (5-16)$$

Similar to the zero-order analysis, the NH<sub>4</sub><sup>+</sup>-N flux through the diffusion layer at steady state can be calculated as follows :

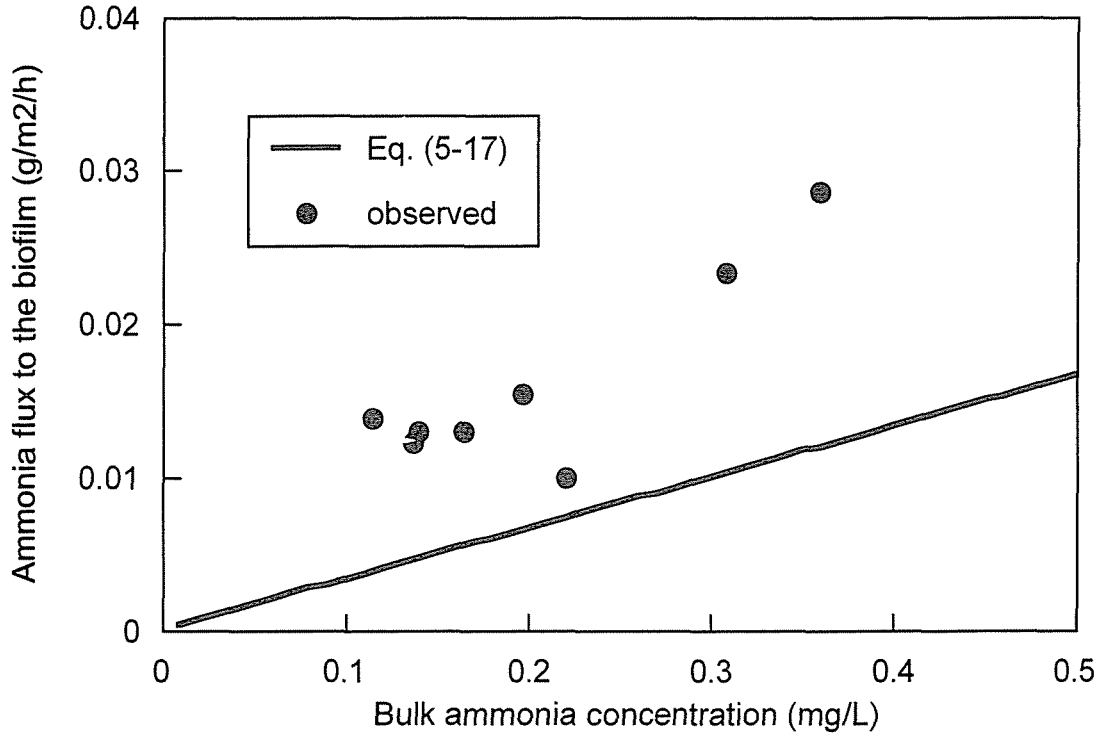


Fig. 5-9. Comparison between the calculated ammonia flux and the observed ones (first-order).

$$F_b = \left( \frac{D_w}{L_d} \right) \frac{D_f r_1 \tanh(r_1 L)}{D_f r_1 \tanh(r_1 L) + (D_w / L_d)} C_b \dots (5-17)$$

Fig. 5-9 shows the comparison of the observed  $\text{NH}_4^+$ -N fluxes in the continuous filter run and the calculated  $\text{NH}_4^+$ -N flux using Eq. (5-17). In opposition to what was found from the zero-order analysis (Fig. 5-7), the observed fluxes were higher than the calculated ones. This shows the enhancement of the mass transport toward the biofilm due to the advection flow.

Taking the advection flow into consideration, Eq. (5-13) can be modified as:

$$D_f \frac{d^2 C}{dz^2} - u \frac{dC}{dz} - kC = 0 \dots (5-18)$$

where  $u$  is the advection flow rate to the biofilm ( $\text{mh}^{-1}$ ), equal to the membrane permeate flux. Solving Eq. (5-18) with the same boundary conditions as Eq. 5-13 yields:

$$C = Ae^{\lambda_1 z} + Be^{\lambda_2 z} \dots (5-19)$$

$$A = \frac{-\lambda_2 e^{\lambda_2 L}}{\lambda_1 e^{\lambda_1 L} - \lambda_2 e^{\lambda_2 L}} C_s \dots (5-20)$$

$$B = \frac{\lambda_1 e^{\lambda_1 L}}{\lambda_1 e^{\lambda_1 L} - \lambda_2 e^{\lambda_2 L}} C_s \dots (5-21)$$

$$\lambda_1 = \frac{u/D_f + \sqrt{(u/D_f)^2 + 4k/D_f}}{2} \dots (5-22)$$

$$\lambda_2 = \frac{u/D_f - \sqrt{(u/D_f)^2 + 4k/D_f}}{2} \dots (5-23)$$

Even when taking the advection flow into consideration, the  $\text{NH}_4^+$ -N flux outside the diffusion layer and the flux at the biofilm surface should be identical. Therefore, the following equation can be formulated:

$$\frac{D_w}{L_d} (C_b - C_s) + uC_b = -D_f \left( \frac{dC}{dz} \right)_{z=0} + uC_s \dots (5-24)$$

From Eq. (5-24),  $C_s$  can be determined as:

$$C_s = \frac{\left( \frac{D_w}{L_d} + u \right) C_b}{\left( \frac{D_w}{L_d} + u \right) - \frac{e^{\lambda_1 L} - e^{\lambda_2 L}}{\lambda_1 e^{\lambda_1 L} - \lambda_2 e^{\lambda_2 L}} \lambda_1 \lambda_2 D_f} \dots (5-25)$$

Now, the  $\text{NH}_4^+$ -N flux with the advection flow can be given as follows:

$$F_b = \frac{D_w}{L_d} (C_b - C_s) + uC_b \dots (5-26)$$

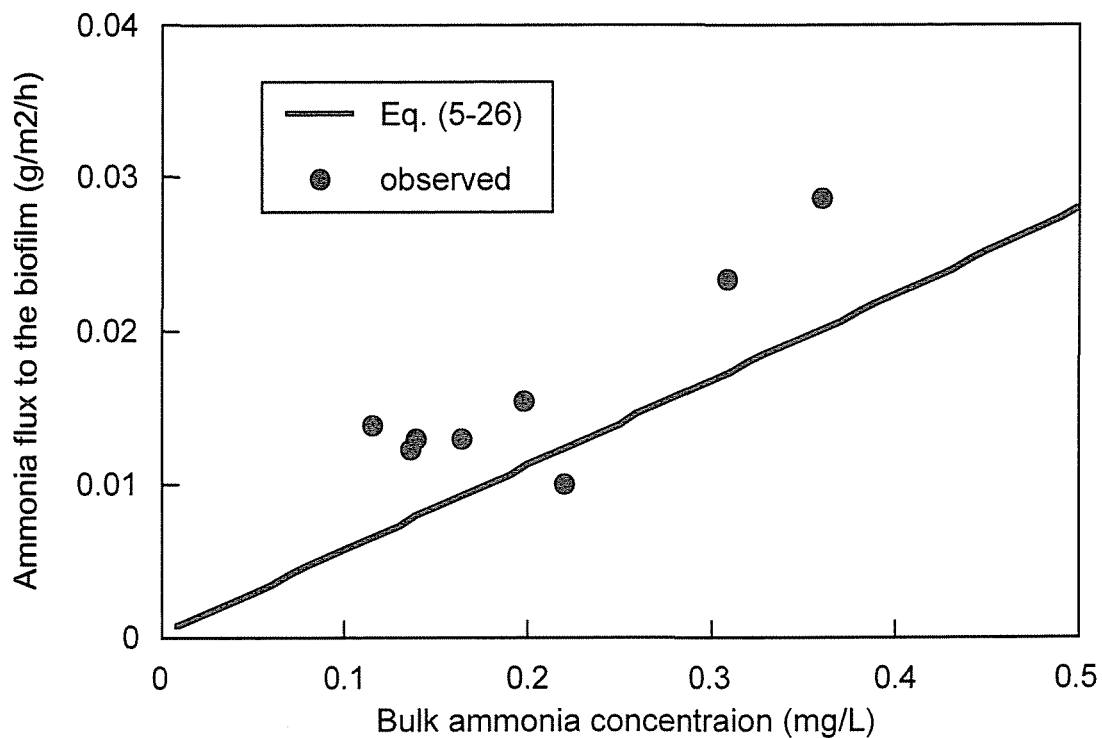


Fig. 5-10. Comparison between the ammonia flux with Eq. (5-26) and the observed fluxes.

The calculated flux considering the advection flow is drawn in Fig. 5-10 and was found to correspond better with the measured data even though the observed flux is still higher than the calculated one. Similar calculations were implemented with Eq. (5-26) substituting higher values of  $k$  and the results are shown in Fig. 5-11. The flux calculated with higher values of  $k$  fitted with the measured data well, which means that the magnitude of the first-order reaction constant,  $k$ , might have been underestimated.

In BMR, treated water is collected from the bottom of the biofilm where  $\text{NH}_4^+\text{-N}$  concentration should be the lowest in the system. This can certainly improve the treatment efficiency. In order to assess this advantage with BMR, the  $\text{NH}_4^+\text{-N}$  concentration profile in the biofilm was calculated with Eq. (5-19) and

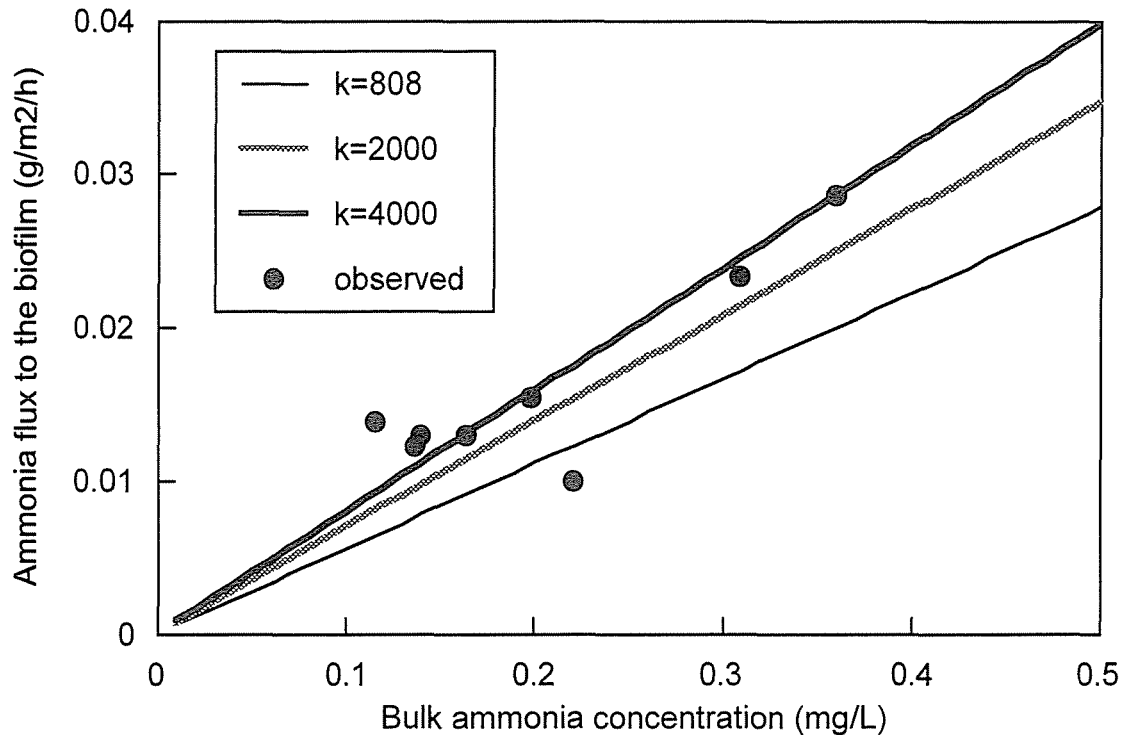


Fig. 5-11. Calculation of the ammonia flux with Eq. (5-26) substituting various  $k$ .

compared with the experimental results obtained in the continuous filter run.

Calculations were carried out using two different values of  $k$ ,  $809 \text{ h}^{-1}$  (the value previously determined in this chapter) and  $4000 \text{ h}^{-1}$ . Figs. 5-12 and 5-13 show the results of the comparisons. The comparisons were made with respect to the last three sampling occasions. In determining  $C_s$ , Eq (5-25) was employed. The other parameters used in the calculation were the same as the ones used in the calculations for Figs. 5-10 and 5-11. The model calculation and experimental data were fairly close, which demonstrated that our hypothesis was reasonable. Similar to the  $\text{NH}_4^+\text{-N}$  flux calculation, the model could express the experimental results better when  $k$  larger than  $809 \text{ h}^{-1}$  was employed. It should be recognized that, therefore, there was an underestimation in the determination of  $k$ . The accurate value

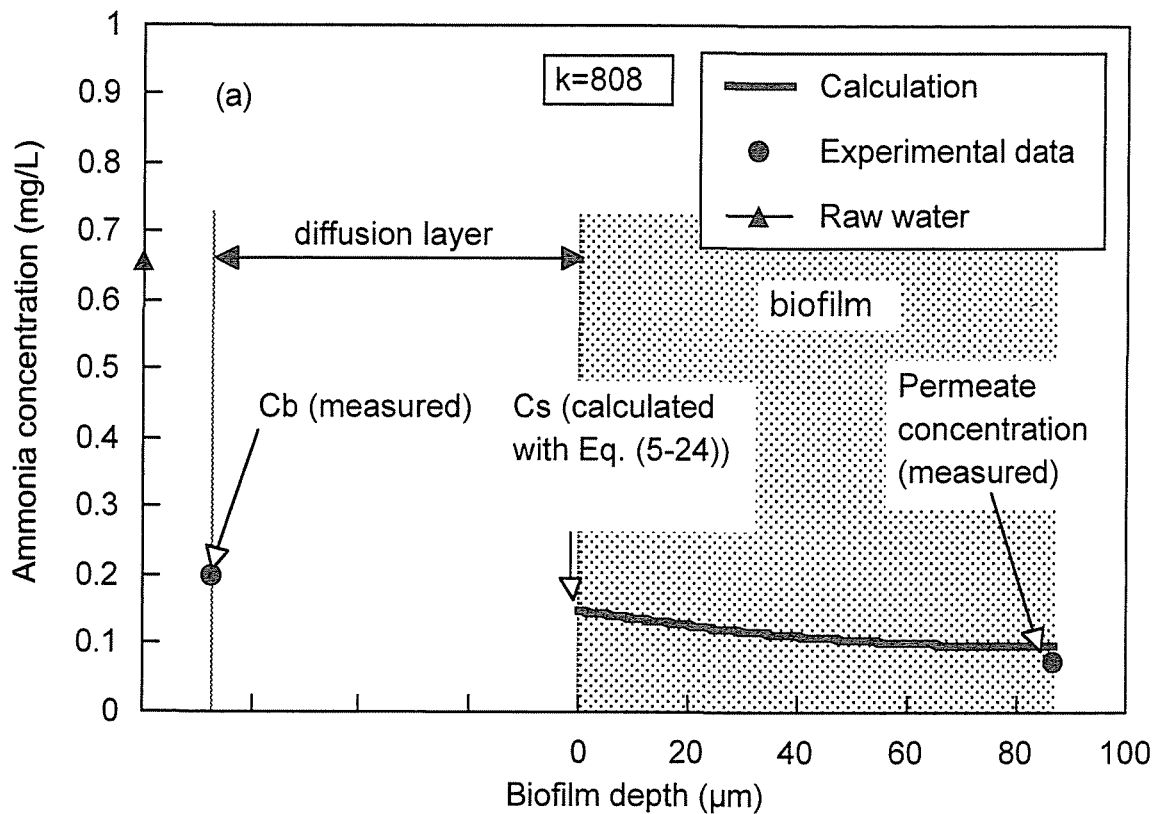


Fig. 5-12. Comparison between the calculated ammonia concentration profiles in the biofilm and the measured ammonia concentrations. ( $k=808 \text{ h}^{-1}$ ,  $C_b$ : ammonia concentration in the bulk water,  $C_s$ : ammonia concentration at the surface of the biofilm.)

of  $k$  within the biofilm seemed to be around  $4000 \text{ h}^{-1}$ .

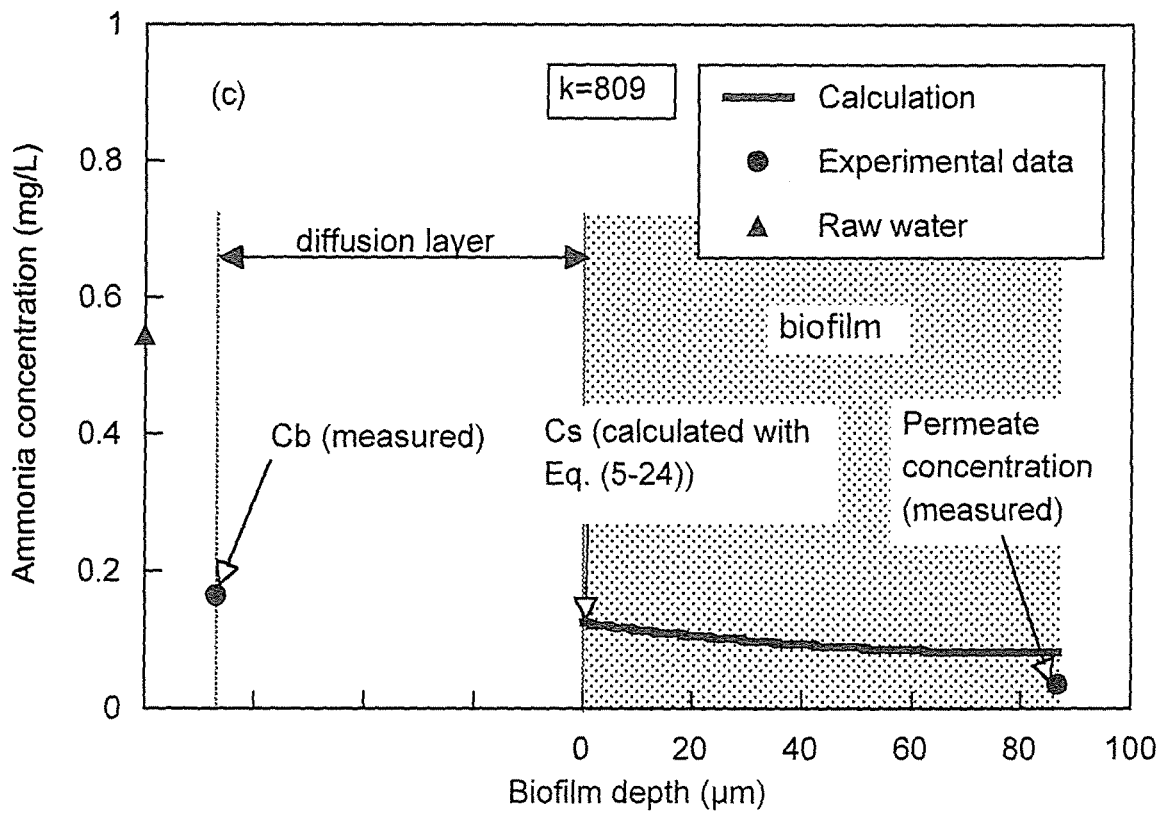
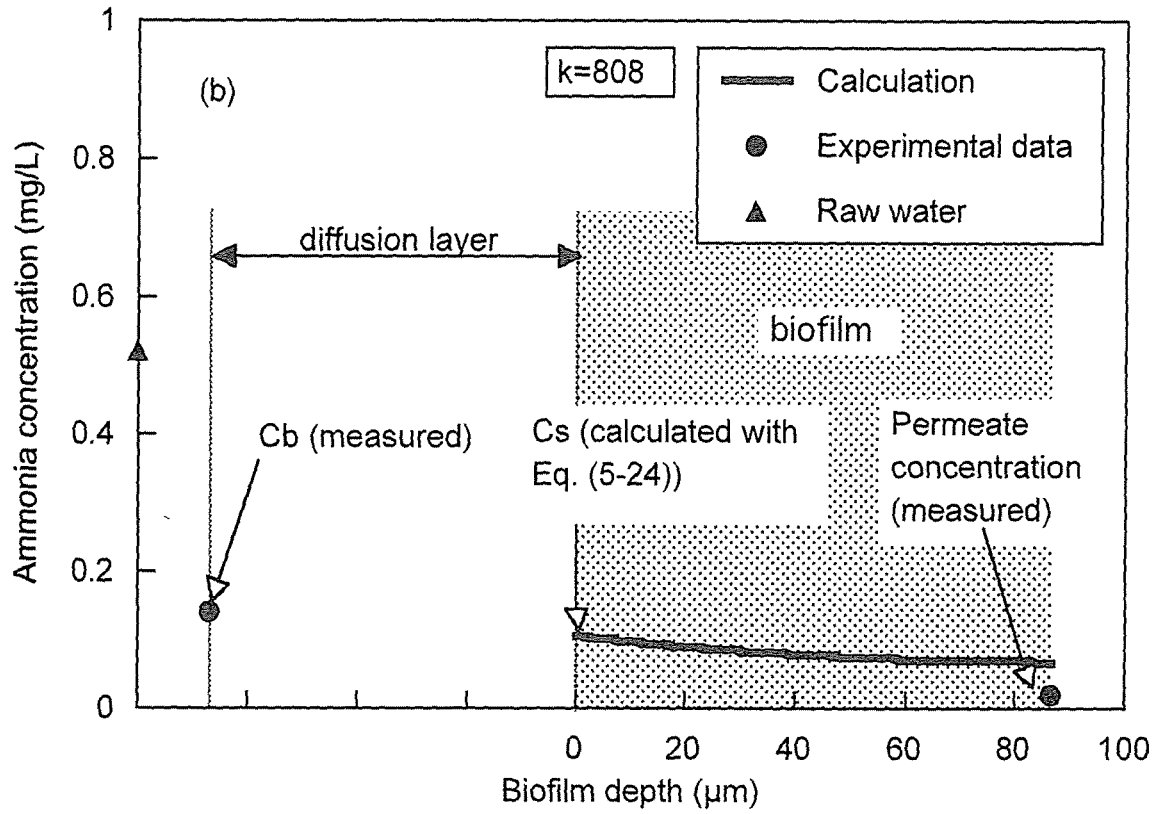


Fig. 5-12. (continued)



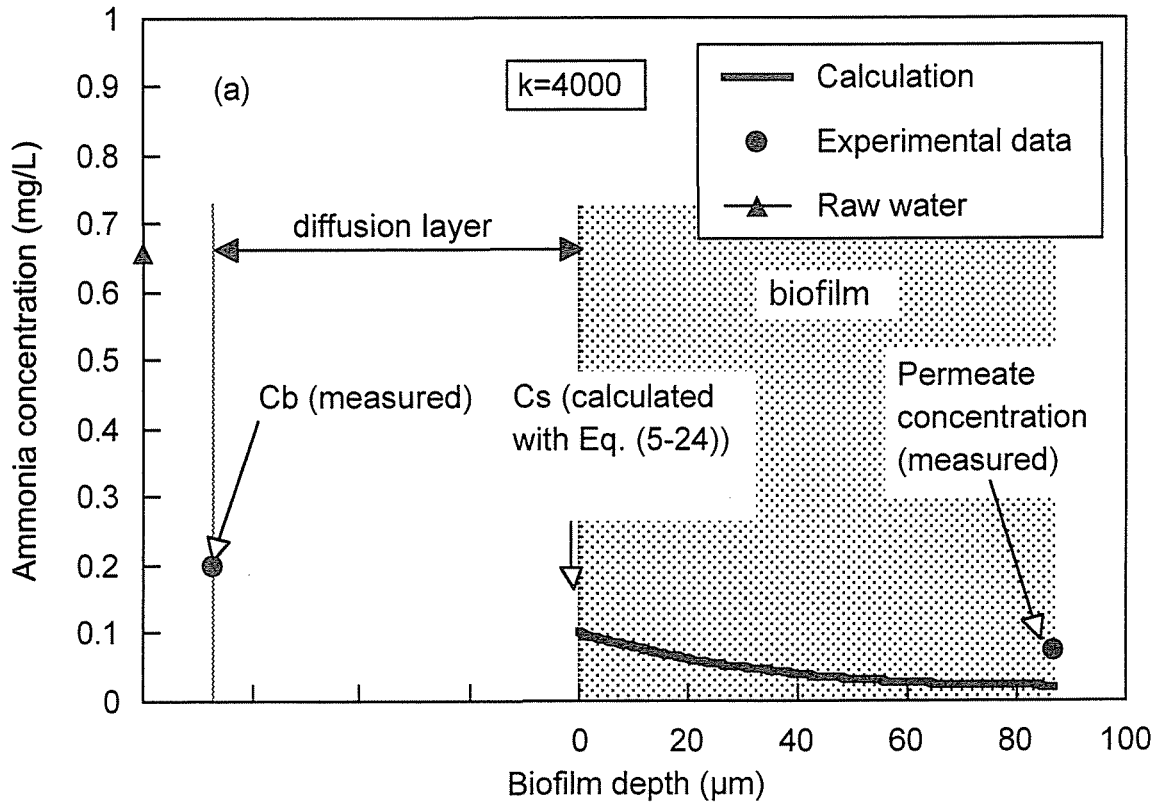


Fig. 5-13. Comparison between the calculated ammonia concentration profiles in the biofilm and the measured ammonia concentrations. ( $k=4000 \text{ h}^{-1}$ ,  $C_b$ : ammonia concentration in the bulk water,  $C_s$ : ammonia concentration at the surface of the biofilm.)

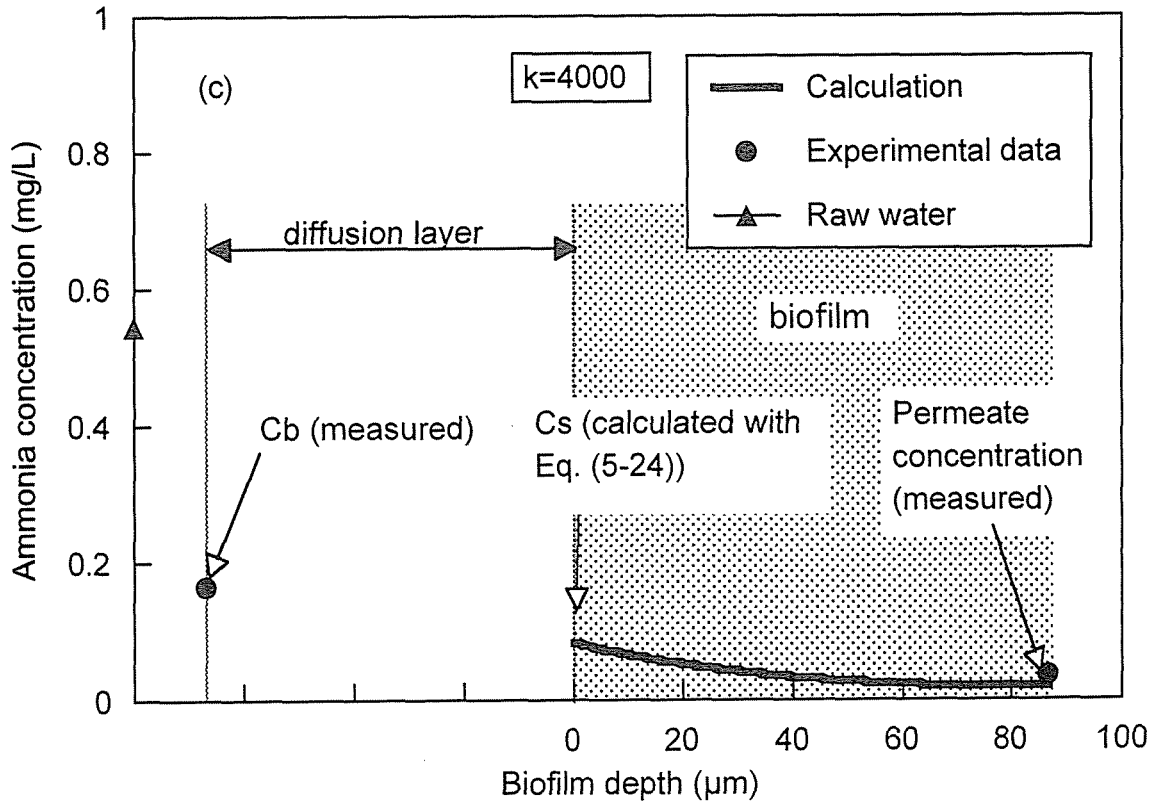
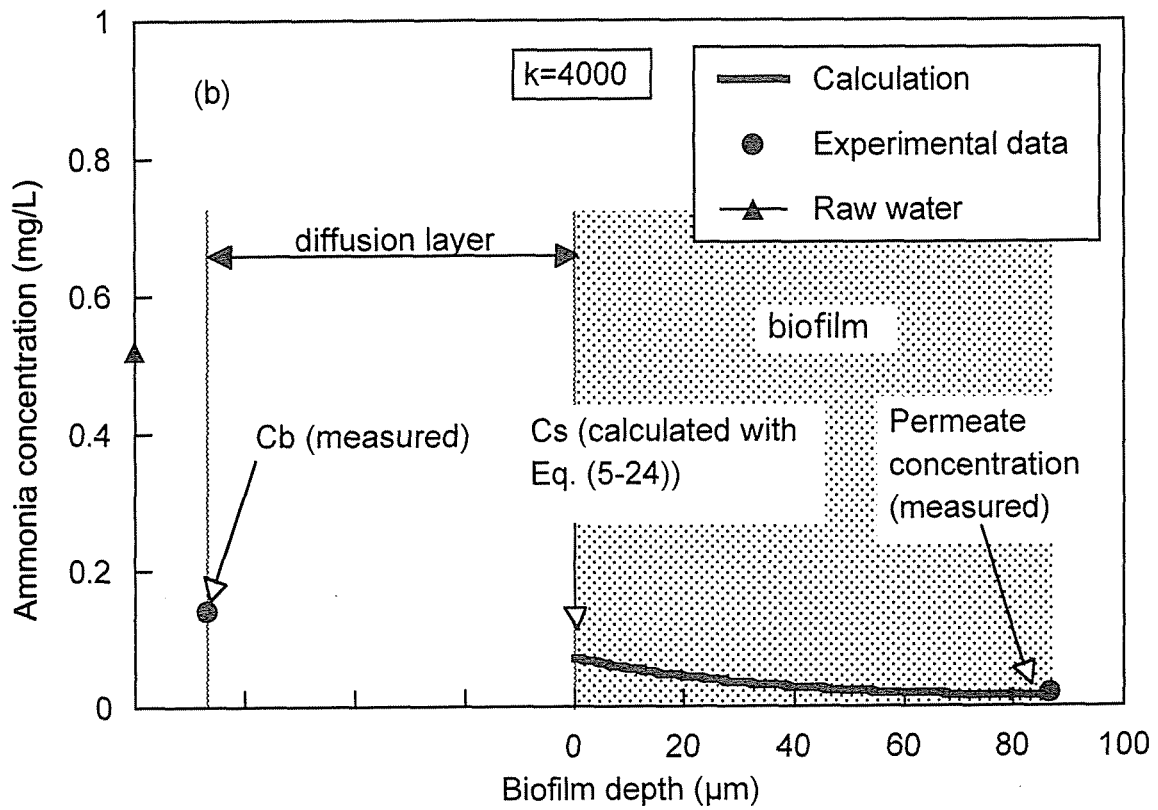


Fig. 5-13. (continued)

### 5.3. SUMMARY

In this chapter, the applicability of the conventional biofilm model to the analysis of the performance of the biofilm developing in BMR was examined. Also, the experimental data obtained in the continuous filter run was analyzed with the conventional model. The results can be summarized as follows:

(1) Although the conventional model was formulated assuming the simple (i.e. flat, homogeneous and continuous) biofilm structure, it was found to be appropriate for the analysis of the biofilm developing in the proposed process. This was because the biofilm actually had a simple structure, which was confirmed by cryosectioning.

(2) When the model is applied to the case dealing with low concentrations of  $\text{NH}_4^+\text{-N}$ , first-order kinetics should be used in the data analysis, and then the model can predict the performance of the proposed process well.

(3) The nitrification efficiency of the BMR is high, which can be explained by two reasons. Firstly, the enhancement of mass transport to the biofilm due to the membrane filtration. Secondly, the collection of treated water from the bottom of the biofilm where  $\text{NH}_4^+\text{-N}$  concentration is the lowest in the system.

### REFERENCES

de Beer, D., Stoodley, P. and Lewandowski, Z. (1994) Liquid flow in heterogeneous biofilms. *Biotech. and Bioeng.* **44**, 636-641.

de Beer, D., Schramm, A., Santegoeds, C. M. and Kühl, M. (1997) Nitrite microsensor for profiling environmental biofilms. *Appl. Environ. Microbiol.* **63**, 973-977.

Famularo J., Mueller J. A. and Mulligan T. (1978) Application of mass transfer to rotating biological contactors. *Jour. WPCF.* **50**(4), 653-671.

Gönenc I. E. and Harremöes P. (1985) Nitrification in rotating disk systems-I, Criteria for transition from oxygen to ammonia rate limitation. *Wat. Res.* **19**(9), 1119-1127.

Huang J.-C. and Bates V. T. (1980) Comparative performance of rotating biological contactor using air and pure oxygen. *Jour. WPCF* **52**(11), 2686-2703.

Levich, V. G. (1962) *Physicochemical Hydrodynamics*, Printice-Hall Inc., New Jersey

Lide, D. R. (eds.) (1998) *The handbook of chemistry and physics*, the 79th edition, CRC Press, Florida

Massol-Deya, A. A., Whallon, J., Hickey, R. F. and Tiedje, J. M. (1995) Channel structures in aerobic biofilms of fixed-film reactors treating contaminated groundwater. *Appl. Environ. Microbiol.* **61**, 769-777.

Melcer, H., Parker W. J. and Rittmann B. E. Modeling of volatile organic contaminants in trickling filter systems. *Wat. Sci. Tech.* **31**(1), 95-104.

Mueller J. A., Paquin P. and Famularo J. (1980) Nitrification in rotating biological contactors. *J. WPCF.* **52**(4), 688-710.

Horn, H. and Hempel, D. C. (1997) Substrate utilization and mass transfer in an autotrophic biofilm system: Experimental results and numerical solution. *Biotech. and Bioeng.* **53**(4), 363-371.

Okabe, S., Kuroda, H. and Watanabe, Y. (1998) Significance of biofilm structure on transport in inert particulates into biofilms. *Wat. Sci. Tech.* **38**(8-9), 163-170.

Watanabe, Y. and Nishidome, K. (1989): Design procedure of RBC based on mass transfer model, *J. of Japan Sewage Works Association*, **26**(6), 34-42 (in Japanese).

Watanabe, Y., Lee, C., Koike, M. and Ishiguro, M (1990): Nitrification kinetics and simultaneous removal of biomass and phosphorus in rotating biological contactors, *Wat. Sci. Tech.* **22**(3/4) 169-178.

Williamson, K. and McCarty, P. L. (1976) A model of substrate utilization by bacterial films, *Jour. WPCF* **48**, 281-296.

---

# CHAPTER

## 6

---

### PILOT SCALE STUDY OF THE NOVEL BIOFILM-MEMBRANE REACTOR (BMR)

Various characteristics of the BMR for advanced drinking water treatment, in which nitrifiers are fixed on the membrane surface, have been described so far. Based on the knowledge obtained in the previous experiments using the bench-scale equipment, a pilot scale study was conducted at an actual water purification plant. The results obtained in the pilot study will be demonstrated in this chapter.

#### 6.1. MATERIALS AND METHODS

##### 6.1.1. Characteristics of raw water

The pilot study was conducted at Kami-Ebetsu water purification plant in Ebetsu City, located 20-km northeast of Sapporo. The plant draws water from Chitose River. This river runs through cities, farming areas as well as peat bog areas before reaching the treatment plant. There are also several wastewater treatment facilities upstream the plant. As a result, the water is severely polluted before it reaches the water intake point. Throughout the year, the raw water contains a considerable

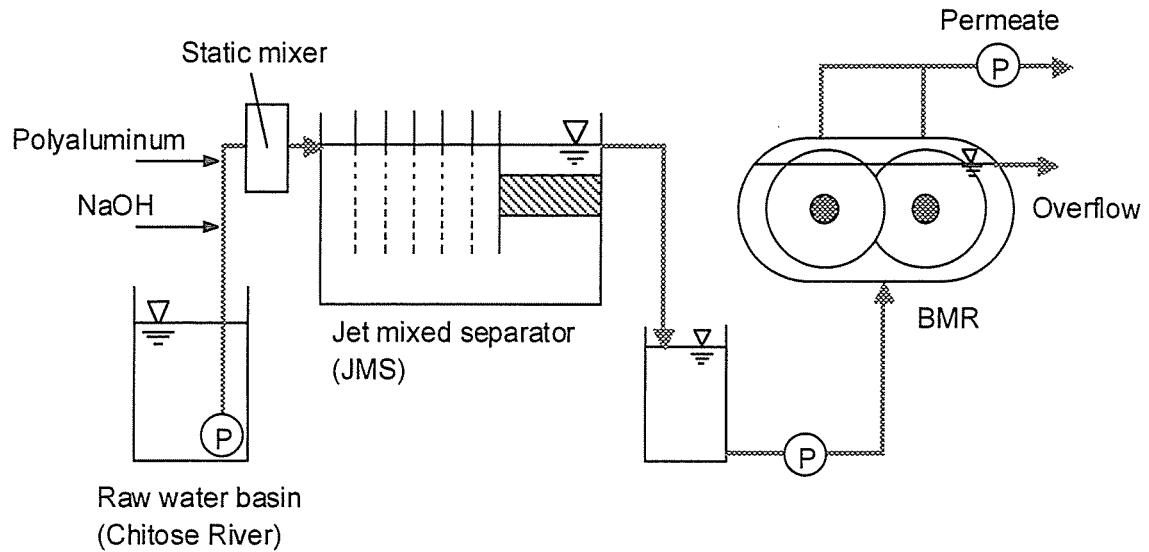


Fig. 6-1. Flowchart of the pilot test.

amount of organic substances (up to 10 mg-DOC/L (Kasahara, 1997)). The fluctuation of turbidity in the raw water is substantial, from 5 turbidity units (TU) to 300 TU. The water temperature decreases to a low level in winter (i.e. around 1 C°), resulting in relatively high concentrations of  $\text{NH}_4^+\text{-N}$  and manganese during winter.

#### 6.1.2. Experimental apparatus

A pilot scale rotating membrane disk module was installed at Kami-Ebetsu water treatment plant. Fig. 6-1 shows flowchart of the pilot experiment and Photo 6-1 shows the overall view of the experimental apparatus. Table 6-1 shows the module characteristics employed in this part of the study. One section of the membrane disks was always above the water surface during the filter run. This membrane module is commercially available (Hitachi Plant & Construction, Tokyo, Japan) and has already been used in full-scale night soil treatment plants for solid-liquid separation. Coagulation with a aluminum coagulant (poly-aluminum chloride) and flocculation/sedimentation in a

Table 6-1. Specification of the pilot-scale membrane module.

---

Water Volume	300 liters
Diameter of disk	750 mm
Area of membrane	4.5 m <sup>2</sup>
Material of membrane	polysulfone
Cut-off molecular weight of membrane	750000

---

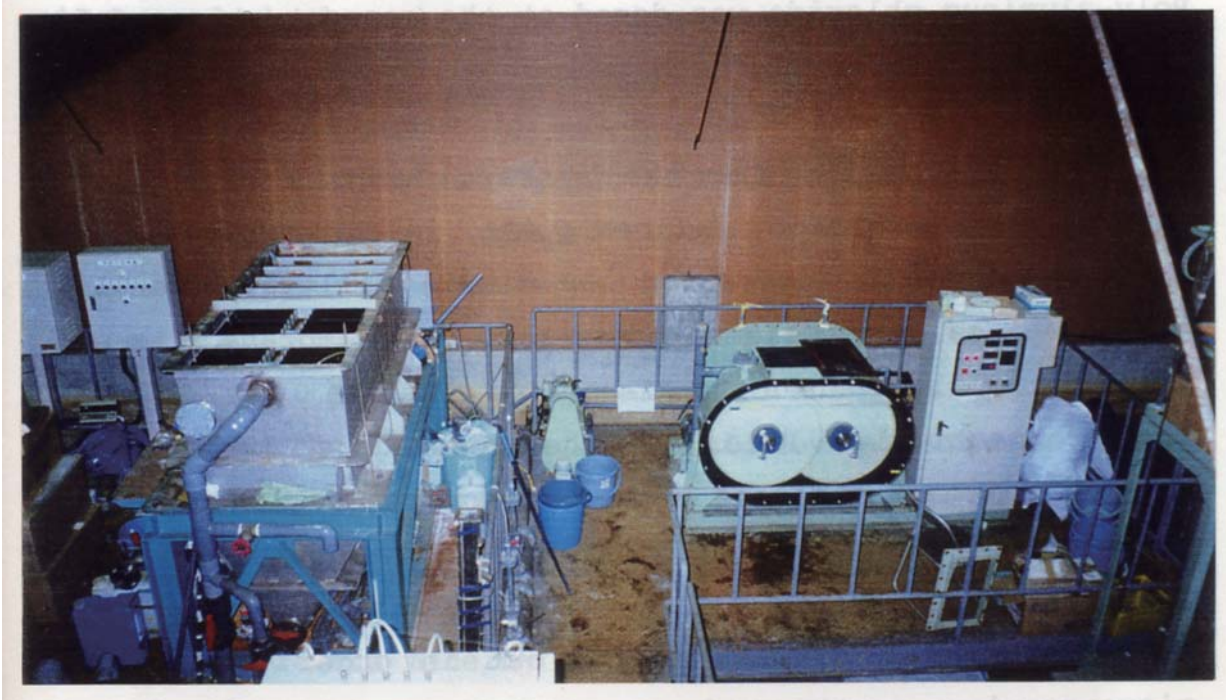


Photo. 6-1. Overall view of the pilot scale equipment.



Jet Mixed Separator (JMS) (Watanabe et al., 1990), were implemented as pre-treatment because the raw water contains substantial organic substances. Many researchers have pointed out the negative influence of natural organic matter (NOM) on the membrane fouling (Mallevalle et al., 1989; Jucker and Clark, 1994; Anselme and Jacobs, 1996; Chang and Benjamin, 1996; Cho et al., 1998; Thorsen, 1999). Coagulation is considered as an efficient way to reduce membrane fouling by NOM (Lahoussine-Turcaud et al., 1990; Wiesner and Laine, 1996)

#### 6.1.3. Experimental conditions

Poly-aluminum chloride was dosed at the concentration of 5-10 mg as Al/L. NaOH was dosed to control the pH of coagulated water in the range between 6.5-7.5. The plant was always operated with overflow from the membrane chamber, resulting in a water recovery ratio, defined  $Q_p/Q_{in}$ , in the range of 0.9-0.95. Intermittent operation, 30 minutes filtration and 2 minutes pause, was implemented as well. The membrane flux and the rotational speed of the disks were fixed at 0.5 m/d and 10 rpm, respectively. Prior to the continuous filter run, microorganisms were seeded in the membrane chamber. The seeding microorganisms were collected from a biofilter installed at the same place, in which active nitrification was observed. Dead-end filtration was carried out in order to fix the microorganisms on the membrane surface.

#### 6.1.4. Analytical methods

The concentrations of ammonia, humic substances (UV absorbance at 260 nm) and turbidity were measured at the plant as soon as samples were taken. With respect to metals, samples were preserved with 0.1 N HNO<sub>3</sub> and measured with graphite furnace

atomic absorption spectrometry (Hitachi Z-5700). Assessment of concentrations of assimilable organic carbon (AOC) was carried out following the procedure described by van der Kooij *et al.* (1982).

## 6.2. RESULTS AND DISCUSSION

### 6.2.1. Increase of the transmembrane pressure difference

After fixation of the biomass, the continuous filter run started on 21 January 1999. Fig. 6-2 shows the change in the transmembrane pressure difference. The pressure difference increased slowly and the operation could be continued for more than 4 months without any membrane cleaning. The first sponge cleaning (see Chapter 4) was carried out on 10 May. After stopping the suction pump and introducing sponge particles into the membrane chamber, the rotational speed of the disk was increased from the normal speed of 10 rpm to 70 rpm. During the cleaning, the overflow valve was shut off and the water surface was elevated to a level sufficient to submerge the membrane disks fully. The sponge particles could move more freely in that situation. One concern was that the shape of the reactor might reduce the mobility of the sponge particle. Photo. 6-2 shows the sponge particles used in the first sponge cleaning. The sponges used were made by cutting sponges normally used for housekeeping. Compared to the experiment in Chapter 4, the size of the sponge particles was enlarged. The apparent volume of the sponge particles introduced was approx. 2000 ml. Sponge cleaning was implemented for 1 hour. In accordance with what was found in the preliminary experiments (see Chapter 4), this sponge cleaning was found to be very effective in removing accumulated cake even in the practical situation. Photo. 6-3 shows the effect of the sponge cleaning. One can see from Photo.

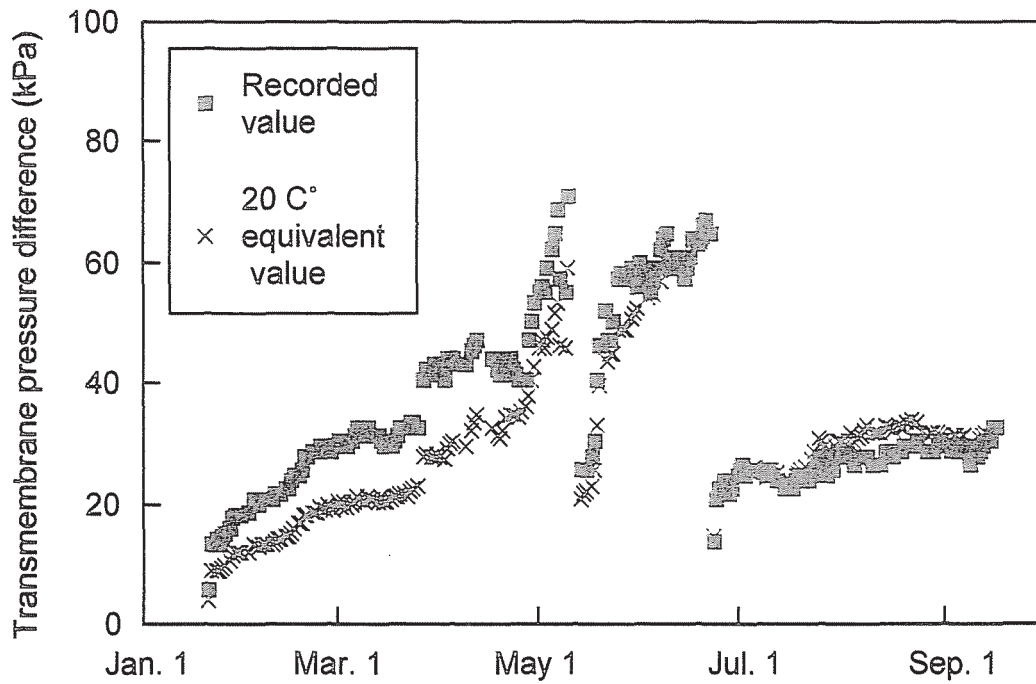


Fig. 6-2. Changes in the transmembrane pressure difference.

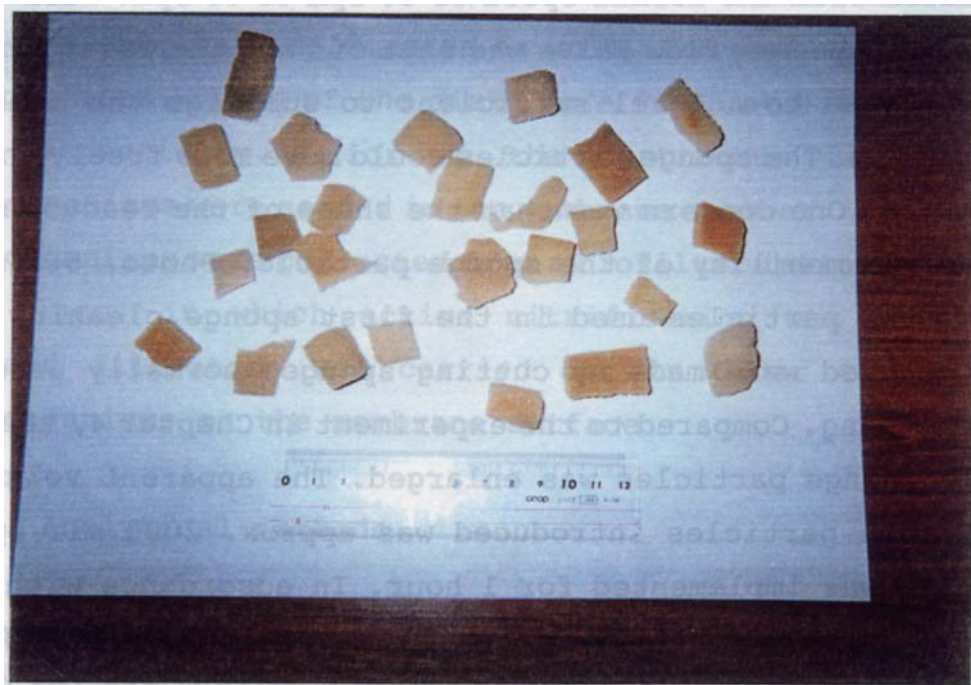
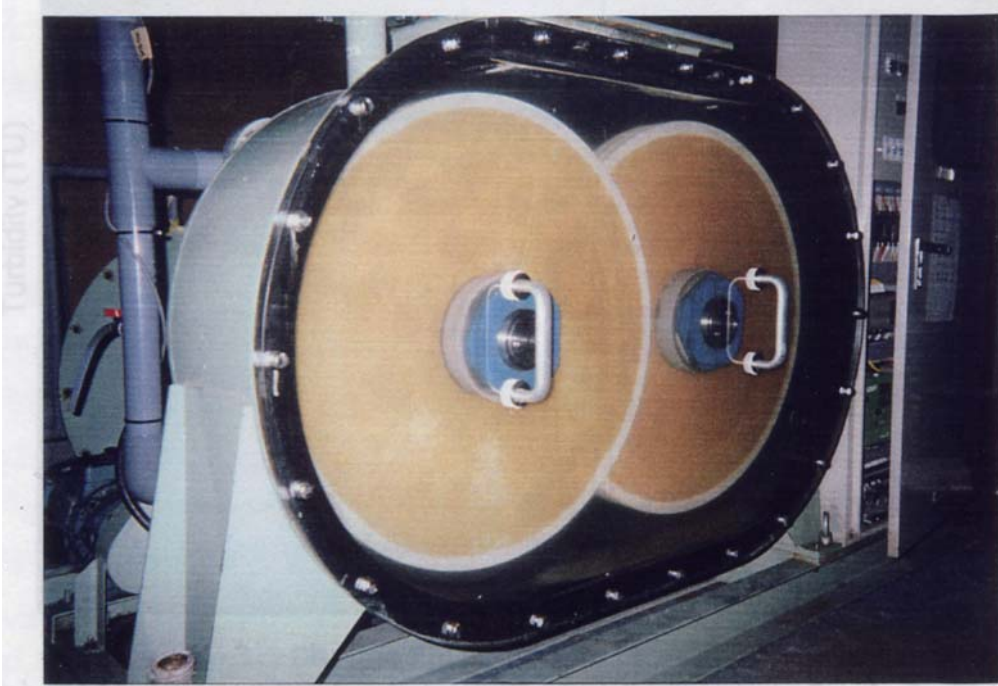


Photo. 6-2. Sponge particles used in the first cleaning.

Before cleaning



After cleaning

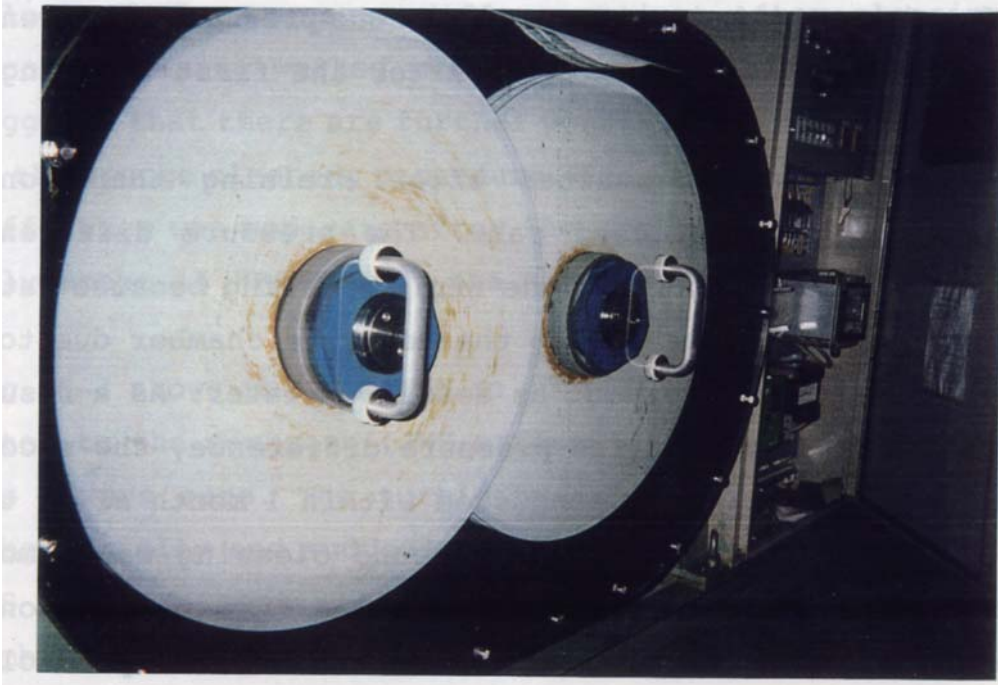


Photo. 6-3. Effect of sponge cleaning in the pilot study.



Photo. 6-4. Sponge particles used in the second cleaning.

6-3 that the accumulated cake was almost completely removed by this cleaning procedure. The transmembrane pressure difference decreased to approx. 20 kPa just after the first cleaning.

The operation was re-started after draining the sponge particles and the detached cake. The pressure difference increased very rapidly after the first cleaning because water with high turbidity was fed to the membrane chamber due to a failure in the pre-treatment as described later. As a result of the rapid increase of the pressure difference, the second sponge cleaning had to be conducted within 1 month after the first one. The procedure of the second cleaning was almost identical to the first one, except for the size of the sponge particles. As shown in Photo. 6-4, the size of the particles was reduced in the second cleaning. The apparent volume of the sponge particles introduced in the second cleaning was approx.

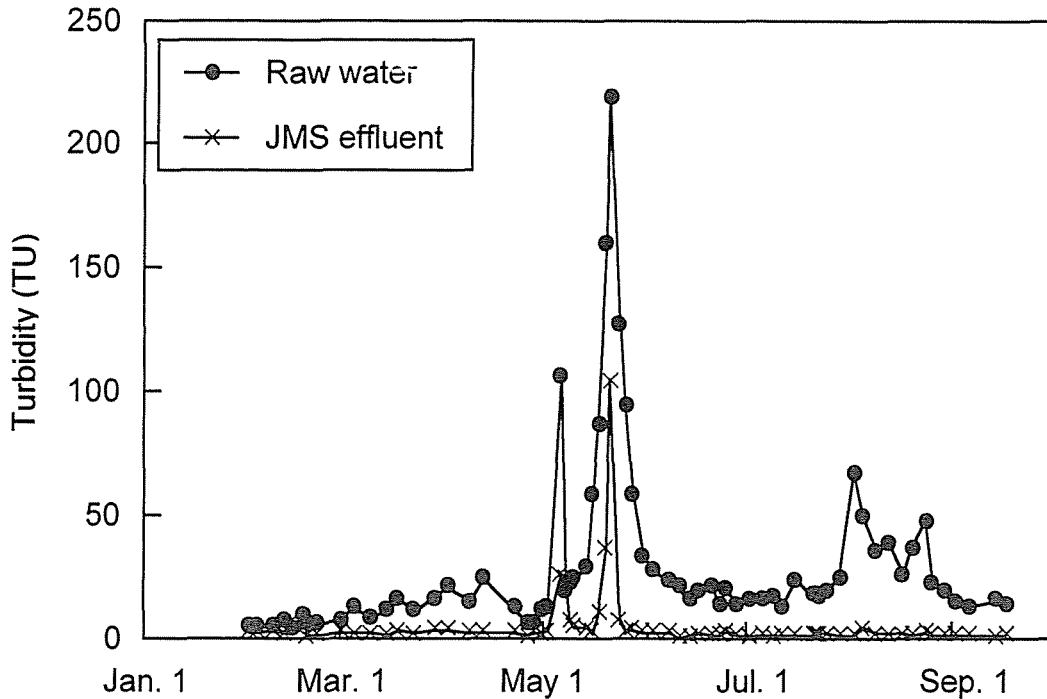


Fig. 6-3. Changes in turbidity in the raw water and the JMS effluent.

2000 ml, the same as in the first one. Judging from the recorded values of the pressure difference just after cleaning, the second cleaning worked much better than the first one. This suggests that there are further possibilities for optimization of the sponge cleaning procedure. The increment of the pressure difference was moderate after the second cleaning, increasing only about 15 kPa during the three months.

Fig. 6-3 shows the changes in turbidity in raw water and feed water to the membrane (JMS effluent). The permeate turbidity was always zero. The turbidity in the raw water fluctuated substantially and suddenly exceeded 200 TU in May. Due to the JMS pre-treatment, the turbidity in the feed water to the membrane was maintained around 2 TU except for some instances in the period from late April to late May. These two peaks corresponded to similar peaks in the raw water during that period. The peaks of the JMS effluent turbidity were certainly

because of a failure in the pre-treatment. The pumps used for the addition of coagulant and alkaline solution did not work well during the high turbidity period. Without the pump failure, turbidity in the feed water would have been at low level regardless of the sudden turbidity increase in the raw water. From Figs. 6-2 and 6-3, the increase of the pressure difference was found to correspond to the increase of turbidity in the feed water. Even with the implementation of continuous overflow and the intermittent operation, the BMR had difficulties in dealing with feed water containing turbidities as high as 100 TU. As experienced in many crossflow systems, membrane systems might not be affected by increase of turbidity in feed water if sufficiently high shear force is continuously applied. It is not reasonable to apply that high shear force to the BMR, however, because it will lead to washing out microorganisms fixed to the membrane. In order to continue stable membrane filtration with BMR, therefore, it is important to remove turbidity sufficiently well from the feed water by some sort of pre-treatment. The moderate increase of the pressure difference after the second sponge cleaning, when the JMS pretreatment was successful, reflects the importance of the pretreatment.

It should be pointed out that the rotational speed of the disks set in this filter run (10 rpm) was not necessarily the optimum one. Probably a higher rotational speed could be employed without resulting in microorganism wash-out. This can be expected to be quite effective in retarding the increase of the pressure difference. This point will, however, need further experiments and consideration.

### 6.2.2. $\text{NH}_4^+$ -N oxidation efficiency

#### 6.2.2.1. Time course change of nitrification

Figs 6-4 and 6-5 show the changes over time in  $\text{NH}_4^+$ -N concentration and the water temperature in the membrane chamber, respectively. In spite of the fact that the seeding bacteria were collected from the biofilter in which active nitrification occurred, almost no nitrification was observed in the early stage of the filter run. A possible explanation for this might be the very low water temperature (around  $5\text{ C}^\circ$ ) as shown in Fig. 6-5. For rapid start-up of nitrification with the BMR, start-up should be carried out in a season when the water temperature is high. Corresponding to the rise in water temperature around mid April, nitrification became significant. Even though almost complete nitrification was observed by the time when the first sponge cleaning was implemented (10 May), the nitrification efficiency declined considerably after the cleaning. This was most probably due to the removal of the microorganisms fixed on the membrane. Three weeks were required to get high nitrification efficiency similar to the one observed just before the first cleaning. Stable nitrification was observed after that. However, the pressure difference rapidly increased in the same period and therefore the second sponge cleaning had to be conducted as described in the previous section.

After the second sponge cleaning, a part of the detached cake (corresponding to 4 % of the whole cake) was returned to the membrane chamber in order to restore the nitrification efficiency rapidly. Dead-end filtration for the fixation of the biomass was not implemented. These re-inoculation procedures were almost the same as those used in Chapter 4 (2 % of the cake returned), which turned out to be effective in recovering the



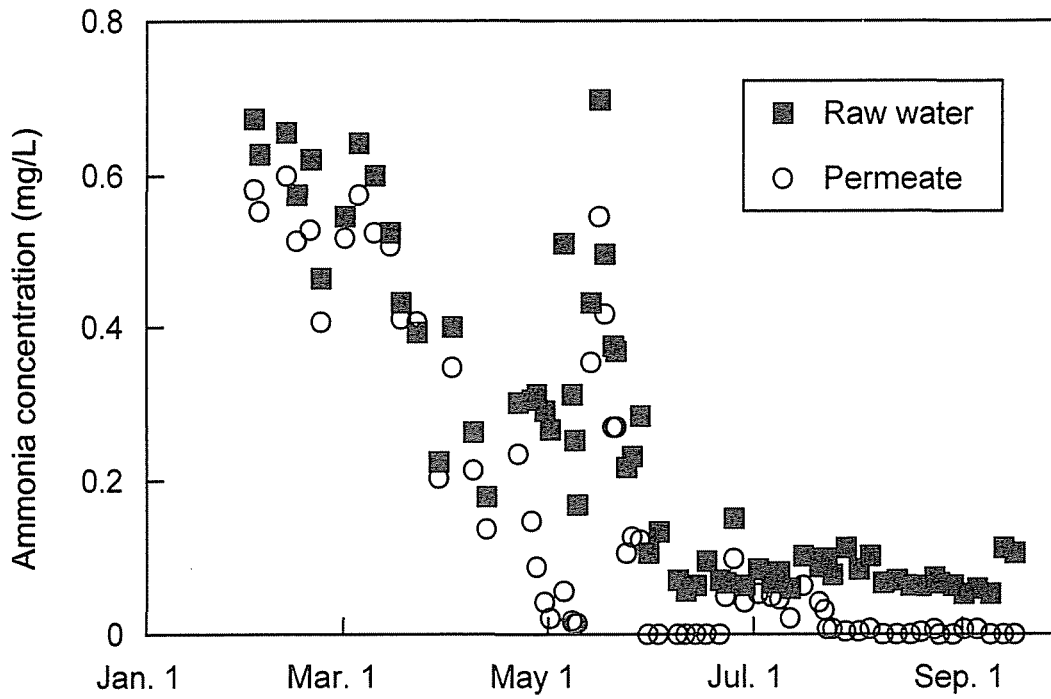


Fig. 6-4. Changes in  $\text{NH}_4^+$ -N concentrations.

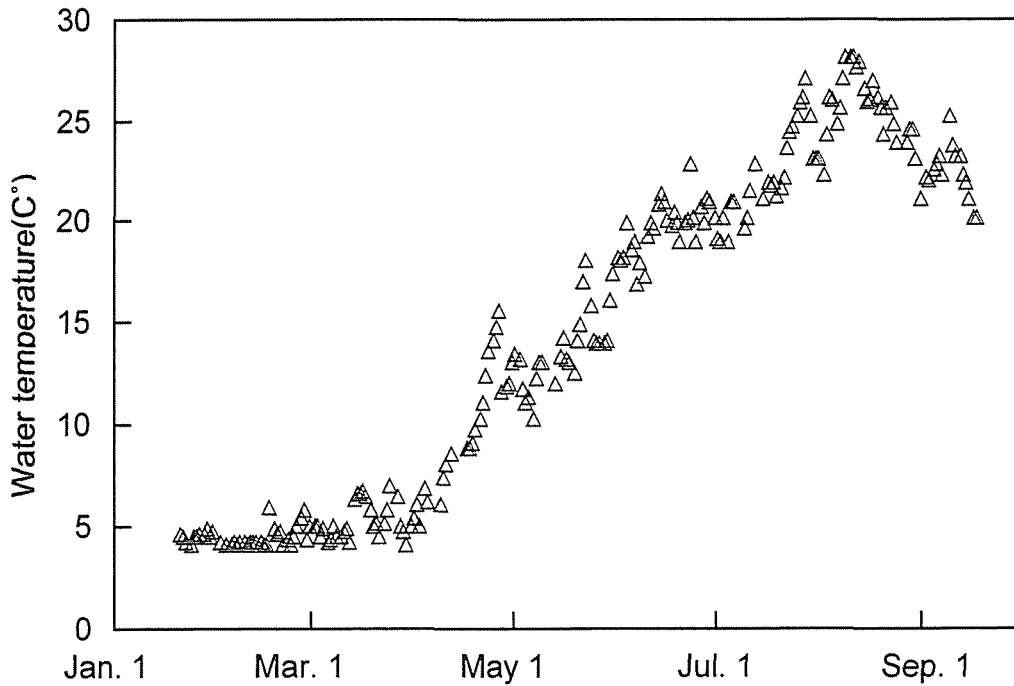


Fig. 6-5 Change in the water temperature in the membrane chamber.

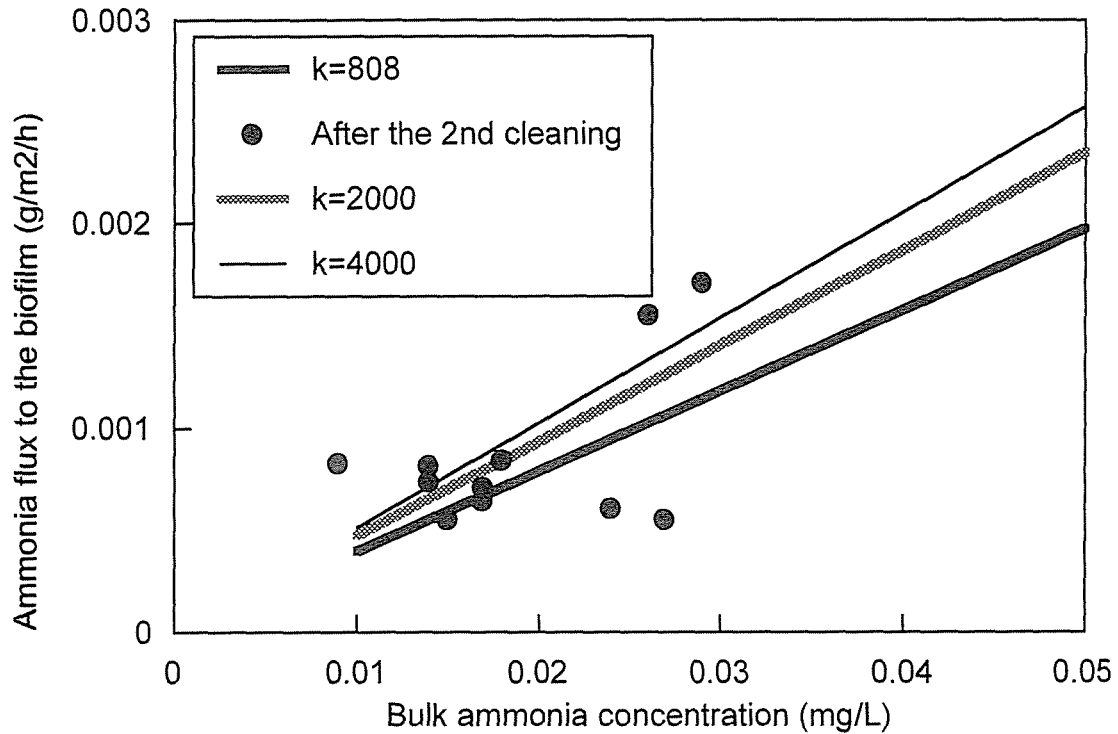


Fig. 6-6. Comparison between calculated  $\text{NH}_4^+$ -N flux and observed ones.

nitrification efficiency then. As it is seen in Fig. 6-4, however, it took about one month to acquire good nitrification after the second cleaning. The reason of the difference between the laboratory experiment and the pilot study is not clear, and, some efficient measures for the biomass fixation after cleaning will have to be investigated. Stable nitrification had, however, been maintained since the middle of July.

#### 6.2.2.2. Application of the biofilm model to the pilot study

The biofilm model developed in Chapter 5 was examined in order to express the experimental data obtained in the pilot study. Eqs. (5-18-26) were used for the calculation. In the calculation, the parameter values were assumed to be identical to the ones used in Chapter 5 except for the that of the diffusion layer thickness,  $L_d$ , and first-order reaction constant,  $k$ . By the use

of Eq. (5-7),  $L_d$  for the disks rotating at 10 rpm was determined to be 137  $\mu\text{m}$ . With respect to  $k$ , three different values, 808, 2000, 4000 1/h, were examined. The value 808 1/h is identical to the one found in Chapter 5. Fig. 6-6 shows the calculated  $\text{NH}_4^+\text{-N}$  flux as well as the  $\text{NH}_4^+\text{-N}$  flux observed in the pilot study. In Fig. 6-6, only the data obtained after 23 July, when stable nitrification was observed, are included. Selection of different  $k$ -values did not affect the results of the calculation significantly. Even though the parameter values were not specific for the pilot study and the model did not take into account that a part of the membrane was above the water surface, the general trend of the observed data seemed to be expressed by the calculation. This indicates the feasibility of the model in practical situations.

### 6.2.3. Removal of other substances

In this pilot study where the actual drinking water source was used, various strains of microorganisms other than nitrifiers should inhabit the biofilm developed on the membrane surface. Due to these microorganisms, the removal of substances other than  $\text{NH}_4^+\text{-N}$  should be expected. Such substances as humic substances (UV absorbance at 260 nm, expressed as E260), AOC, manganese, iron and aluminum were examined.

#### 6.2.3.1. Humic substances expressed by E260

Fig. 6-7 shows the E260 in the raw water, the JMS effluent (i.e. feed water to the membrane) and the membrane permeate over time. E260 was measured with 1-cm quartz cell. As seen from Fig. 6-7, mainly the coagulation and sedimentation with the JMS resulted in removal of E260 while the BMR did not reduce E260 to any measurable extent. Coagulation is suitable for removing high

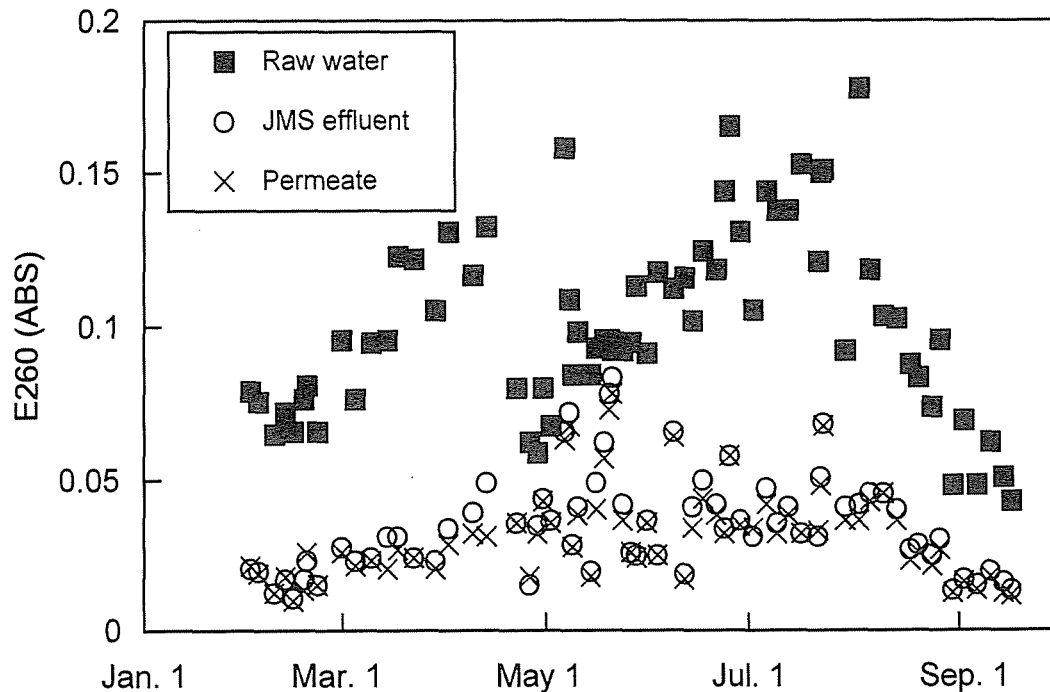


Fig. 6-7. Changes in E260.

molecular weight organic substances but inefficient in removing low molecular weight organic substances (Tambo and Kamei, 1978). The effluent from the JMS can be expected to contain mainly the low molecular weight organic substances, not removable by the membrane employed (cut-off molecular weight: 750,000 Da). Adsorption of humic substance (or often referred as natural organic matter, NOM) by biomass has been investigated by some researches (Zhou and Banks, 1993; Carlson and Silverstein, 1997 and 1998). However, this kind of "biosorption" of organic matter was not significant in this experiment.

Fig. 6-8 shows the changes in pH of the JMS effluent and in the membrane chamber. The optimum pH for nitrifiers is considered to be weakly alkaline, in the range between 7.2-8.4 (Bitton, 1994). In this filter run, the pH in the membrane chamber often fell below 7 especially after the second cleaning. From Figs. 6-4 and 6-8, one can find, however, that the nitrification efficiency was not adversely affected by the low pH condition.

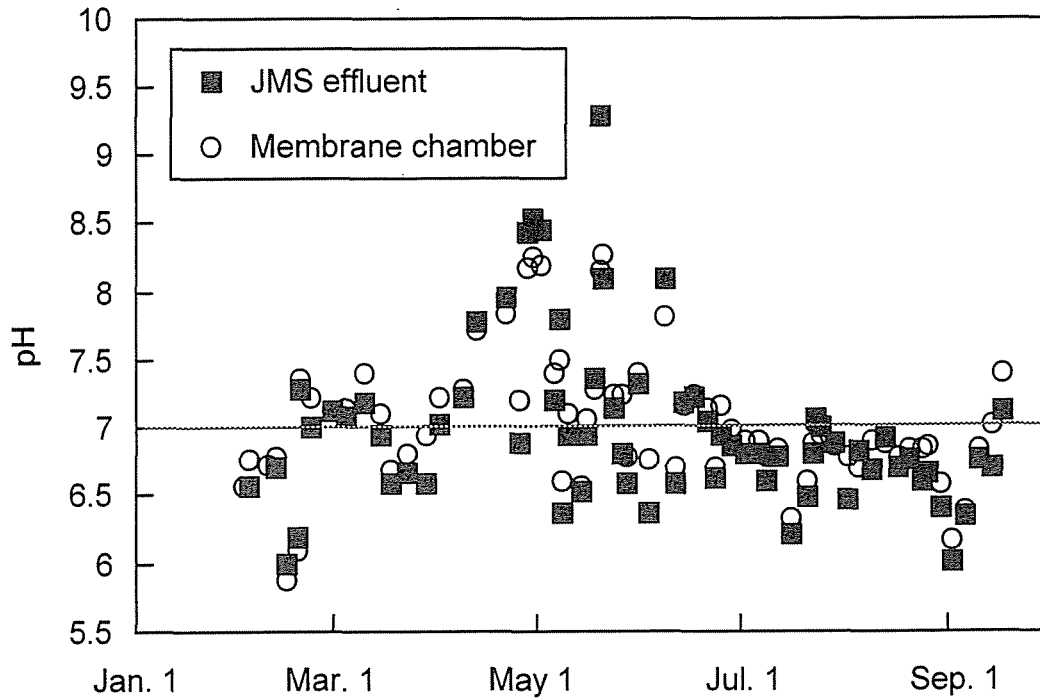


Fig. 6-8. Changes in pH.

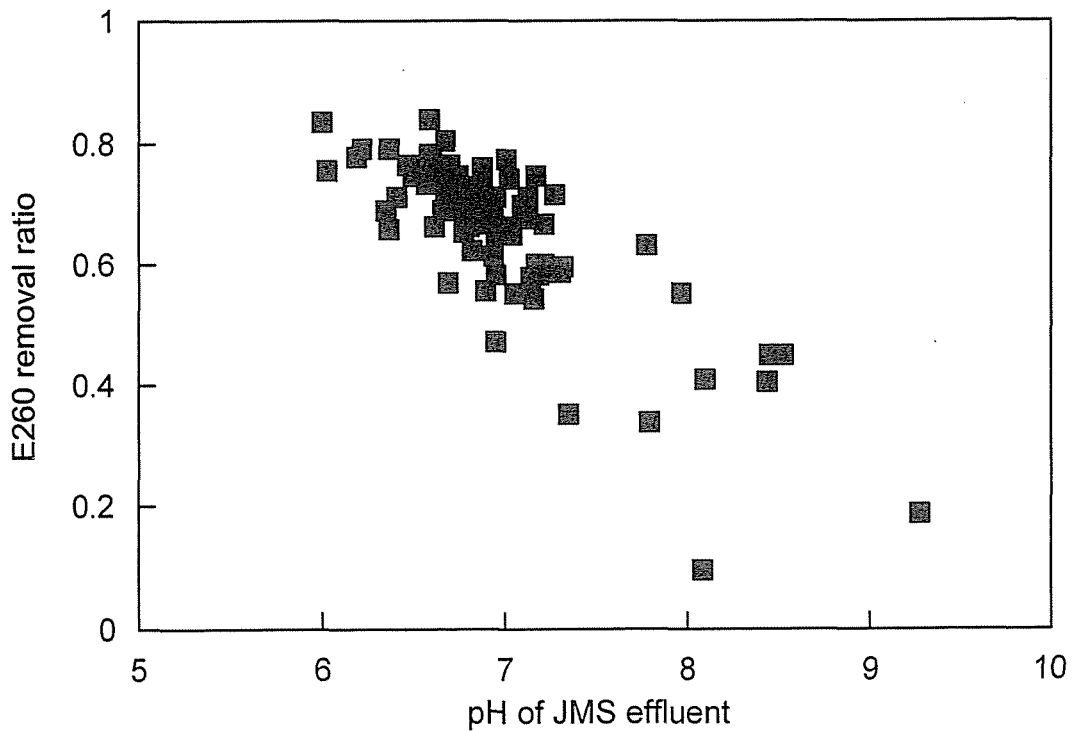


Fig. 6-9. Relationship between pH of JMS effluent and E260 removal ratio defined as  $(1 - E260_{\text{JMS effl.}} / E260_{\text{raw water}})$ .

As is commonly known, pH should be controlled at a weakly acid range in order to remove non-biodegradable organic substances efficiently by coagulation. The total removal of E260 increased by 10-20 % when pH was slightly shifted to the weak acidic region, which was observed in this filter run (Fig. 6-9). Therefore, it can be concluded that coagulation as the pre-treatment for the BMR may be implemented in weak acidic condition as normal. This allows the improvement in the removal of E260 without deterioration of nitrification efficiency.

#### 6.2.3.2. AOC

Fig. 6-10 shows the results of the AOC assessment. Van der Kooij (1992) suggested that AOC concentrations should be less than 10  $\mu\text{g-C/L}$  to limit the regrowth of heterotrophs during distribution. Using the same water source as in this study, an advanced water purification system, consisting of coagulation, sedimentation, sand-filtration and biological activated carbon (BAC) with/without ozonation, was also examined by Kasahara (1997). Kasahara *et al.* (1998) carried out intensive AOC assessment with respect to the system and found that it was difficult to reduce AOC concentration below 35  $\mu\text{g-C/L}$ . In this study, however, the AOC concentration was reduced below 10  $\mu\text{g-C/L}$  on 30 August when biofilm on the membrane was well established. The reason for the fact that the results from 11 June were not so good, may be that the biofilm on the membrane was not well established at this time. These results may indicate that the BMR might be superior to the advanced purification system in removing AOC and establishing biologically stable water.

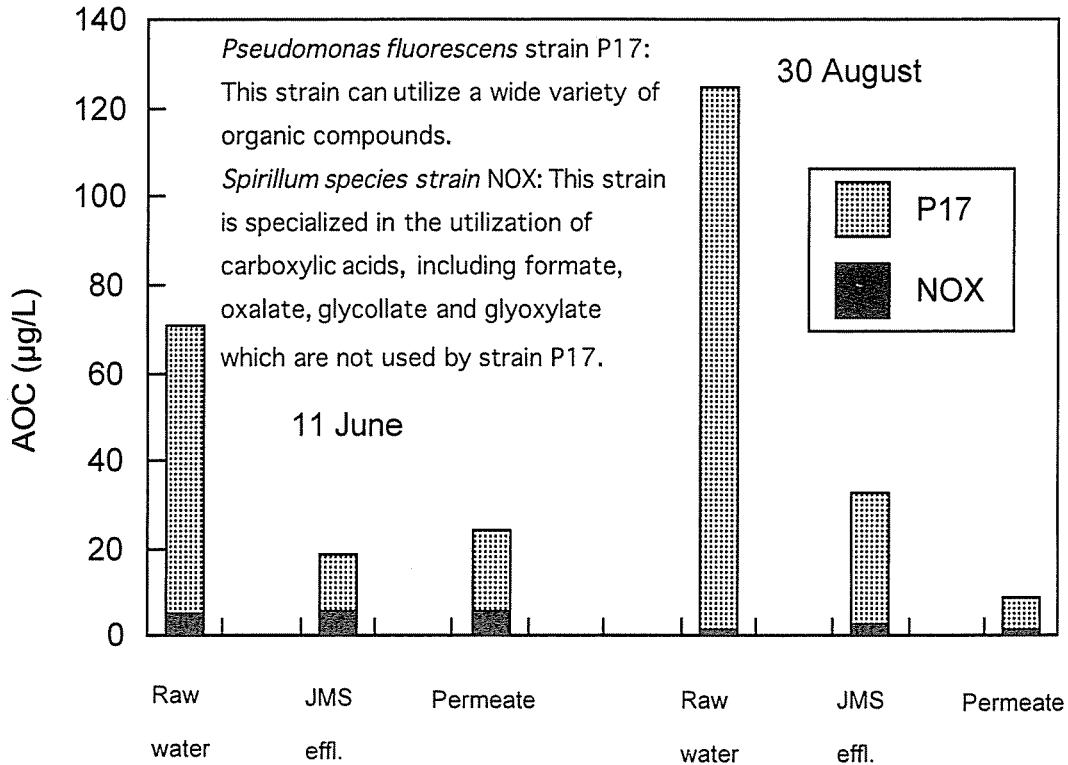


Fig. 6-10 Result of AOC assessment.

6.2.3.3. Metals

Fig. 6-11 shows the results of the measurement of manganese concentration. On 5 March when the water temperature was still low and nitrification was not significant, manganese was hardly removed either. With the increase of water temperature (samples of 17 June and 5 August), manganese concentration decreased to low levels. This was probably due to biological oxidation of manganese. A close relationship between biological nitrification and biological manganese oxidation has been pointed out (Rittmann and Snoeyink, 1984; Vandenabeele et al., 1995). The concentration of iron and aluminum (Figs. 6-12 and 6-13, respectively) were both reduced to low levels regardless of water temperature. The removal of iron and aluminum was, however, not due to microorganisms but due to the membrane sieve effect of iron and aluminum flocs. It should be noted that the

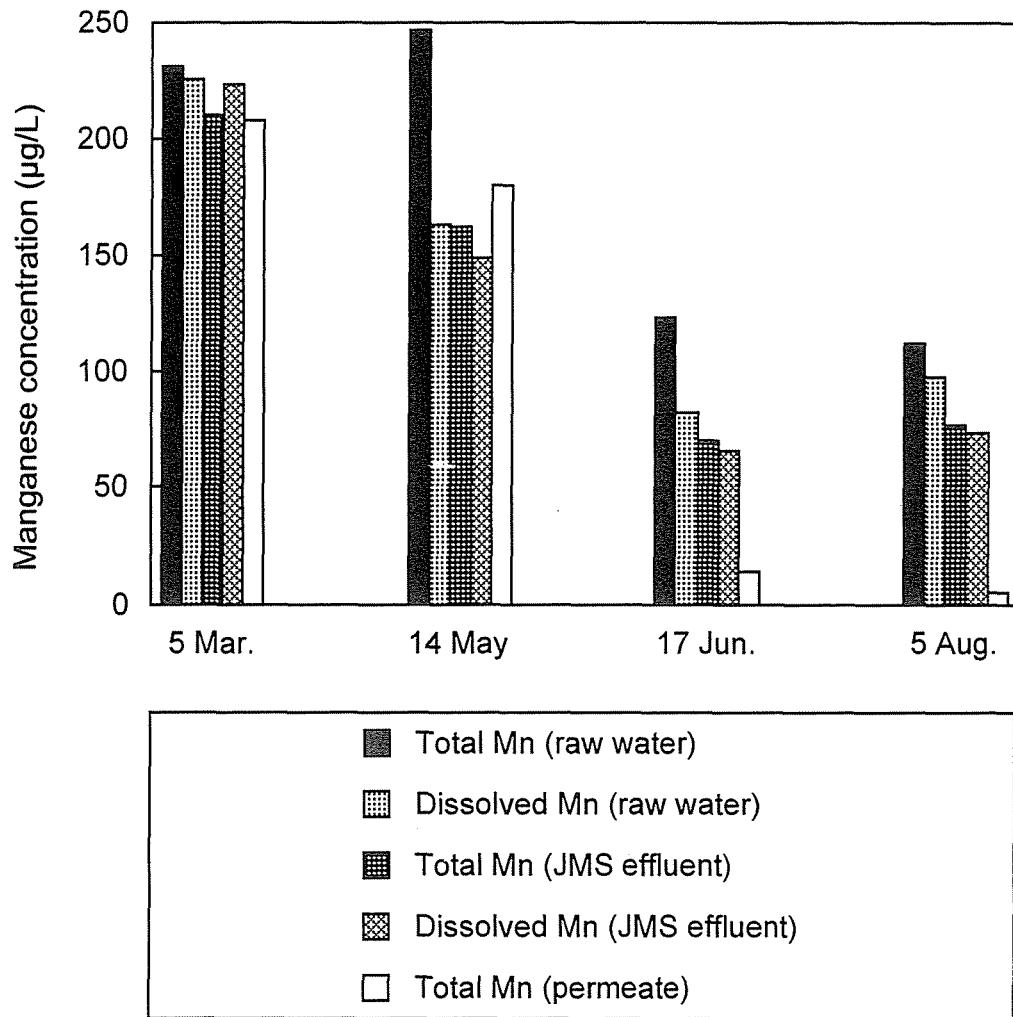


Fig. 6-11. Reduction of manganese concentration with the BMR.

concentration of dissolved (less than  $0.45 \mu\text{m}$ ) aluminum in the JMS effluent was not stable and it was especially high on 9 June. This was certainly due to the implementation of coagulation. Srinivasan *et al.* (1999) pointed out the possibility of leakage of colloidal organic aluminum to treated water associated with inadequate coagulation. Use of membrane could absorb instability in coagulation and could minimize the residual aluminum in treated water.



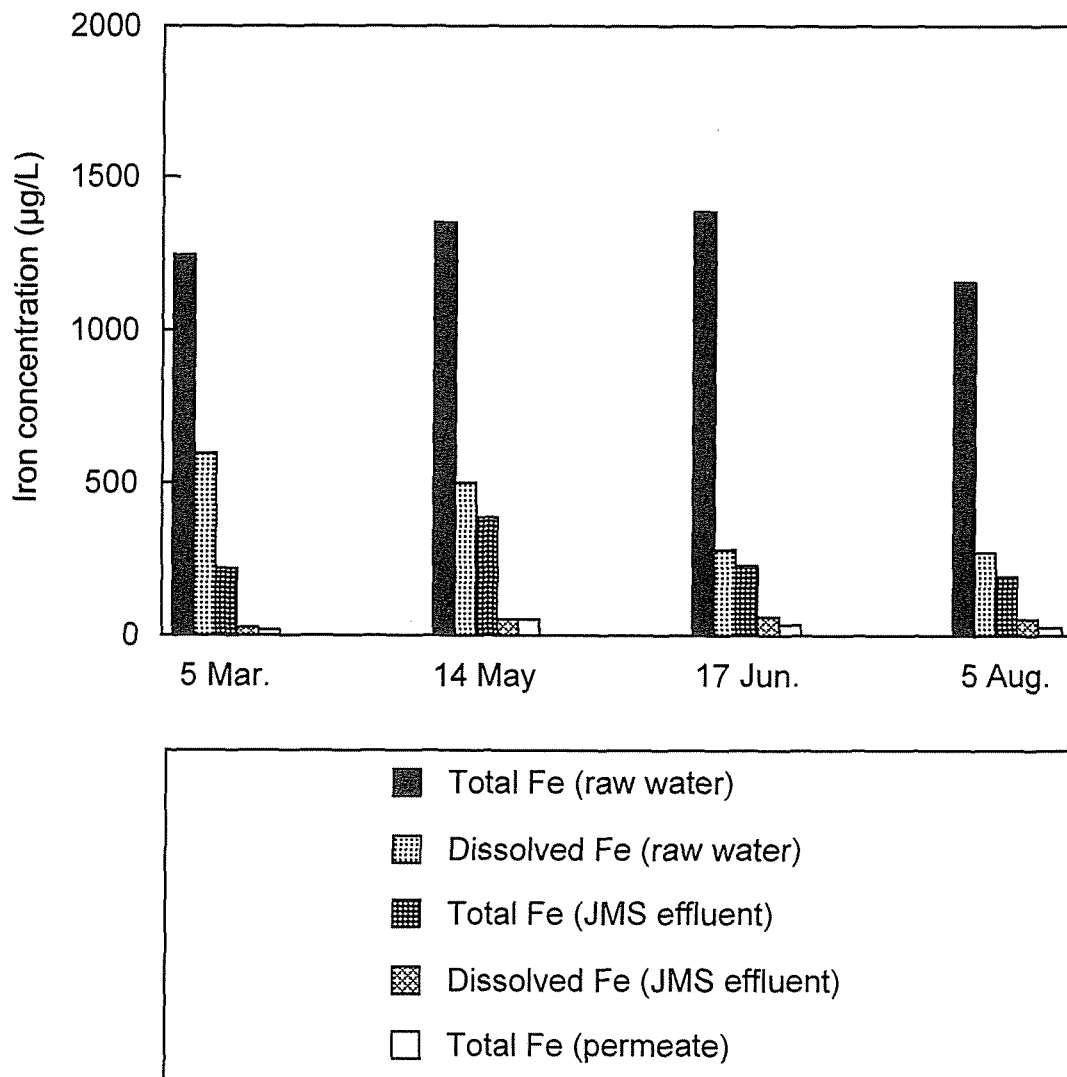


Fig. 6-12. Reduction of iron concentration with the BMR.

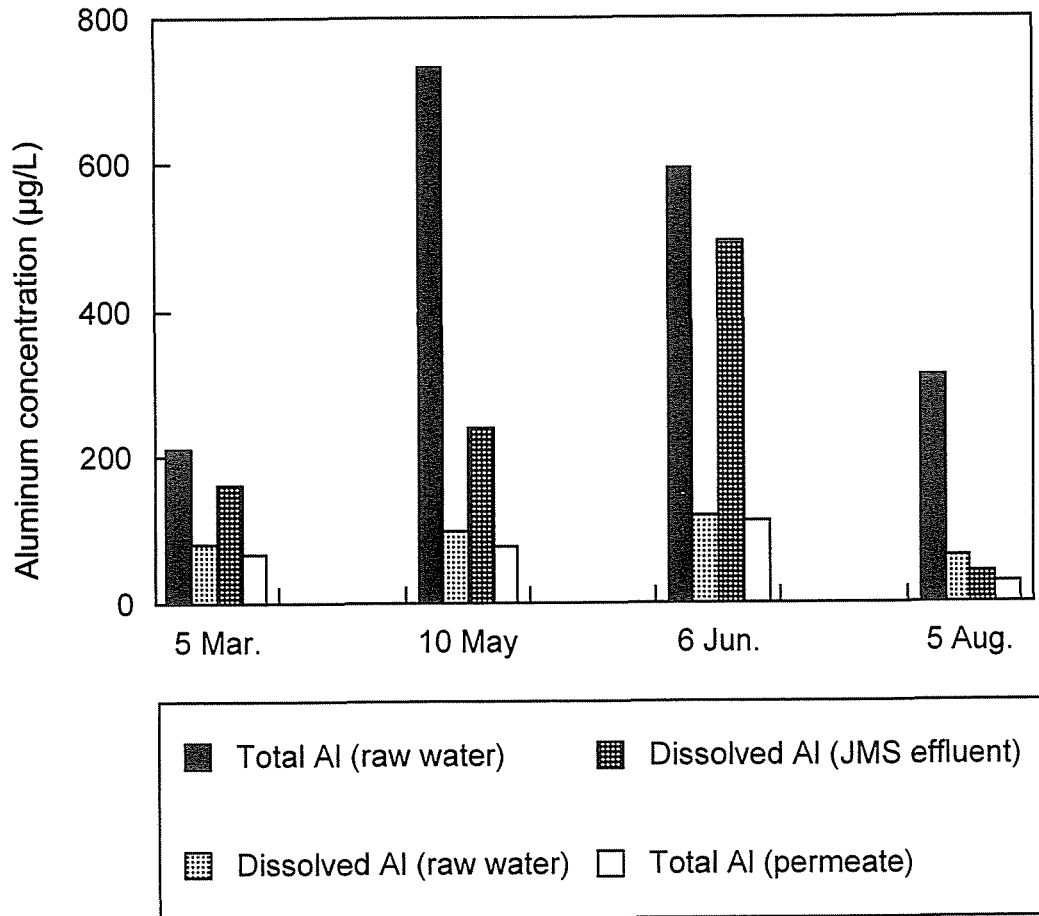


Fig. 6-13. Reduction of aluminum concentration with the BMR.

### 6.3. SUMMARY

Based on the knowledge obtained in the previous chapters, a pilot study of the novel biofilm-membrane reactor (BMR) was conducted using an actual drinking water source. The experimental results obtained from the pilot study can be summarized as follows;

(1) A pilot scale filter run could be carried out successfully even with the water from an actual drinking water source. By Implementation of pre-treatment (coagulation and sedimentation with JMS), the filter run could be continued more than eight months without any chemical washing.

(2) The sponge cleaning developed (see Chapter 4) was found to be very effective even in the pilot study. This indicates that the accumulated cake resistance ( $R_c$ ) is dominant in the practical situation as well.

(3) Sufficient nitrification was observed when water temperature was high. The biofilm model developed in Chapter 5 may be useful the practical operation of a BMR plant.

(4) If coagulation is employed as pre-treatment of the BMR, coagulation should be implemented at weak acidic condition, which can allow improvement in the removal of organic substances without the deterioration of nitrification. In this experiment, nitrification was not deteriorated even at around 6.0 of pH.

(5) In addition to the nitrification, removal of AOC and manganese can be expected with the BMR. In this study, both AOC and manganese concentration in the permeate decreased to the level less than 10  $\mu\text{g/L}$ .

(6) The operating conditions employed in this pilot study were not necessarily optimum ones. More experiments and investigation are needed in order to optimize the process.

#### REFERENCES

Anselme C. and Jacobs E. P. (1996) Ultrafiltration. *Membrane process: Water treatment*, Mallevalle J., Odendaal P. E. and Wiesner M. R. eds., McGraw-Hill, New York

Bitton G. (1994) *Wastewater Microbiology*. John Willey & Sons, New York

Carlson G. and Siverstein J. (1997) Effect of ozonation on sorption of natural organic matter by biofilm. *Wat. Res.* **31**(10), 2467-2478

Carlson G. and Siverstein J. (1998) Effect of molecular size and charge on biofilm sorption of organic matter. *Wat. Res.* **32**(5), 1580-1592

Chang Y. and Benjamin M. M. (1996) Iron oxide adsorption and UF to remove NOM and control fouling. *J. AWWA.* **88**(12), 74-88

Cho J., Amy G., Pellgrino J. and Yoon Y. (1998) Characterization of clean and natural organic matter (NOM) fouled NF and UF membranes, and foulants characterization. *Desalination* **118**, 101-108

Jucker C. and Clark M. M. (1994) Adsorption of humic substances on hydrophobic ultrafiltration membranes. *Jour. Mem. Sci.* **97**, 37-52

Kasahara S. (1997) Development of an advanced water purification system with high efficiency. Doctoral thesis, Hokkaido University, Sapporo, Japan (in Japanese)

Kasahara S., Aizawa T., Watanabe Y., Ozawa G. and Okabe S. (1998) Evaluation of performance of advanced water purification system by assimilable organic carbon. *J. Japan Water Works Association* **67**(11), 12-21

Van der Kooij D, Visser A. and Hijnen W. A. M. (1982) Determining the concentration of easily assimilable organic carbon in drinking water. *J. AWWA* **74**(10), 540-545

Van der Kooij D. (1992) Assimilable organic carbon as an indicator of bacterial regrowth. *J. AWWA* **84**(2), 57-65

Lahoussine-Turcaud V., Wiesner M. R., Bottero J.-Y. and Mallevalle J. (1990) Coagulation pretreatment for ultrafiltration of a surface water. *J. AWWA*. **82**(12), 76-81

Mallevalle J., Anselme C. and Marsigny O. Effects of humic substances on membrane process. Aquatic humic substances: Influences on fate and treatment of pollutants, Adv. in Chem. Ser. No.219. Suffet I. H. and MacCarthy P. eds, Am. Chemical Soc., Washington, D. C., 749-767

Rittmann B. E. and Snoeyink V. L. (1984) Achieving biologically stable drinking water. *J. AWWA*, **76**(10), 106-114

Tambo N. and Kamei T. (1978) Treatability evaluation of general organic matter concept and its application for a regional water and wastewater system. *Wat. Res.* **12**(11), 931-950

Strinivasan P. T., Viraraghavan T. and Bergman J. (1999) Factors influencing residual aluminum levels at the Buffalo Pound Water Treatment Plant, Saskatchewan, Canada. *J Water SRT-Aqua*, **48**(4), 167-175

Thorsen T. (1999) Membrane filtration of humic substances - State of the art. *Wat. Sci. Tech.* **40**(9), 105-112

Vandenabeele J., de Beer D., Germonpré R., Van de Sande R. and Verstraete W. (1995) Influence of nitrate on manganese removing microbial consortia from sand filters. *Wat. Res.* **29**(2), 579-587

Watanabe Y., Fukui M. and Miyanoshita T. (1990) Theory and performance of a jet mixed separator. *J. Water SRT-Aqua*, **39**(6), 387-395

Watanabe Y., Kasahara S. and Iwasaki Y. (1998) Enhanced flocculation/sedimentation process by a jet mixed separator. *Wat. Sci. Tech.* **37**(10), 55-67

Wiesner M. R. and Laîné J.-M. (1996) Coagulation and membrane separation. *Membrane process: Water treatment* Mallevalle J., Odendaal P. E. and Wiesner M. R. eds., McGraw-Hill, New York

Zhou J. L. and Banks C. J. (1993) Mechanism of humic acid colour removal from natural waters by fungal biomass biosorption. *Chemosphere*, **27**(4), 607-620

---

# CHAPTER

## 7

---

### SUMMARY AND CONCLUSION

#### 7.1. SUMMARY

The author has proposed a novel biofilm-membrane reactor (BMR), in which nitrifiers are fixed on the membrane surface, for advanced drinking water treatment. With the BMR, biological nitrification and complete solid-liquid separation can be performed simultaneously. Through this doctoral thesis, various characteristics of the BMR were shown and the feasibility of the BMR was examined. Experiments were carried out in bench-scale equipment using synthetic raw water (CHAPTERS 2-5) as well as in a pilot-scale plant using raw water from an actual drinking water source (CHAPTER 6).

In CHAPTER 1, the background for the development of the BMR was described. The present state of water use in Japan as well as problems concerned with ammonia nitrogen ( $\text{NH}_4^+\text{-N}$ ) in drinking water treatment was reviewed.

In CHAPTER 2, the potential of using the rotating membrane disk module as the BMR was examined. The rotating membrane was found to be usable as the BMR. The experimental results obtained with the bench-scale equipment, indicated that it was possible to perform membrane filtration even though biofilm was attached

to the membrane surface.

In CHAPTER 3, membrane filtration resistance in the BMR was investigated. The type and quantity of seeding bacteria had a significant influence on the increase of the filtration resistance. In order to minimize the increase of the filtration resistance, it is important to use bacteria acclimated to an autotrophic environment. It was sufficient to apply bacteria at the amount of 0.3 g-SS/m<sup>2</sup>-membrane for the oxidation of low concentrations of NH<sub>4</sub><sup>+</sup>-N (i.e. 1.0 mg/L). In the operation of the BMR, the cake filtration resistance was dominant and therefore development of an efficient method for removing the accumulated cake was found to be important. Increasing the rotational speed of the disks, was found to be an efficient cleaning method (shear cleaning). Some organic substances, most probably humic substances and carbohydrates caused irreversible membrane fouling. The increase in filtration resistance resulting from this, was caused mostly by substances contained in the raw water. In other words, bacteria fixed on the membrane surface for the oxidation of low concentrations of NH<sub>4</sub><sup>+</sup>-N hardly created filtration resistance.

In CHAPTER 4, simultaneous oxidation of NH<sub>4</sub><sup>+</sup>-N and removal of suspended solids with the BMR was examined and an efficient cleaning method for the BMR was developed. Dead-end filtration mode was found to be unsuitable for treating suspended solids due to the intensive accumulation of the cake. Shear cleaning, utilizing the shear stress by the increased rotational speed, did not work well for the removal of the accumulated cake when feed water contained turbidity. By establishing an overflow from the chamber as well as intermittent operation and an supplementary cleaning method, stable operation of the BMR could be accomplished. Sponge cleaning utilizing a small



quantity of sponge particles improved the cleaning efficiency considerably. Even when feed water contained turbidity, the accumulated cake was completely removed by this modified cleaning method. Implementing the sponge cleaning once every 1000-1500 hours, more than 3000 hours of operation could be carried out in the experiment. For quick recovery of the  $\text{NH}_4^+\text{-N}$  oxidation rate, however, a part of the removed cake should be fixed on the membrane again after sponge cleaning.

In CHAPTER 5, a kinetic analysis of the nitrifying biofilm developed in the BMR was conducted, by the use of a conventional biofilm model (assuming flat, homogeneous and continuous structure). The conventional biofilm model was found to be useful for analysis of the biofilm in the BMR due to the fact that the biofilm in the BMR actually had a simple structure (thin, flat and homogeneous). This was confirmed by cryosectioning of the biofilm and the microelectrode measurement. It can be expected that the nitrification efficiency of the BMR is higher than that of a conventional biofilm reactor. There are two distinct reasons for this; (1) reinforcement of mass transport toward the biofilm with advection flow (membrane filtration) (2) collection of treated water from the bottom of the biofilm where concentration of  $\text{NH}_4^+\text{-N}$  should be the lowest in the system. Model calculations supported these hypotheses.

In CHAPTER 6, a pilot study of the BMR was carried out using raw water from an actual drinking water source. Coagulation and sedimentation were implemented as pre-treatment in the pilot run. Simultaneous oxidation of  $\text{NH}_4^+\text{-N}$  and complete removal of suspended solids was successfully achieved. The filter run could be continued for more than 8 months without any chemical washing. The sponge cleaning was found to be very effective also in the pilot study. Sufficient nitrification was observed only

when the water temperature was higher than 10 °C. The recommended pH during coagulation in the pre-treatment of the BMR was found to 6.5-7.0 of pH. This can allow improvement in the removal of organic substances without the deterioration of nitrification. In addition to nitrification, biological oxidation of assimilable organic carbon (AOC) and manganese was experienced.

## 7.2. CONSIDERATIONS FOR FULL SCALE APPLICATION

In order to optimally design and operate the BMR, however, more pilot scale study is needed. Some considerations for full scale application is made in this section.

### (a) rotational speed

In the pilot scale study, the disk rotational speed was fixed at 10 rpm. The rotational speed can be fixed at a higher speed (e.g. 20-30rpm) without the detachment of microorganisms. By increasing the rotational speed, the rate of cake accumulation is supposed to be lowered. The optimum speed, however, should be determined taking energy consumption into account.

### (b) type of membrane and membrane flux

For the fixation of microorganism on the membrane, the employed membrane might be too tight. Molecular weight cut-off of the membrane was 750,000, equivalent to the pore size of 0.03  $\mu\text{m}$ . By employing looser membrane, membrane permeate flux can be increased. Material of the membrane is also important. Polysulfone is not necessarily optimum for this type of membrane application.

### (c) Pretreatment

Turbidity (suspended solids) in the raw water should be less

than 10 TU for the efficient operation of the BMR. However, the BMR would accept higher turbidity by increasing the disk rotational speed. When dealing with the raw water containing higher turbidity, coagulation and sedimentation can be recommended as the efficient pretreatment for the BMR.

(d) condition of coagulation

Aluminum salt is superior to iron salt for the pretreatment for the BMR. When using iron salt, low pH is required to achieve good treatment. This can lead to the deterioration of nitrification in the BMR. The recommended pH during aluminum coagulation in the pre-treatment of the BMR is 6.5-7.0 of pH. This can allow improvement in the removal of organic substances without the deterioration of nitrification.

(e) Others (investigation needed in the future)

Especially, rapid recovery of the treatment efficiency after sponge cleaning is the problem to be solved. Maintaining the nitrification efficiency during low water temperature period and optimizing the sponge cubes for cleaning (i.e. material, size etc.) can also be listed as interesting issues.

### 7.3. CONCLUSION

It can be concluded that the BMR proposed through this thesis has significant potential for being used as advanced drinking water treatment process. The BMR can perform complete solid-liquid separation and biological oxidation of  $\text{NH}_4^+\text{-N}$  and other substances (e.g. manganese) simultaneously. Efficiency of biological oxidation in the BMR can be expected to be high even when the concentrations of contaminants are quite low. This was shown by model calculation in this study. Effective cleaning method utilizing sponge cubes, "sponge cleaning" was developed

for the operation of the BMR. This cleaning was found to completely cancel the filtration resistance due to the accumulated cake. By implementing the sponge cleaning at an appropriate interval, filter run could be continued for several months without any chemical membrane washing. These features of the BMR were recognized in a pilot study using raw water from an actual drinking water source as well.

The membrane in the BMR might be categorized as an "The Multi-function Membrane" defined as a membrane with other functions than sieving. The author thinks this novel process can expand the possibility of membrane technology.